Introduction to Plasma Physics and Plasma Processes

07. Dec. 2018

Ho Jun Kim

Assistant Professor

Department of Mechanical Engineering, Dong-A University

EDUCATION

Ph.D. Texas A&M University,
College Station, Texas, 2008
Major: Mechanical Engineering

M.S. Texas A&M University,
College Station, Texas, 2004
Major: Mechanical Engineering

B.S. Hanyang University,
Seoul, South Korea, 2002
Major: Mechanical Engineering

EXPERIENCE

Assistant Professor Dong-A University, Department of Mechanical Engineering.
(3/18 – *)
Principal Engineer Samsung Electronics, Memory Thin Film Technology Team.
(3/14 – 2/18)
Senior Engineer Samsung Electronics, Memory Thin Film Technology Team.
(8/08 – 2/14)
Research Expert Korea Institute of Industrial Technology, Fuel Cell Group.
(3/08 – 7/08)
Research Associate Old Dominion University, Department of Mechanical and Aerospace Engineering.
(1/07 – 2/08)
Research Assistant Texas A&M University, Department of Mechanical Engineering. (9/03 – 12/06)

Source: **Demetre J. Economou, Hybrid Simulation of Low Temperature Plasmas: A Brief Tutorial**

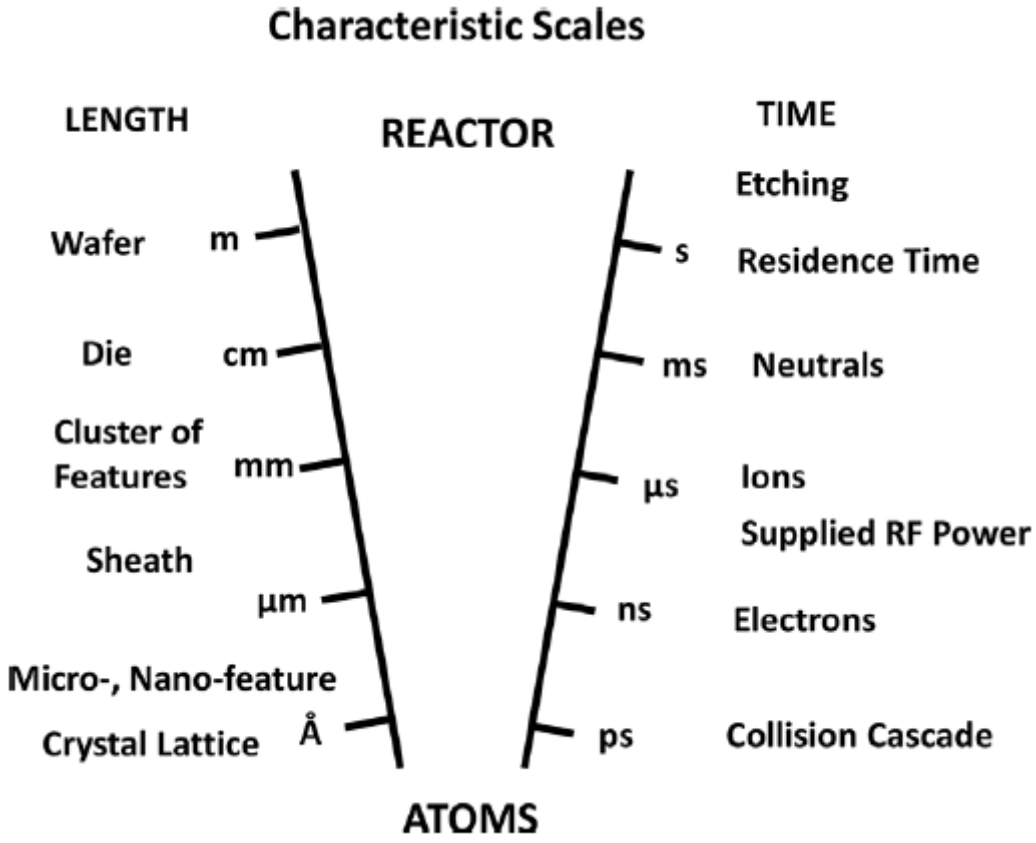

Complex Flows and Plasma Physics Laboratory (CFPPL)

Chaotic Transport

- Computation of stretching and its efficiency in chaotic flows
- Mixing, reaction and chaos in multi-dimensional flows
- Periodic point and invariant manifold in chaotic flows

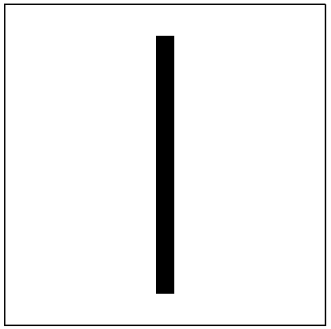

Chaotic cavity flow

Plasma Discharge

- Process plasma (CCP) simulations: PE-TEOS, PE-SiN, PE-SiON, ACL, PE-ALD
- Process plasma (ICP) simulations: HDP-SiO_2, HDP-SiN, HDP-ACL
- Remote plasma: fluorine chemistry, NF_3 plasma dissociation, fluorine transport

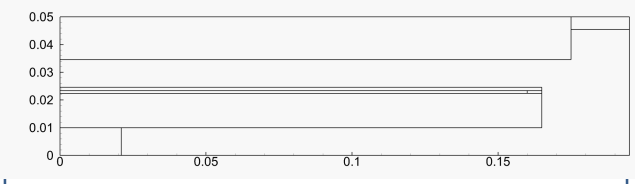

Electron density

Surface Chemistry

- Molecular dynamics: deposition, etching
- Ab initio calculation: reaction rate, activation energy
- Computational chemistry: reaction rate, reaction pathway

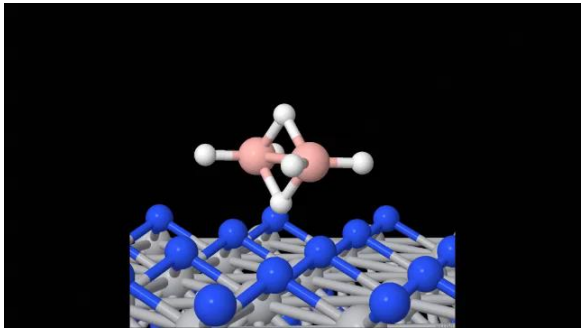

Dissociation reaction of B_2H_6 on TiN surfaces

Complex Flows and Plasma Physics Laboratory (CFPPL)

Chaotic Transport

- Computation of stretching and its efficiency in chaotic flows
- Mixing, reaction and chaos in multi-dimensional flows
- Periodic point and invariant manifold in chaotic flows

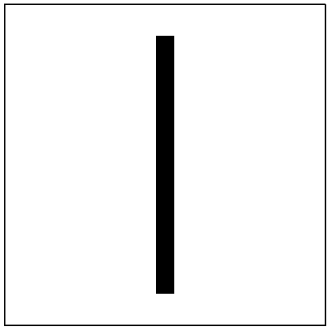

Chaotic cavity flow

Plasma Discharge

- Process plasma (CCP) simulations: PE-TEOS, PE-SiN, PE-SiON, ACL, PE-ALD
- Process plasma (ICP) simulations: HDP-SiO_2, HDP-SiN, HDP-ACL
- Remote plasma: fluorine chemistry, NF_3 plasma dissociation, fluorine transport

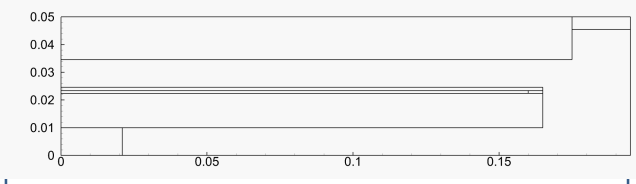

Electron density

Surface Chemistry

- Molecular dynamics: deposition, etching
- Ab initio calculation: reaction rate, activation energy
- Computational chemistry: reaction rate, reaction pathway

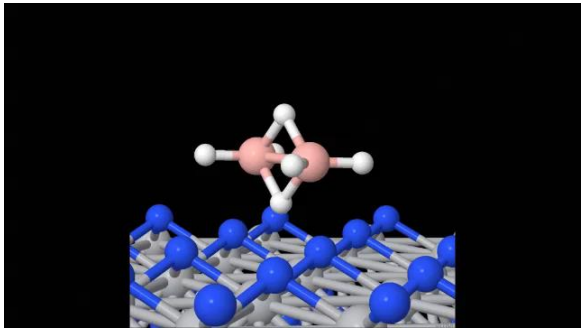

Dissociation reaction of B_2H_6 on TiN surfaces

Process simulation: Electroplating of Cu

Active type (moving stirrer) reactor: vortex contour

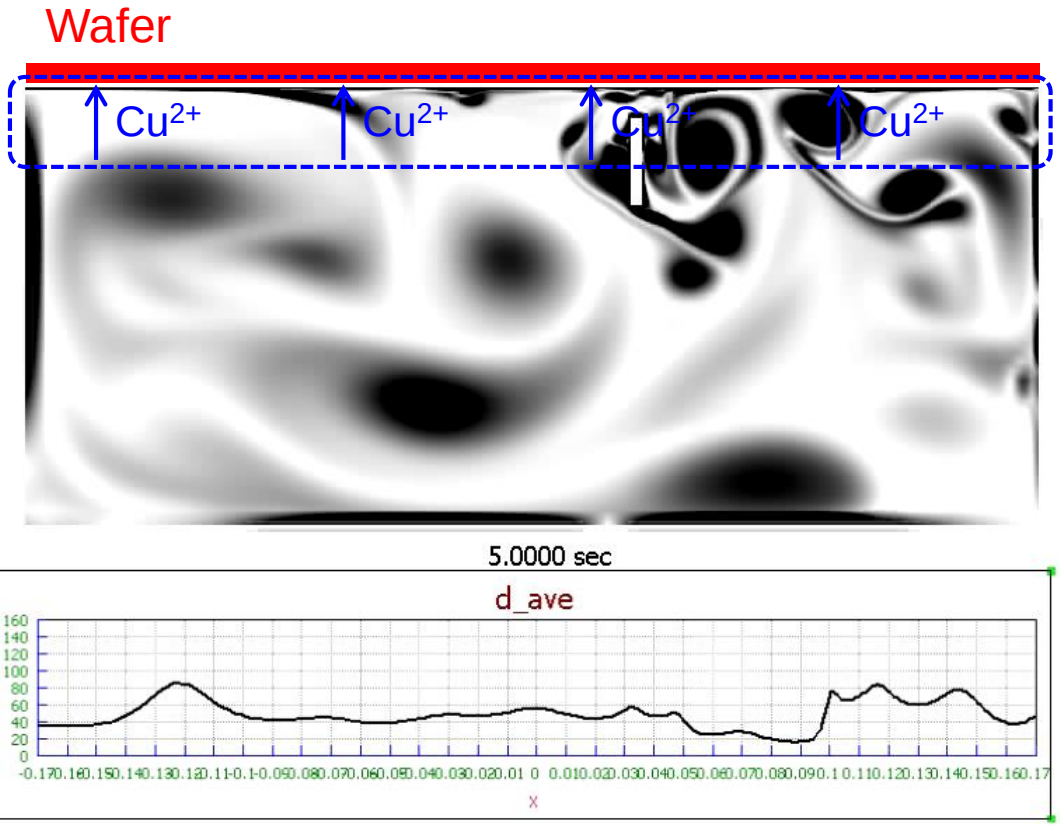

By the vortex movement, the surface flux of Cu ion is uniformly formed along the wafer surface.

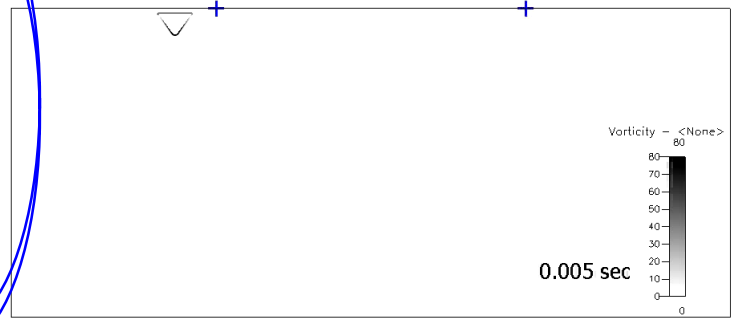

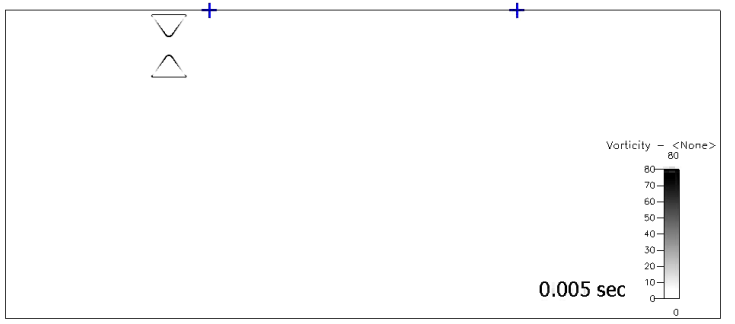

Examples of stirrer design

Electroosmotically stirred chaotic micro mixer

$$U_{HS} = -\frac{\zeta \varepsilon E_x}{\mu}$$

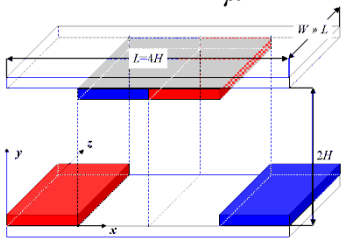

+

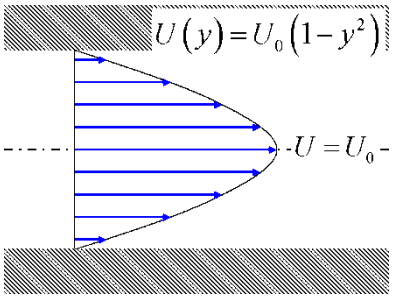

=

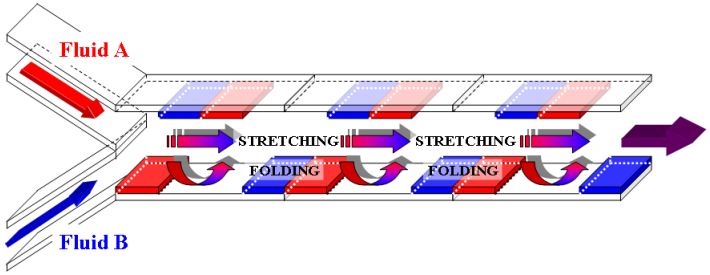

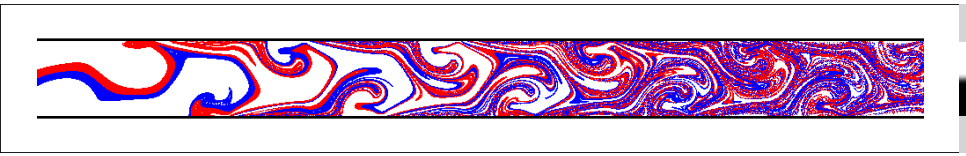

Particle Dispersion

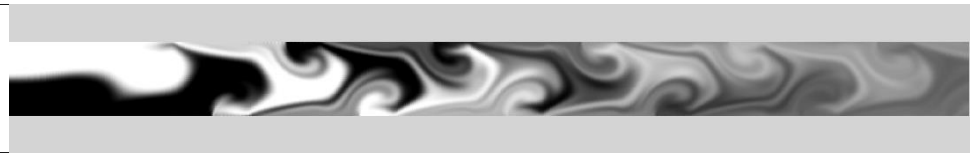

Mixing Simulation, Pe = 1000

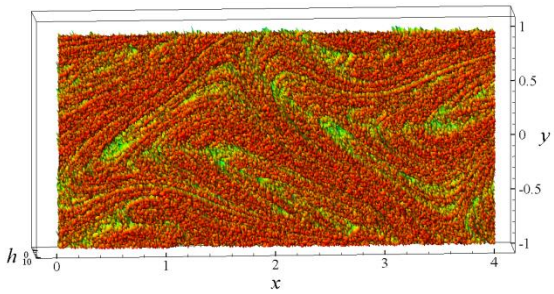

$$h = \frac{|l|}{|l(0)|}$$

$l(0)$ is the initial length of fluid filament

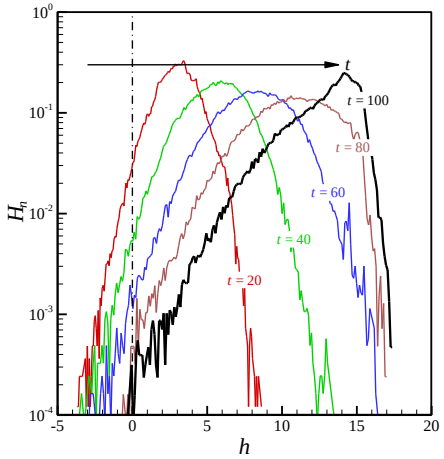

$$H_n(\ln h) = \frac{dN(\ln h)}{d(\ln h)}$$

$dN(\ln h)$ is the number of particles experiencing the stretching values in the range of [ln h, ln h + d(ln h)]

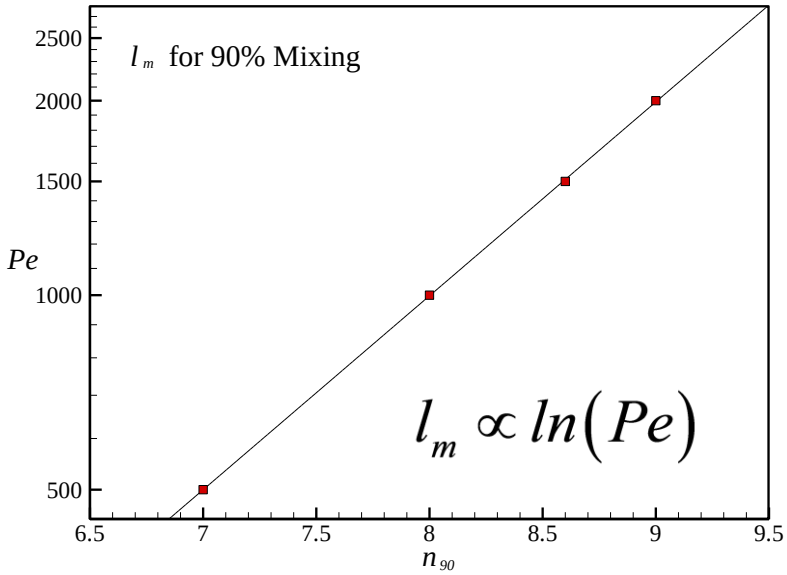

Peristaltic meso scale mixer

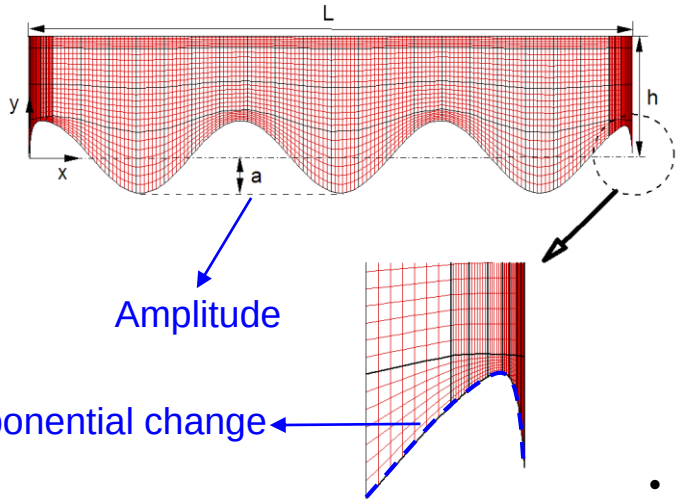

Spectral element mesh

$Re = 6000,\ Pe = 6000$

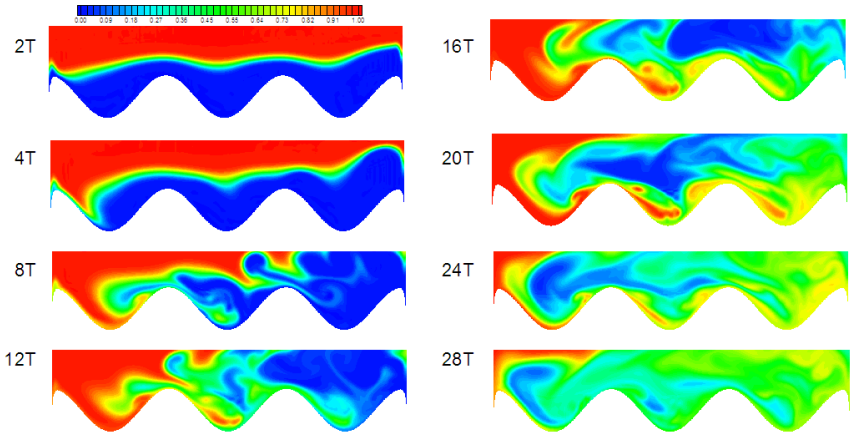

- Bottom wall is flexible membrane.
- Waves traveled through wall and induced peristaltic motion that resulted in predictable mixing.

$$M = \frac{\sigma}{\theta_o} = \sqrt{\frac{1}{(N-1)}\sum_{i=1}^{N}\left(\frac{\theta_i}{\theta_o} - 1\right)^2}$$

θ_i is the concentration in box i

θ_o is the concentration of the perfect mix

$$90\%\ \text{Mixing} \Rightarrow 0.45 \le \theta \le 0.55$$

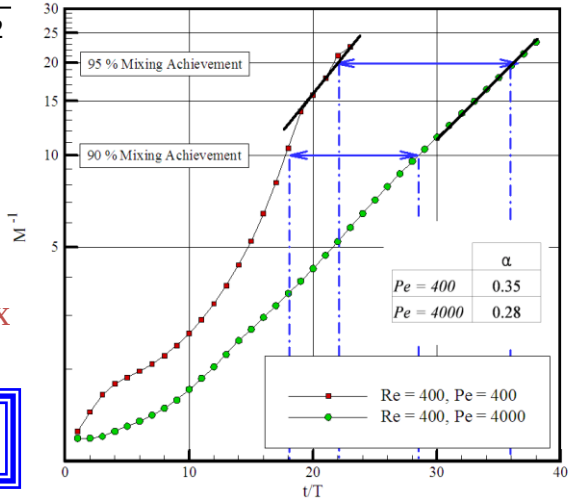

$Re = 400,\ Pe = 400$

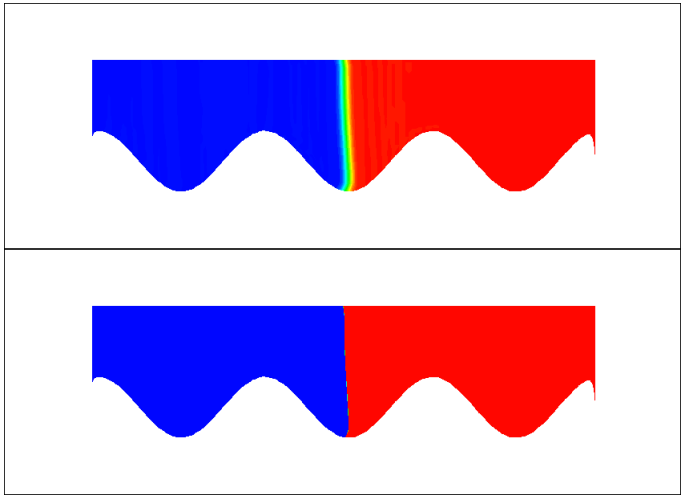

Nonconforming spectral element method

Moving Gaussian Hill

$Pe = 10^6$

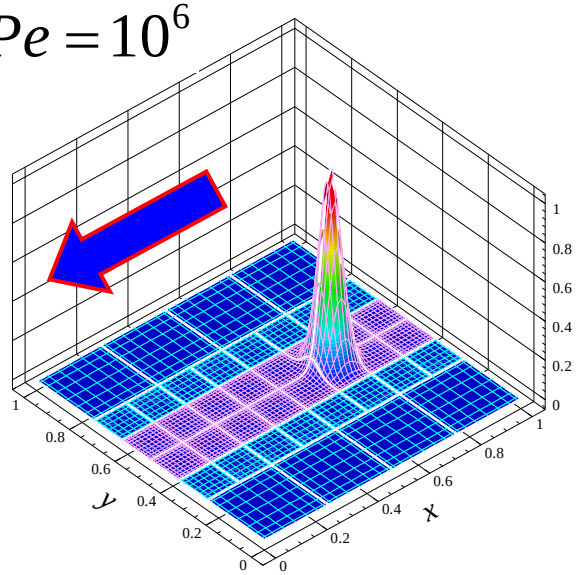

Singular cavity flow, Re =1,000

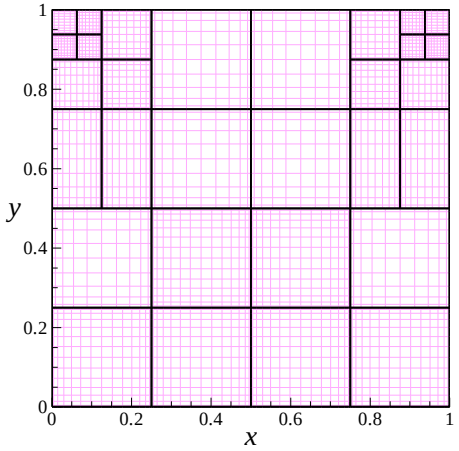

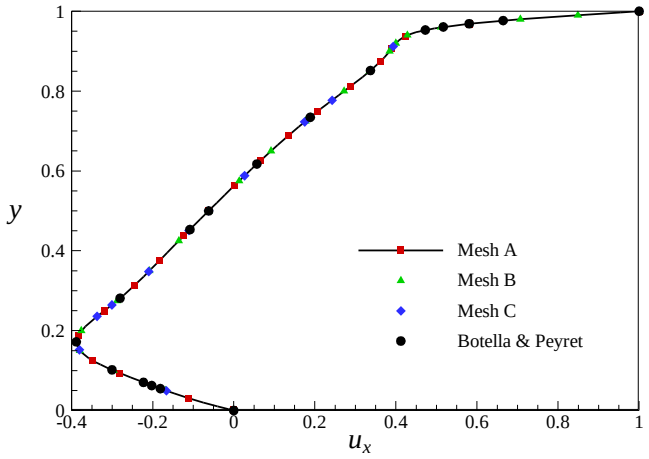

u_x velocity distribution along the x = 0.5 line

Boussinesq approximation: Natural convection

$$\frac{\partial u}{\partial x}+\frac{\partial v}{\partial y}=0$$

$$\frac{\partial u}{\partial t}+u\frac{\partial u}{\partial x}+v\frac{\partial u}{\partial y}=-\frac{\partial p}{\partial x}+\frac{Pr}{Ra^{1/2}}\left(\frac{\partial^2 u}{\partial x^2}+\frac{\partial^2 u}{\partial y^2}\right)$$

$$\frac{\partial v}{\partial t}+u\frac{\partial v}{\partial x}+v\frac{\partial v}{\partial y}=-\frac{\partial p}{\partial y}+\frac{Pr}{Ra^{1/2}}\left(\frac{\partial^2 v}{\partial x^2}+\frac{\partial^2 v}{\partial y^2}\right)+PrT$$

$$\frac{\partial T}{\partial t}+u\frac{\partial T}{\partial x}+v\frac{\partial T}{\partial y}=\frac{1}{Ra^{1/2}}\left(\frac{\partial^2 T}{\partial x^2}+\frac{\partial^2 T}{\partial y^2}\right)$$

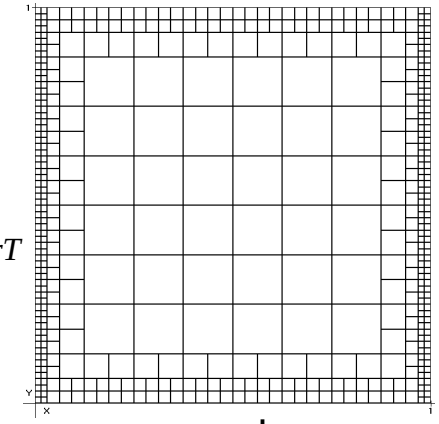

mesh

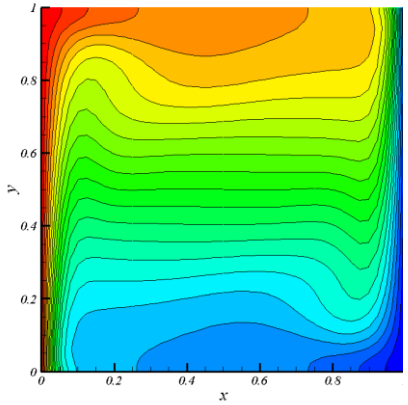

temperature

Chaotic flow in a cavity

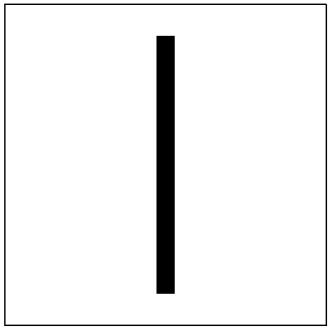

Complex Flows and Plasma Physics Laboratory (CFPPL)

Chaotic Transport

- Computation of stretching and its efficiency in chaotic flows
- Mixing, reaction and chaos in multi-dimensional flows
- Periodic point and invariant manifold in chaotic flows

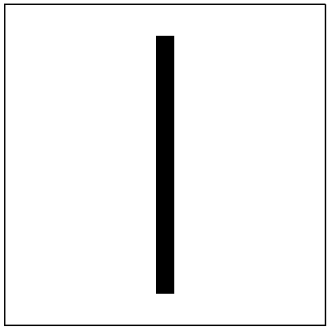

Chaotic cavity flow

Plasma Discharge

- Process plasma (CCP) simulations: PE-TEOS, PE-SiN, PE-SiON, ACL, PE-ALD
- Process plasma (ICP) simulations: HDP-SiO_2, HDP-SiN, HDP-ACL
- Remote plasma: fluorine chemistry, NF_3 plasma dissociation, fluorine transport

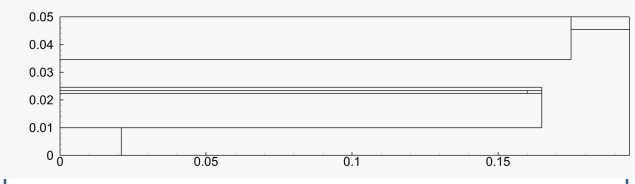

Electron density

Surface Chemistry

- Molecular dynamics: deposition, etching
- Ab initio calculation: reaction rate, activation energy
- Computational chemistry: reaction rate, reaction pathway

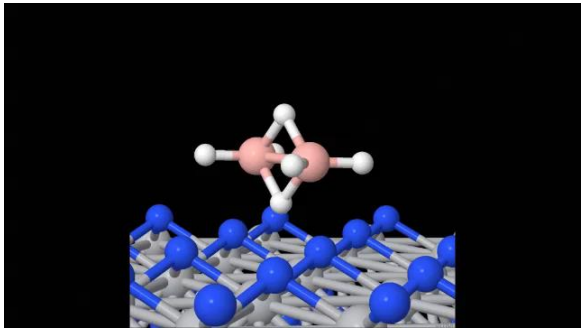

Dissociation reaction of B_2H_6 on TiN surfaces

The optimized structures of ACL and 2D charge density map

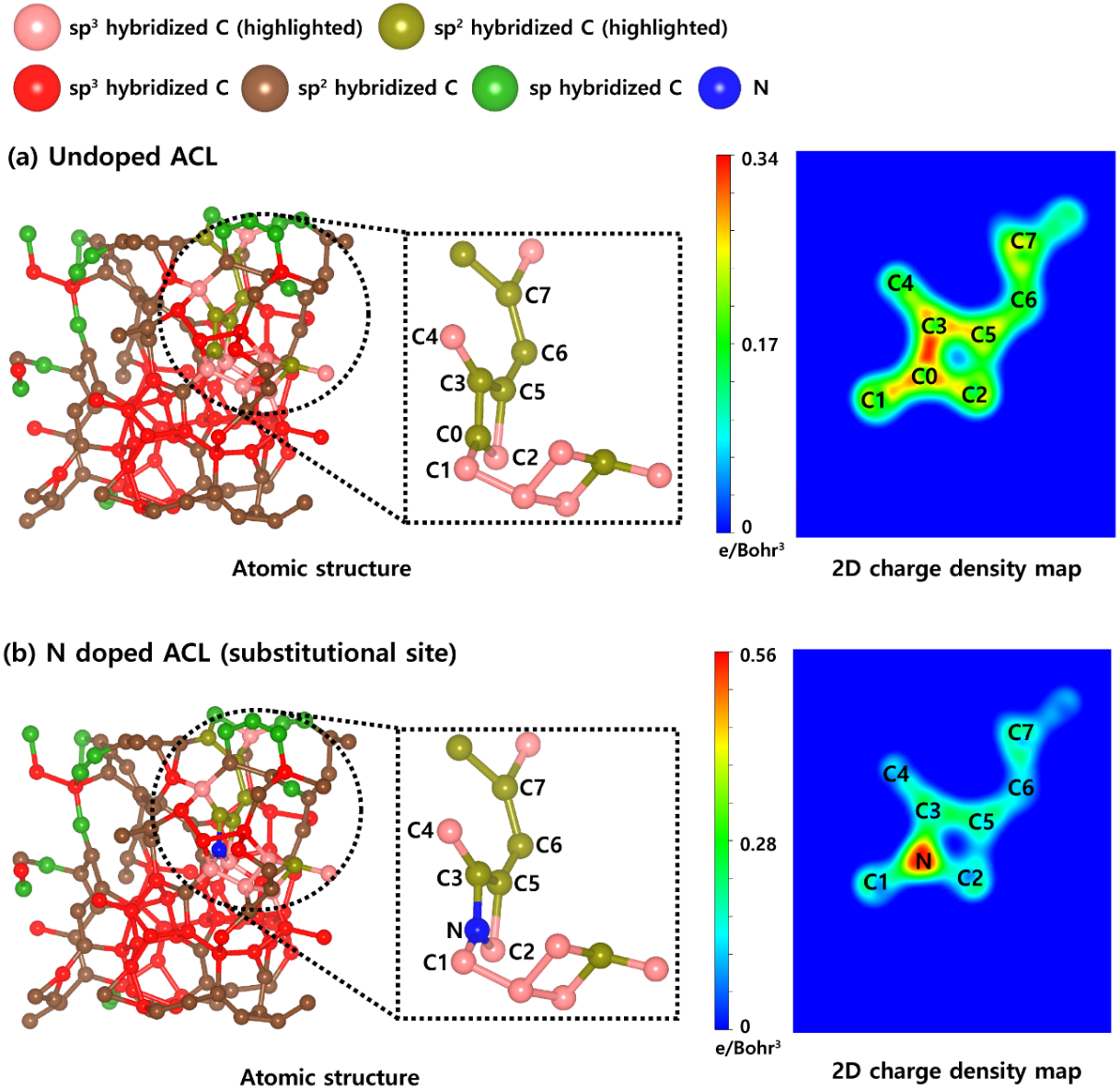

The optimized structures of the ACL (left) and 2D charge density map (right) for (a) undoped ACL and (b) N doped ACL (substitutional site).

In the center of (a-b), several atoms in the dotted black box are highlighted.

2D charge density map contains specified atoms: (a) C0 ~ C7, and (b) N and C1 ~ C7. Charge accumulation (red area) in the vicinity of the N atom can be seen.

Surface phenomena: Molecule dissociation and deposition

Ab initio simulations

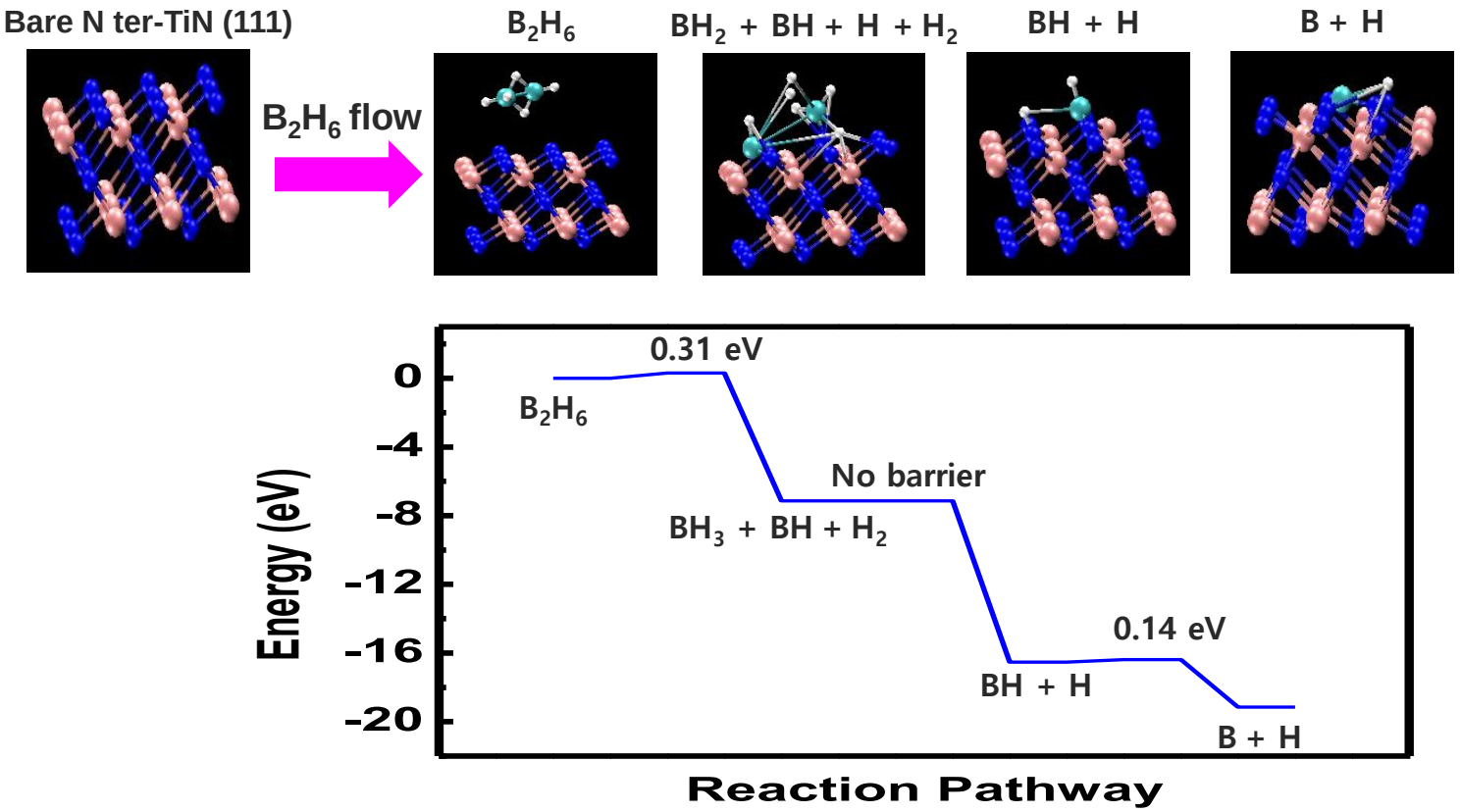

Complex Flows and Plasma Physics Laboratory (CFPPL)

Chaotic Transport

- Computation of stretching and its efficiency in chaotic flows
- Mixing, reaction and chaos in multi-dimensional flows
- Periodic point and invariant manifold in chaotic flows

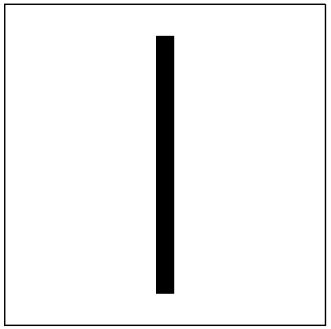

Chaotic cavity flow

Plasma Discharge

- Process plasma (CCP) simulations: PE-TEOS, PE-SiN, PE-SiON, ACL, PE-ALD
- Process plasma (ICP) simulations: HDP-SiO_2, HDP-SiN, HDP-ACL
- Remote plasma: fluorine chemistry, NF_3 plasma dissociation, fluorine transport

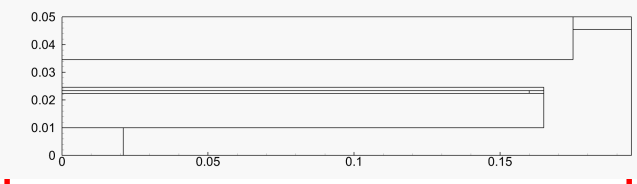

Electron density

Surface Chemistry

- Molecular dynamics: deposition, etching
- Ab initio calculation: reaction rate, activation energy
- Computational chemistry: reaction rate, reaction pathway

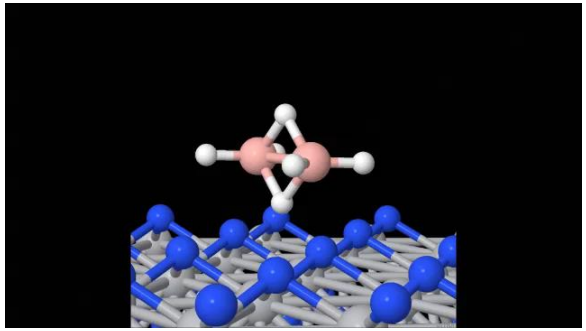

Dissociation reaction of B_2H_6 on TiN surfaces

Recent trend in a semiconductor industry

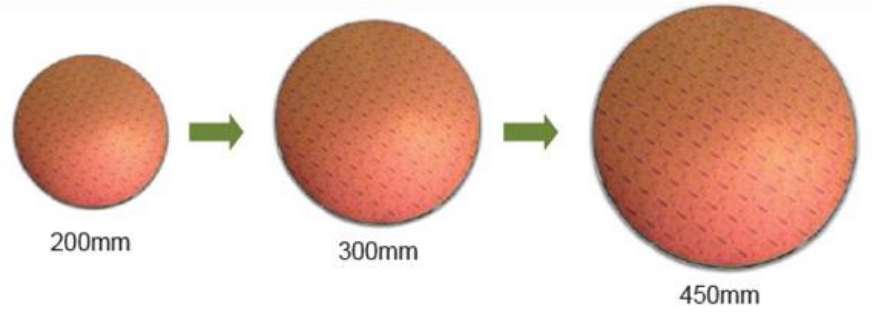

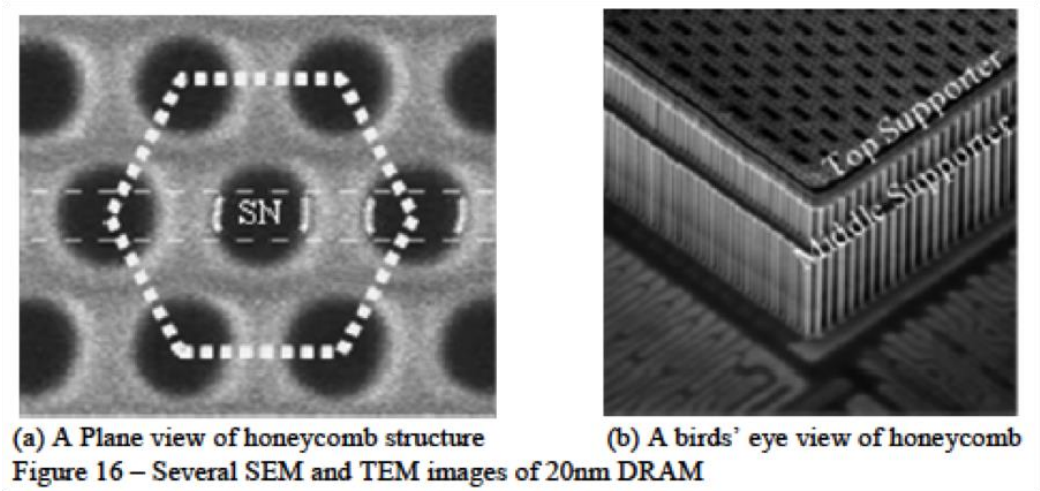

(a) A Plane view of honeycomb structure (b) A birds' eye view of honeycomb

Figure 16 – Several SEM and TEM images of 20nm DRAM

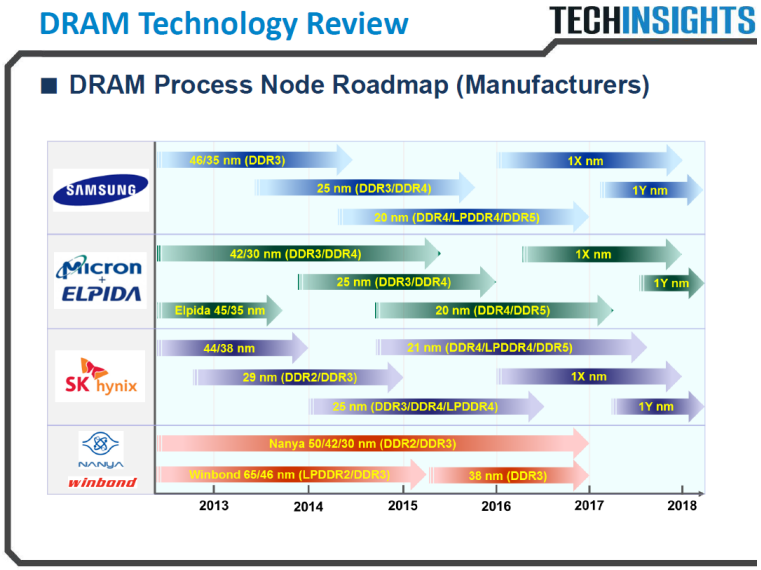

Proposed 3D NAND Structure

	p-BiCS (Toshiba)	TCAT (Samsung)	3D FG (Hynix)	Micron
Structure	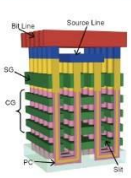 Tanaka. H, VLSIT 2007	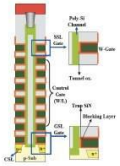 J. Jang, VLSIT 2009	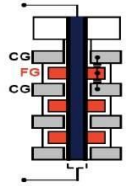 S. Whang, IEDM 2010	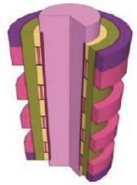 G. Hawk, FMS 2011
Key Features	- P+ SONOS Cell	- TANOS Cell	- Floating Gate	?
Key Issue	- Large Cell Size - Reliability	- Large Cell Size - SL Resistance	- Process of bit separation - Disturbance	?

Source: TechInsights

Semiconductor fabrication process

Semiconductor fabrication consists of the various (total 8) categories of process:

- Photolithography
- Wet Chemical Etching
- Dry Etching
- Diffusion
- Ion Implantation
- Film Deposition – Metallization
- Film Deposition – Dielectric
- Chemical Mechanical Polishing

Plasma is mainly adopted.

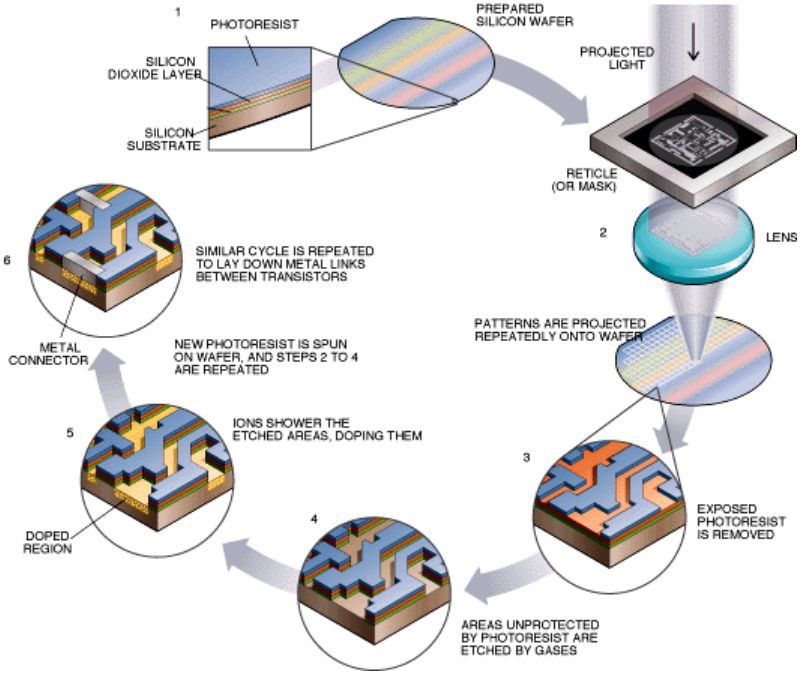

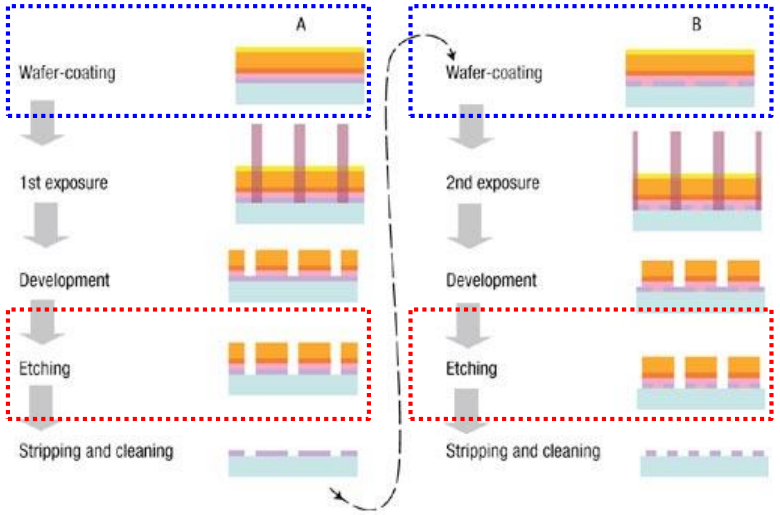

> 50 %, plasma process

Samsung Electronics SCS Engineers

Definition of plasma

Plasmas

A collection of freely moving charged particles which is, on the average, electrically neutral

- Discharges:
  - Driven by voltage or current sources
  - Neutral particles are important
  - There are boundaries at which surface losses are important
  - The electrons are much hotter than the ions
- Device sizes: 30 cm - 1 m
- Driving frequencies: DC to RF (13.56 MHz) to microwaves (2.45 GHz)

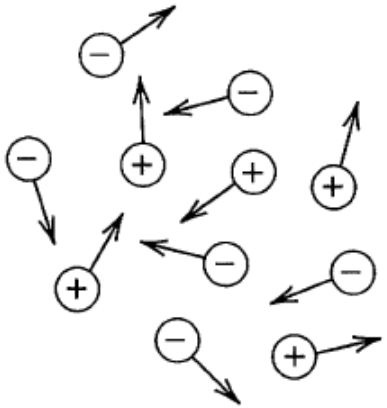

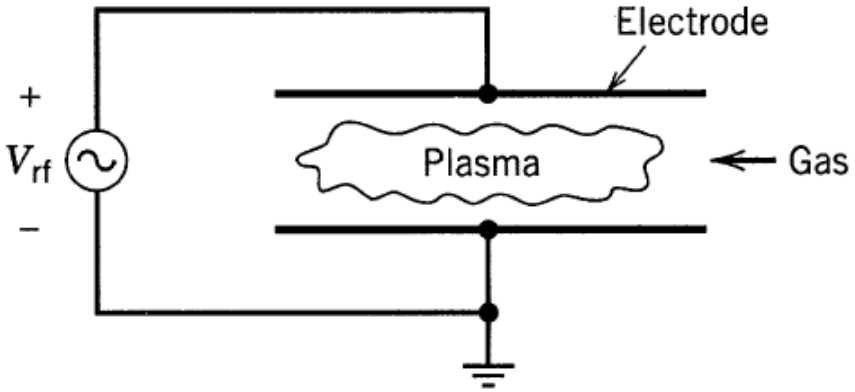

What is Plasma ?

Source: http://pluto.space.swri.edu/image/glossary/plasma.html

Plasma: A plasma is a hot ionized gas consisting of approximately equal numbers of positively charged ions and negatively charged electrons. The characteristics of plasmas are significantly different from those of ordinary neutral gases so that plasmas are considered a distinct “fourth state of matter.” For example, because plasmas are made up of electrically charged particles, they are strongly influenced by electric and magnetic fields (see figure) while neutral gases are not. An example of such influence is the trapping of energetic charged particles along geomagnetic field lines to form the Van Allen radiation belts.

www.geo.mtu.edu/weather/aurora/

Source: CFD ACE+ manual

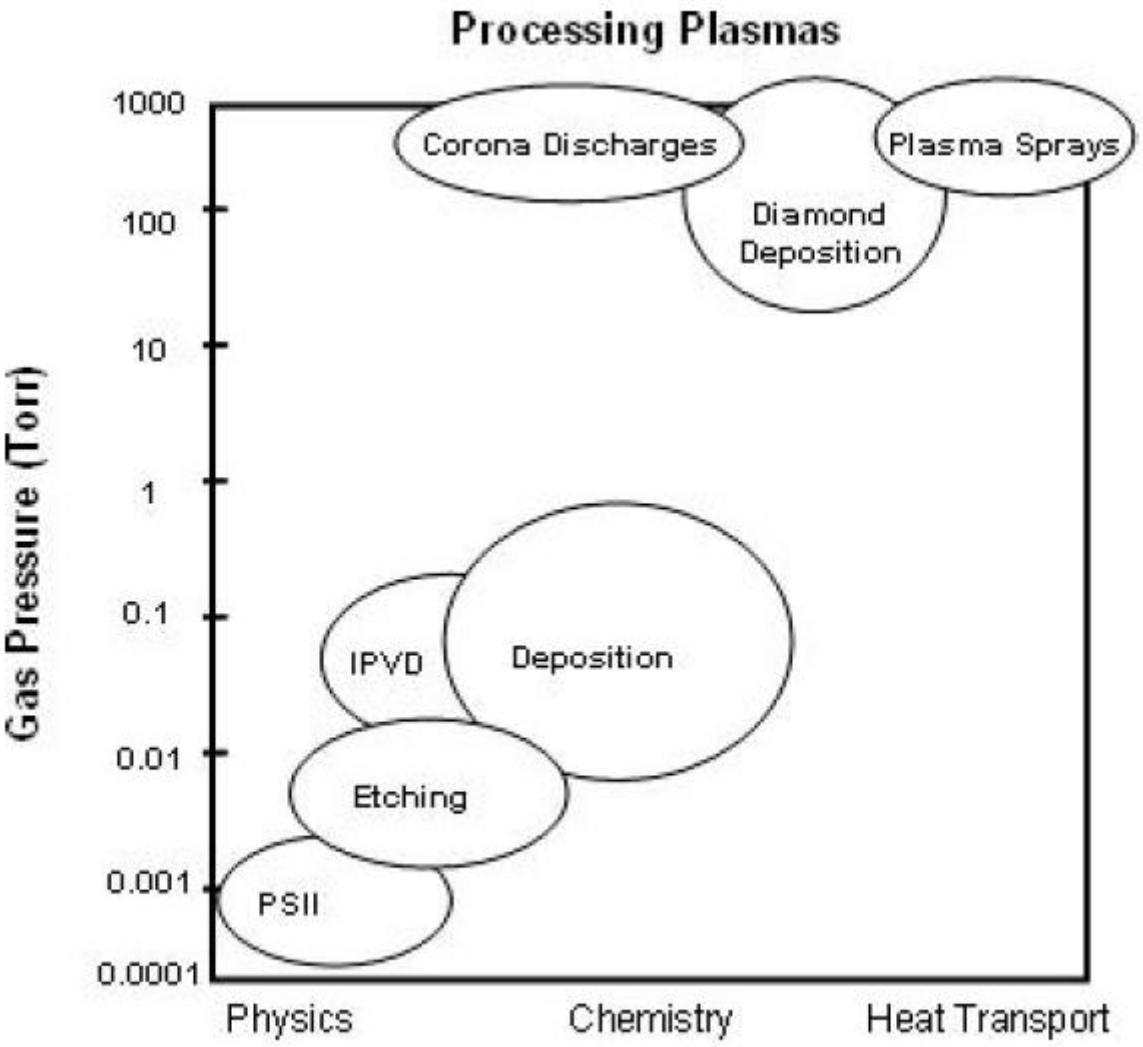

Different Plasma Technologies

Source: CFD ACE+ manual

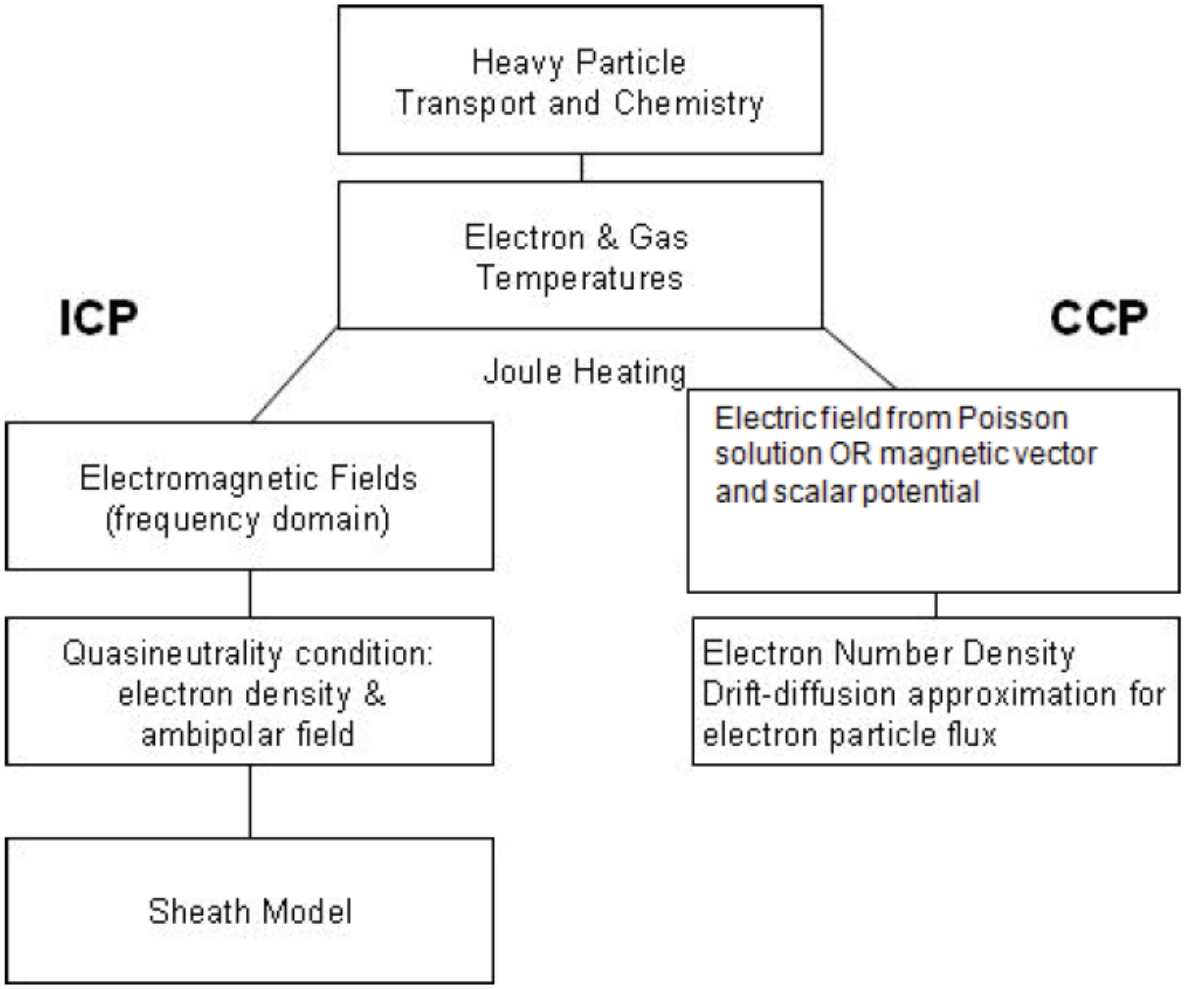

Distinctive Features of athe ICP and CCP Models

Source: CFD ACE+ manual

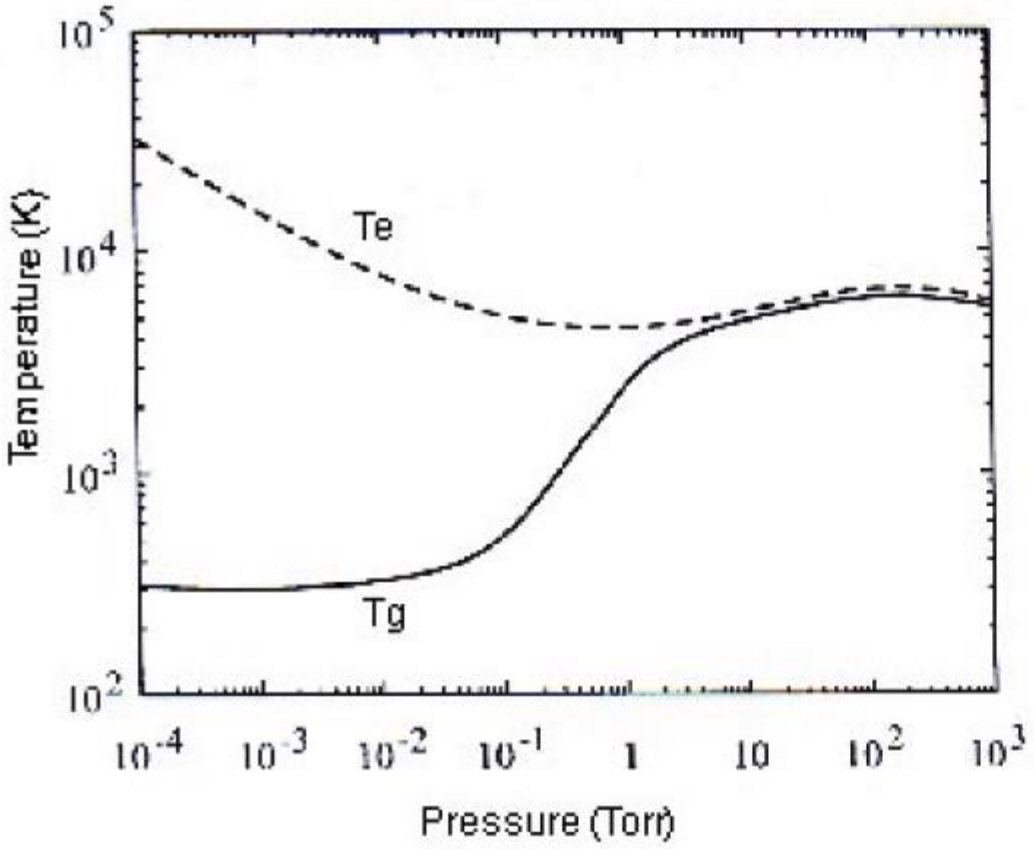

Electron and gas temperatures in a DC discharge of mercury and rare gas mixture at different gas pressures and same current.

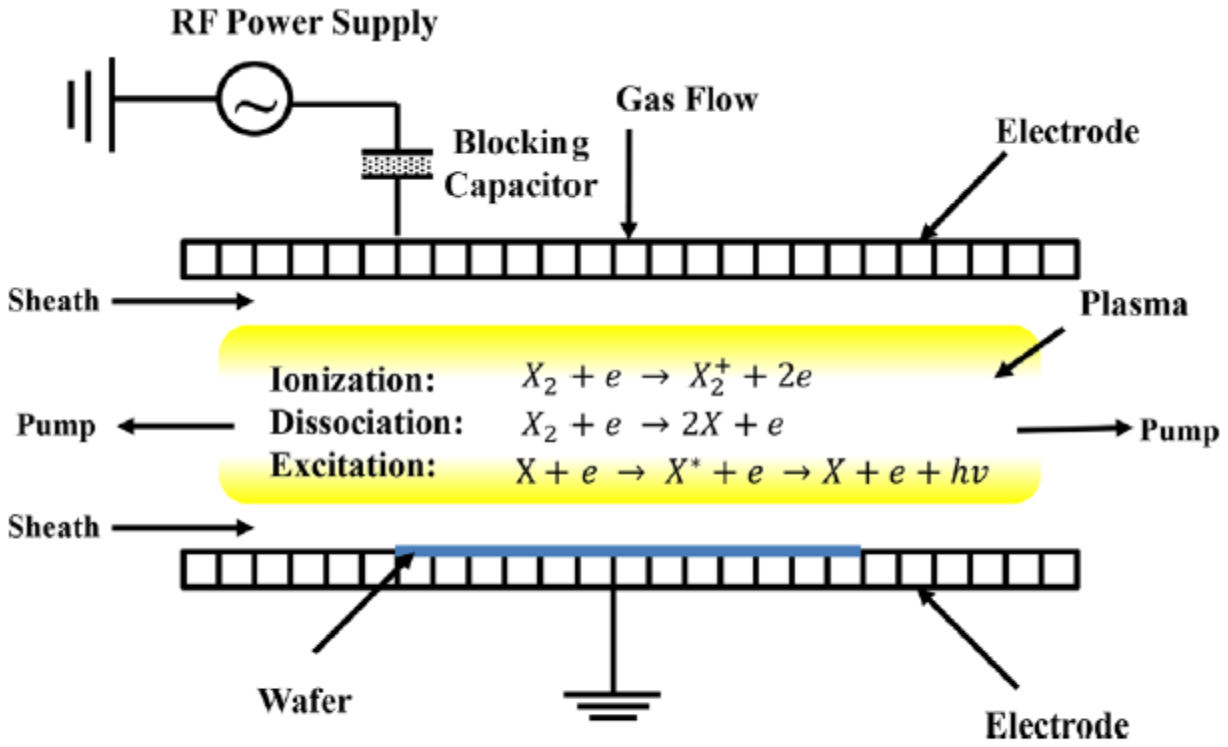

Figure 3. Schematic of a parallel plate capacitively-coupled plasma (CCP) reactor.

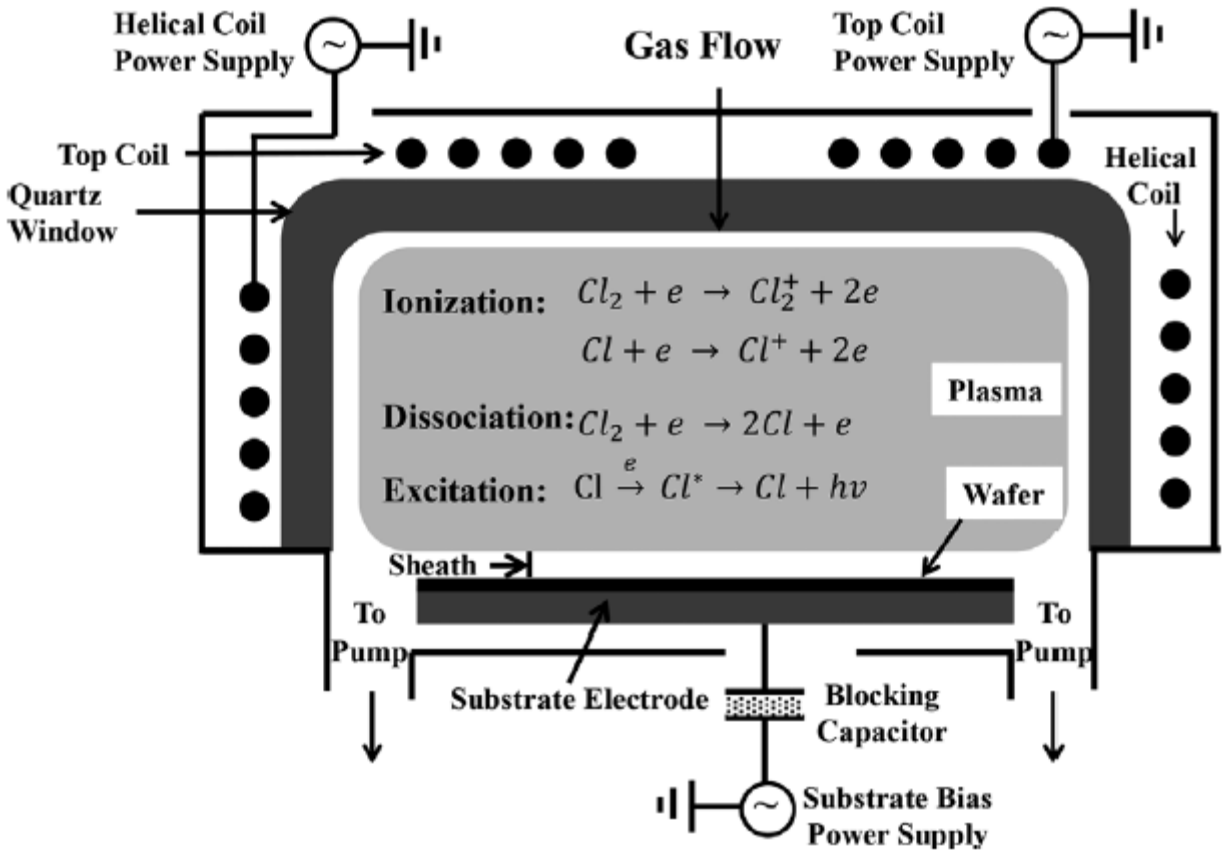

Figure 4. Schematic of a dual coil inductively-coupled plasma (ICP) reactor.

Source: Applied Materials

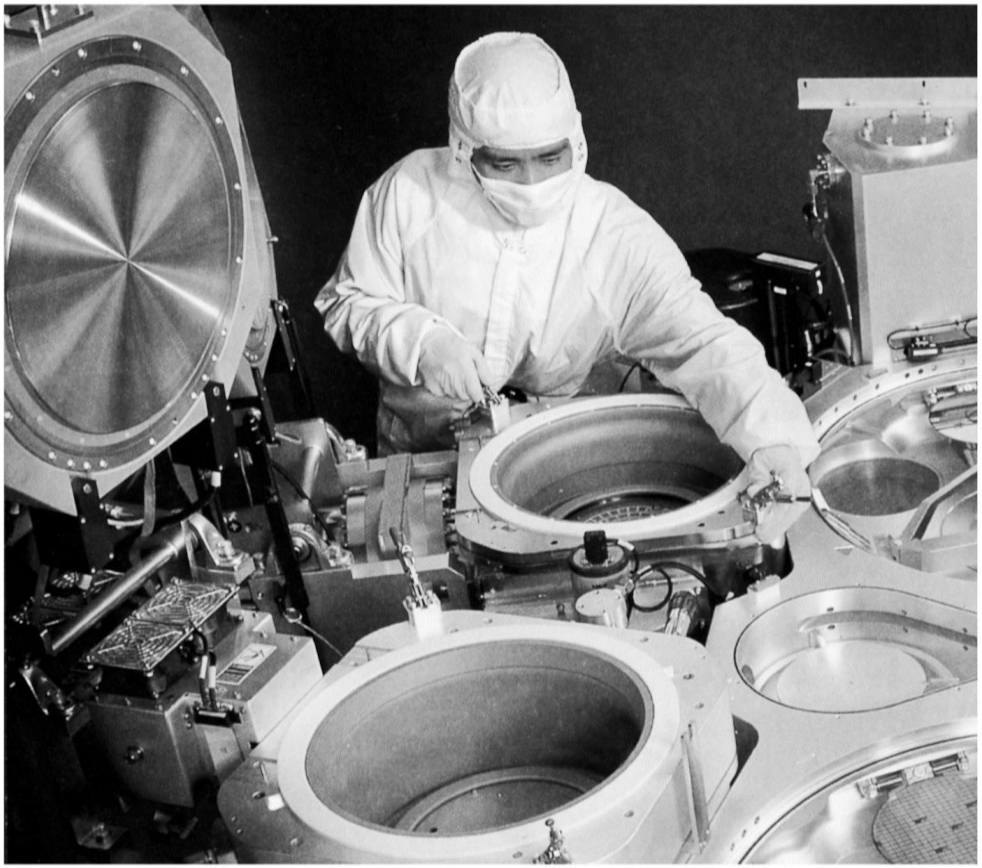

Figure 12.24 The Endura system by Applied Materials uses a number of PVD or CVD chambers fed by a central robot. For conventional and IMP sputtering, targets are hinged to open upward. Two open chambers are shown in this photograph along with the load lock *(from Applied Materials).*

Introduction to Plasma Physics

Source: https://people.eecs.berkeley.edu/~lieber/

PLASMAS AND DISCHARGES

- Plasmas
  A collection of freely moving charged particles which is, on the average, electrically neutral
- Discharges
  Are driven by voltage or current sources
  Charged particle collisions with neutral particles are important
  There are boundaries at which surface losses are important
  The electrons are not in thermal equilibrium with the ions

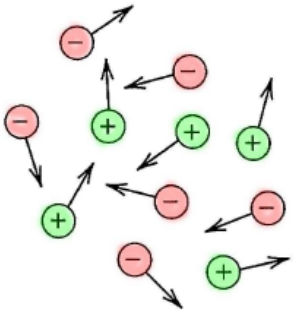

(a)

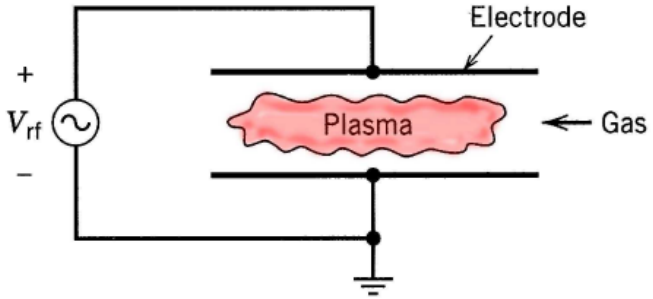

(b)

- Device sizes $\sim$ 30 cm – 1 m
- Frequencies from DC to rf (13.56 MHz) to microwaves (2.45 GHz)

UNITS AND CONSTANTS

- SI units: meters (m), kilograms (kg), seconds (s), coulombs (C)
  $e = 1.6 \times 10^{-19}$ C, electron charge $= -e$
- Energy unit is joule (J)
  Often use electron-volt
  $$1 \text{ eV} = 1.6 \times 10^{-19} \text{ J}$$
- Temperature unit is kelvin (K)
  Often use equivalent voltage of the temperature
  $$\boxed{\text{T}_e(\text{volts}) = \frac{kT_e(\text{kelvins})}{e}}$$

where k = Boltzmann's constant $= 1.38 \times 10^{-23}$ J/K

$$\boxed{1 \text{ V} \Longleftrightarrow 11,600 \text{ K}}$$

- Pressure unit is pascal (Pa); 1 Pa = 1 N/m^2
  Atmospheric pressure $\equiv$ 1 bar $\approx 10^5$ Pa $\approx$ 760 Torr

$$\boxed{1 \text{ Pa} \Longleftrightarrow 7.5 \text{ mTorr}}$$

Source: https://people.eecs.berkeley.edu/~lieber/

PLASMA DENSITY VERSUS TEMPERATURE

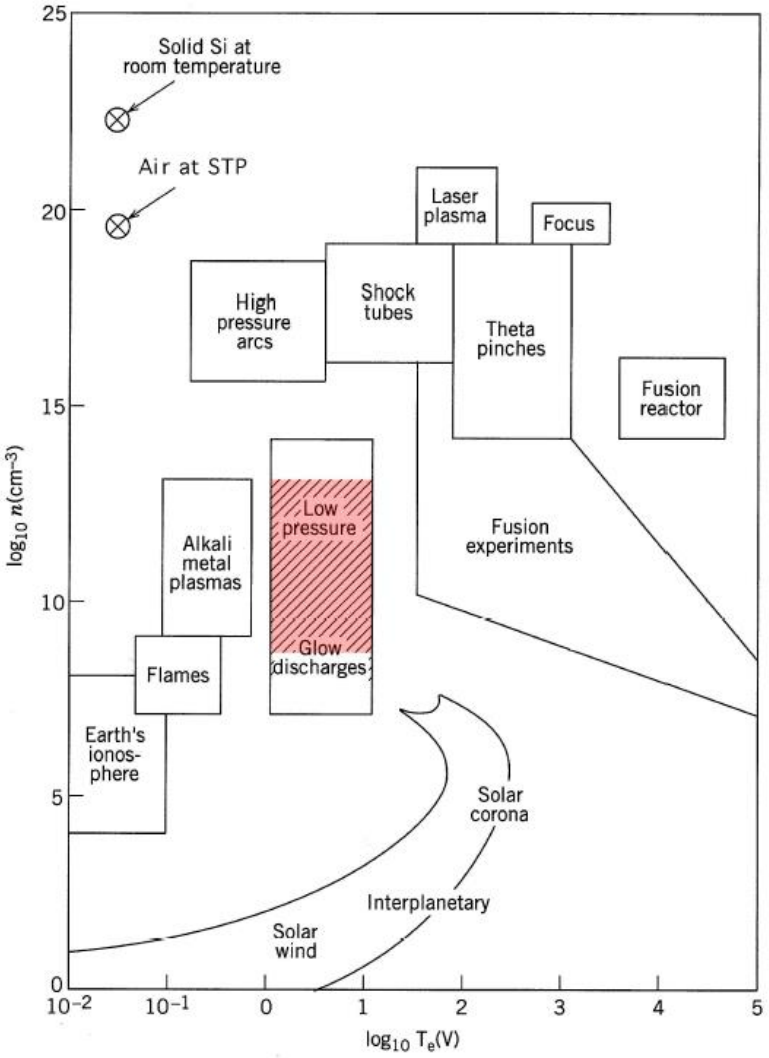

Source: https://people.eecs.berkeley.edu/~lieber/

RELATIVE DENSITIES AND ENERGIES

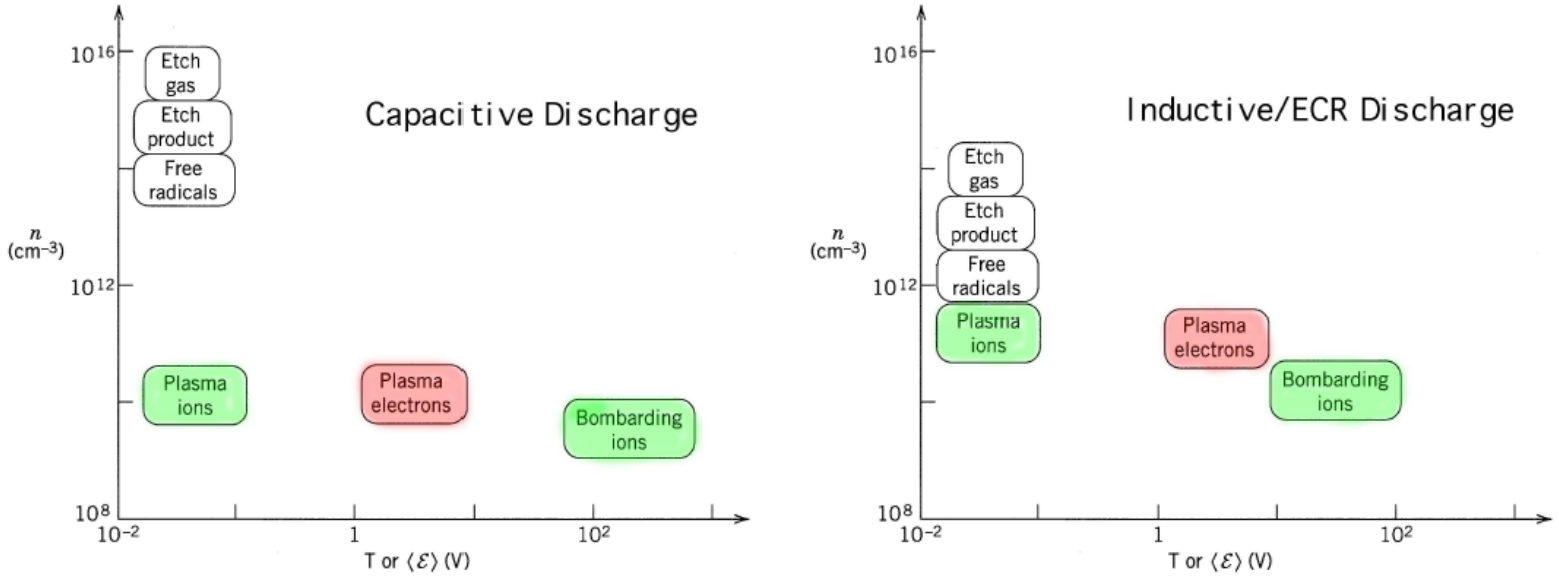

Source: https://people.eecs.berkeley.edu/~lieber/

NON-EQUILIBRIUM

- Energy coupling between electrons and heavy particles is weak

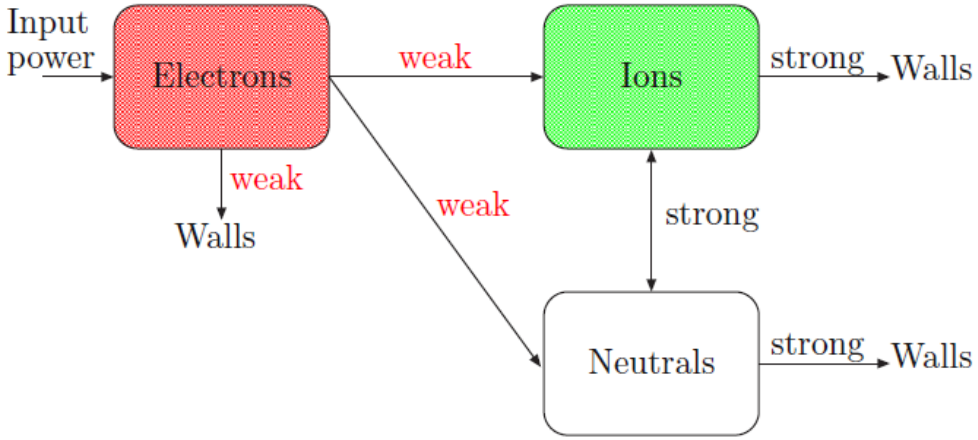

- Electrons are *not* in thermal equilibrium with ions or neutrals

$$T_e \gg T_i \quad \text{in plasma bulk}$$

$$\text{Bombarding ion } \mathcal{E}_i \gg T_e \quad \text{at wafer surface}$$

- "High temperature processing at low temperatures"
  1. Wafer can be near room temperature
  2. Electrons produce free radicals $\Longrightarrow$ chemistry
  3. Electrons produce electron-ion pairs $\Longrightarrow$ ion bombardment

Source: https://people.eecs.berkeley.edu/~lieber/

ELEMENTARY DISCHARGE BEHAVIOR

- Uniform density of electrons and ions n_e and n_i at time $t = 0$
- Low mass warm electrons quickly drain to the wall, forming sheaths

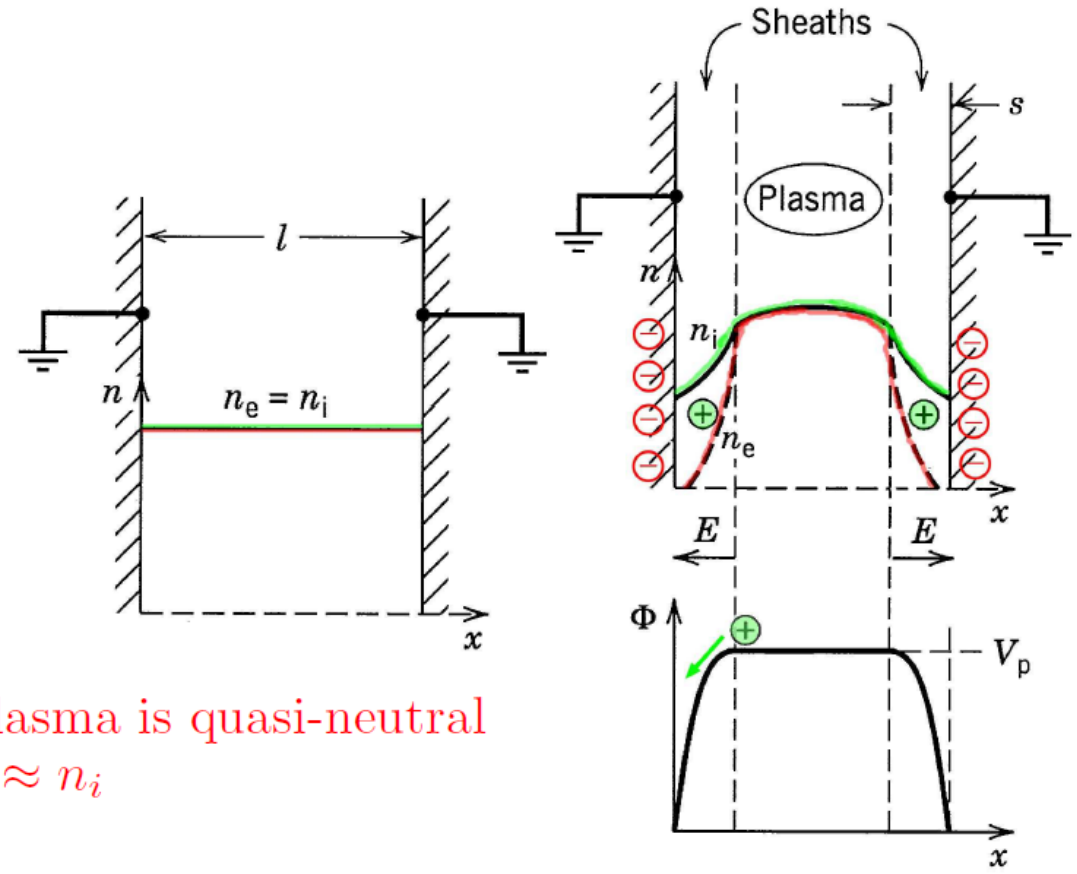

- Bulk plasma is quasi-neutral
  $\Longrightarrow n_e \approx n_i$

- Ions accelerated to walls; ion bombarding energy $\mathcal{E}_i$ = plasma-wall potential V

POISSON'S EQUATION

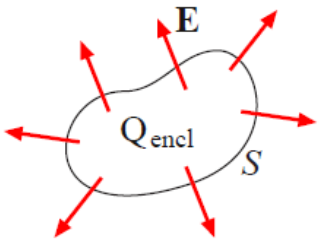

- An electric field can be generated by charges

$$\nabla \cdot \mathbf{E} = \frac{\rho}{\epsilon_0} \quad \text{or} \quad \oiint_S \bar{\mathbf{E}} \cdot d\mathbf{A} = \frac{Q_{\text{encl}}}{\epsilon_0}$$

- For slow time variations (dc, rf, but not microwaves)

$$\mathbf{E} \approx -\nabla\Phi$$

$\mathbf{E}$ = electric field (V/m), ρ = charge density (C/m^3), Φ = potential (V), $\epsilon_0 = 8.85 \times 10^{-12}$ F/m

- In 1D planar geometry

$$\boxed{\frac{dE_x}{dx} = \frac{\rho}{\epsilon_0}, \qquad \frac{d\Phi}{dx} = -E_x}$$

Combining these yields Poisson's equation

$$\boxed{\frac{d^2\Phi}{dx^2} = -\frac{\rho}{\epsilon_0}}$$

- This field powers a capacitive discharge or the wafer bias power of an inductive or ECR discharge

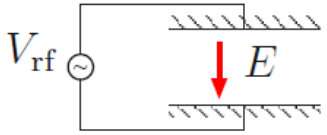

Source: https://people.eecs.berkeley.edu/~lieber/

FARADAY'S LAW

- An electric field can be generated by a time-varying magnetic field

$$\nabla \times \mathbf{E} = -\frac{\partial \mathbf{B}}{\partial t} \qquad \text{or} \qquad \oint_C \mathbf{E} \cdot d\mathbf{l} = -\frac{\partial}{\partial t} \iint_A \mathbf{B} \cdot d\mathbf{A}$$

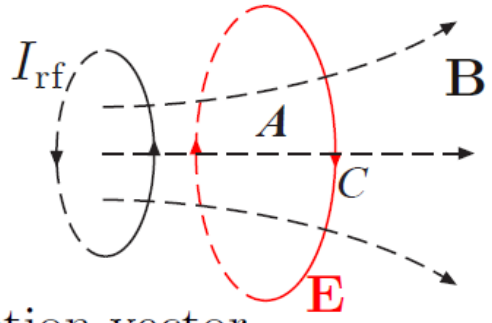

$\mathbf{B}$ = magnetic induction vector

- This field powers the coil of an inductive discharge (top power)

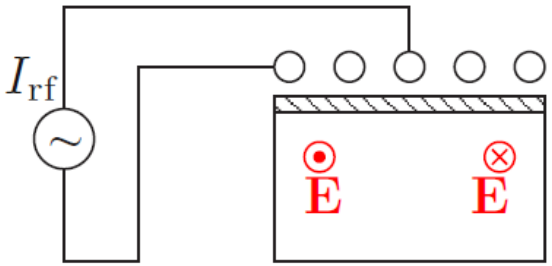

Source: https://people.eecs.berkeley.edu/~lieber/

AMPERE'S LAW

- Both conduction currents and displacement currents generate magnetic fields $\mathbf{H}$

$$\nabla \times \mathbf{H} = \mathbf{J}_c + \epsilon_0 \frac{\partial \mathbf{E}}{\partial t} = \mathbf{J} \qquad [\mathrm{A/m^2}]$$

$\mathbf{J}_c$ = conduction current density (physical motion of charges)
$\epsilon_0 \partial \mathbf{E}/\partial t$ = displacement current density (flows in vacuum)
$\mathbf{J}$ = total current density

- Note the vector identity $\nabla \cdot (\nabla \times \mathbf{H}) = 0 \;\Rightarrow\; \nabla \cdot \mathbf{J} = 0$
- In 1D

$$\boxed{\frac{\partial J(x,\,t)}{\partial x} = 0}$$

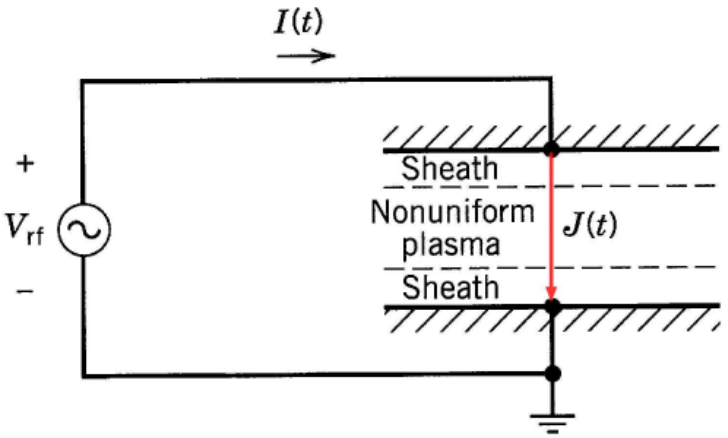

Total current J is independent of x

REVIEW OF PHASORS

- Physical voltage (or current), a real sinusoidal function of time

$$V(t) = V_0 \cos(\omega t + \phi)$$

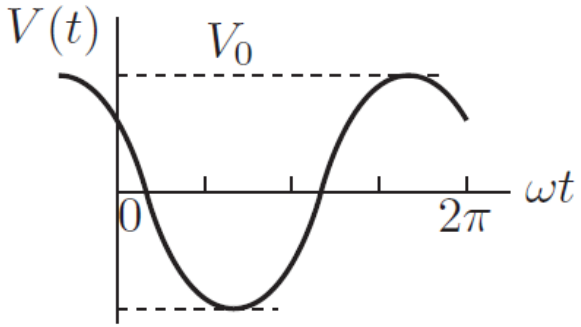

- Phasor voltage (or current), a complex number, independent of time

$$\widetilde{V} = V_0 \, e^{j\phi} = V_R + jV_I$$

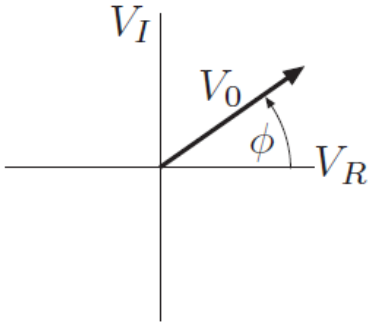

- Note that

$$\boxed{V(t) = \mathrm{Re}\left(\widetilde{V} \, e^{j\omega t}\right)}$$

- Hence

$$V(t) \Longleftrightarrow \widetilde{V} \qquad \text{(given } \omega\text{)}$$

Source: https://people.eecs.berkeley.edu/~lieber/

THERMAL EQUILIBRIUM PROPERTIES

- Electrons generally near thermal equilibrium
  Ions generally *not* in thermal equilibrium
- Maxwellian distribution of electrons

$$f_e(v) = n_e \left(\frac{m}{2\pi k T_e}\right)^{3/2} \exp\left(-\frac{m v^2}{2 k T_e}\right)$$

where $v^2 = v_x^2 + v_y^2 + v_z^2$

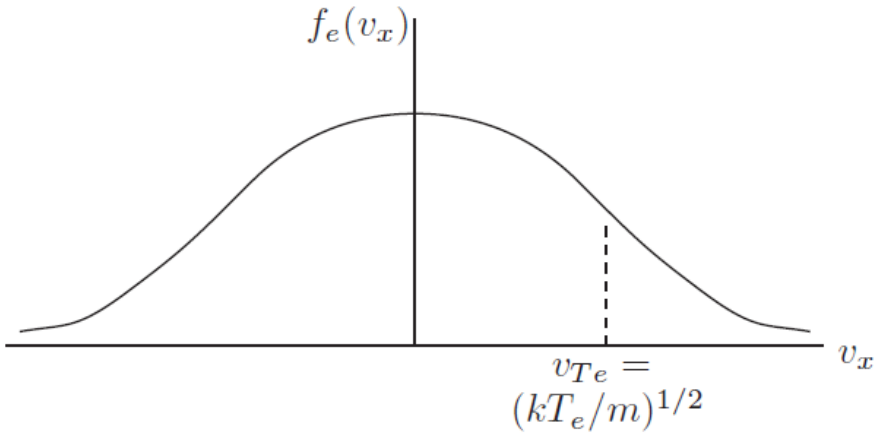

- Pressure $p = nkT$
  For neutral gas at room temperature (300 K)

$$\boxed{n_g(\text{cm}^{-3}) \approx 3.3 \times 10^{16}\, p(\text{Torr})}$$

Source: https://people.eecs.berkeley.edu/~lieber/

AVERAGES OVER MAXWELLIAN DISTRIBUTION

- Average energy

$$\left\langle \tfrac{1}{2}mv^2 \right\rangle = \frac{1}{n_e}\int d^3v \tfrac{1}{2}mv^2 f_e(v) = \tfrac{3}{2}kT_e$$

- Average speed

$$\boxed{\bar{v}_e = \left(\frac{8kT_e}{\pi m}\right)^{1/2}} \qquad \left(= \frac{1}{n_e}\int d^3v\, v f_e(v)\right)$$

- Average electron flux lost to a wall

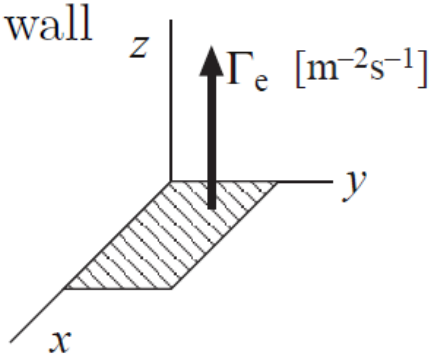

$$\boxed{\Gamma_e = \frac{1}{4}n_e\bar{v}_e} \quad \left(= \int_{-\infty}^{\infty}dv_x \int_{-\infty}^{\infty}dv_y \int_{0}^{\infty}dv_z v_z f_e(v)\right)$$

- Average kinetic energy lost per electron lost to a wall

$$\boxed{\mathcal{E}_e = 2\,\mathrm{T}_e}$$

FORCES ON PARTICLES

- For a unit volume of electrons (or ions)

$$mn_e \frac{d\mathbf{u}_e}{dt} = qn_e\mathbf{E} - \nabla p_e - mn_e\nu_m\mathbf{u}_e$$

mass × acceleration = electric field force +
+ pressure gradient force + friction (gas drag) force

- m = electron mass
  n_e = electron density
  $\mathbf{u}_e$ = electron flow velocity
  $q = -e$ for electrons ($+e$ for ions)
  $\mathbf{E}$ = electric field
  $p_e = n_e kT_e$ = electron pressure
  ν_m = collision frequency of electrons with neutrals [p. 36]

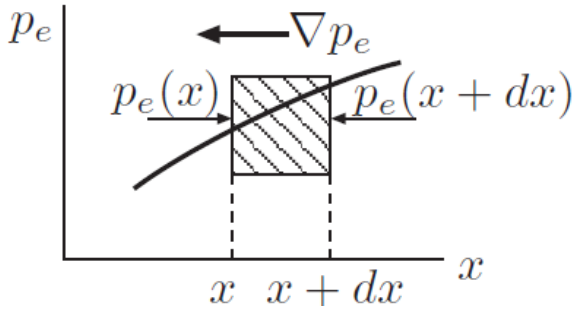

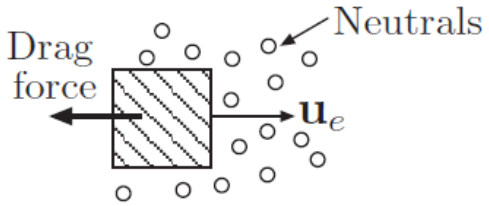

Source: https://people.eecs.berkeley.edu/~lieber/

BOLTZMANN FACTOR FOR ELECTRONS

- If electric field and pressure gradient forces almost balance

$$0 \approx -en_e\mathbf{E} - \nabla p_e$$

- Let $\mathbf{E} = -\nabla\Phi$ and $p_e = n_e kT_e$

$$\nabla\Phi = \frac{kT_e}{e}\frac{\nabla n_e}{n_e}$$

- Put $kT_e/e = \mathrm{T}_e$ (volts) and integrate to obtain

$$\boxed{n_e(\mathbf{r}) = n_{e0}\,\mathrm{e}^{\Phi(\mathbf{r})/\mathrm{T}_e}}$$

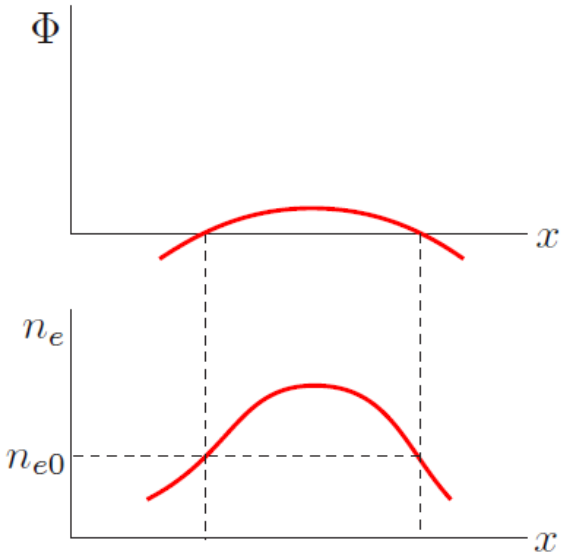

Source: https://people.eecs.berkeley.edu/~lieber/

UNDERSTANDING PLASMA BEHAVIOR

- The field equations and the force equations are coupled

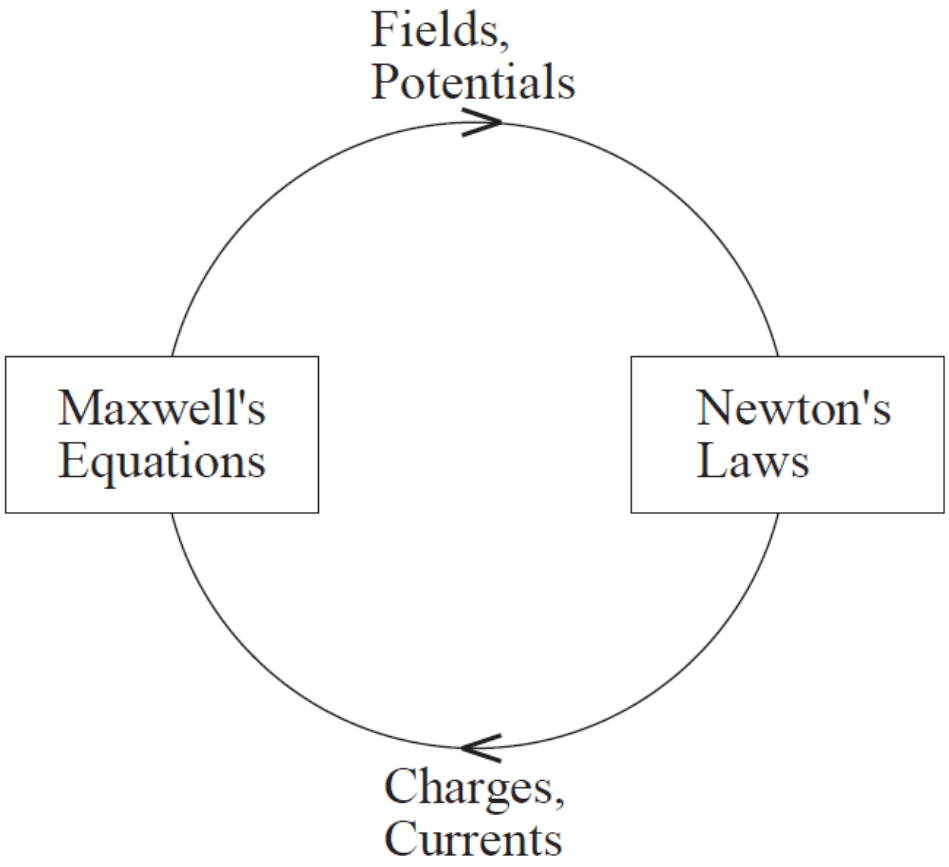

Source: https://people.eecs.berkeley.edu/~lieber/

DEBYE LENGTH λ_{De}

- The characteristic length scale of a plasma
- Low voltage sheaths ~ few Debye lengths thick
- Let's consider how a sheath forms near a wall
  Electrons leave plasma before ions and charge wall negative

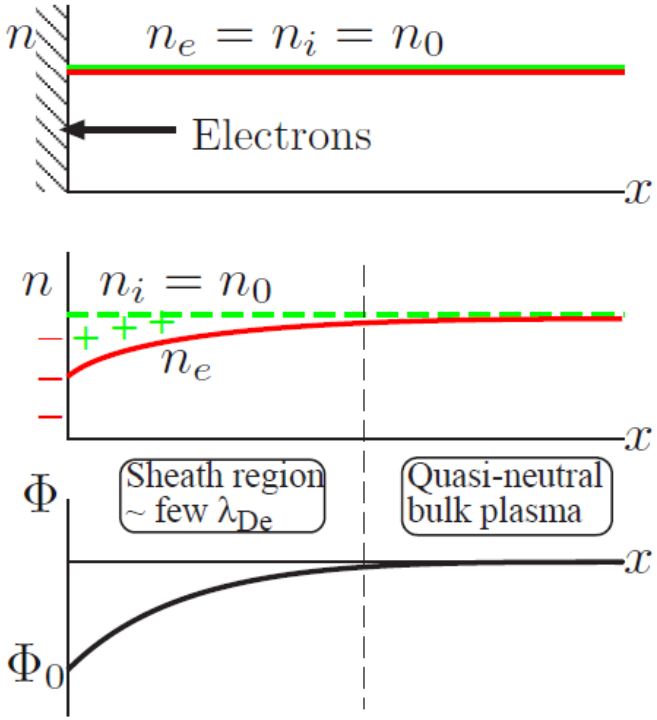

Assume electrons in thermal equilibrium and stationary ions

DEBYE LENGTH λ_{De} (CONT'D)

- Newton's laws [p. 18]

$$n_e(x) = n_0\, e^{\Phi/T_e}, \qquad n_i = n_0$$

- Use in Poisson's equation [p. 12]

$$\frac{d^2\Phi}{dx^2} = -\frac{en_0}{\epsilon_0}\left(1 - e^{\Phi/T_e}\right)$$

- Linearize $e^{\Phi/T_e} \approx 1 + \Phi/T_e$

$$\frac{d^2\Phi}{dx^2} = \frac{en_0}{\epsilon_0 T_e}\Phi$$

- Solution is

$$\Phi(x) = \Phi_0\, e^{-x/\lambda_{De}}, \qquad \boxed{\lambda_{De} = \left(\frac{\epsilon_0 T_e}{en_0}\right)^{1/2}}$$

- In practical units

$$\lambda_{De}(\text{cm}) = 740\sqrt{T_e/n_0}, \qquad T_e \text{ in volts, } n_0 \text{ in cm}^{-3}$$

- Example

  At $T_e = 1$ V and $n_0 = 10^{10}$ cm^{-3}, $\lambda_{De} = 7.4 \times 10^{-3}$ cm

  $\Longrightarrow$ Sheath is ~ 0.15 mm thick (Very thin!)

ELECTRON PLASMA FREQUENCY ω_{pe}

- The fundamental timescale for a plasma
- Consider a plasma slab (no walls). Displace all electrons to the right a small distance x_{e0}, and release them

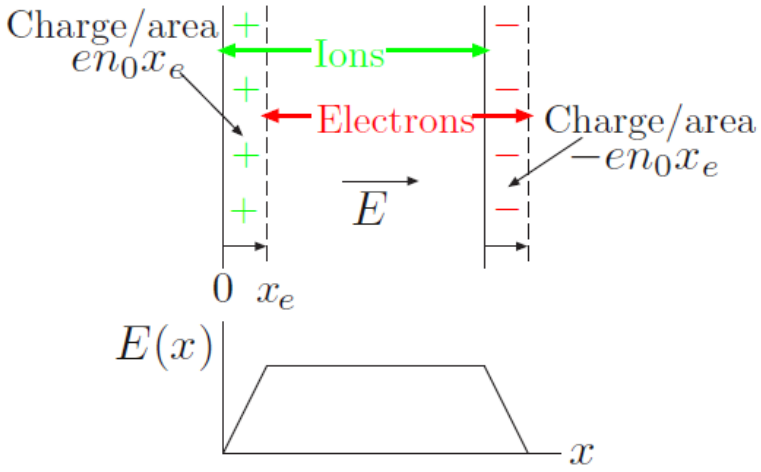

- Maxwell's equations (parallel plate capacitor) [p. 12]

$$E = \frac{en_0x_e(t)}{\epsilon_0}$$

ELECTRON PLASMA FREQUENCY ω_{pe} (CONT'D)

- Newton's laws (electron motion) [p. 18]

$$m\frac{d^2x_e(t)}{dt^2} = -eE = -\frac{e^2n_0}{\epsilon_0}x_e(t)$$

- Solution is electron plasma oscillations

$$x_e(t) = x_{e0}\cos\omega_{pe}t, \qquad \boxed{\omega_{pe} = \left(\frac{e^2n_0}{\epsilon_0 m}\right)^{1/2}}$$

- Practical formula is $f_{pe}(\text{Hz}) = 9000\sqrt{n_0}$, n_0 in cm^{-3}

$\Longrightarrow$ microwave frequencies ($\gtrsim$ 1 GHz) for typical plasmas

Source: https://people.eecs.berkeley.edu/~lieber/

1D SIMULATION OF SHEATH FORMATION

- Particle-in-cell (PIC) simulations with uniform fixed ion density; 4000 electron sheets; solve Newton's laws + Maxwell's equations
- $T_e = 1$ V (random), $n_e = n_i = 10^{13}$ m^{-3} (low), $l = 0.1$ m
- Electron v_x–x phase space at $t = 0.77$ μs

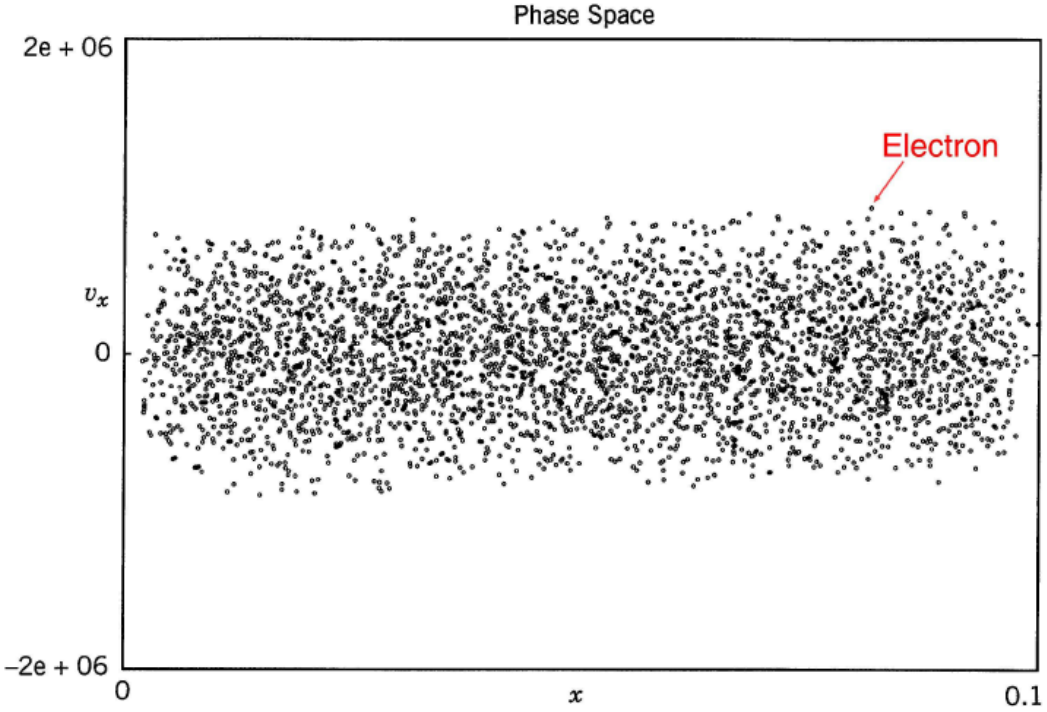

- Note absence of electron sheets near the walls

Source: https://people.eecs.berkeley.edu/~lieber/

1D SIMULATION OF SHEATH FORMATION (CONT'D)

- Electron number $\mathcal{N}$ versus t

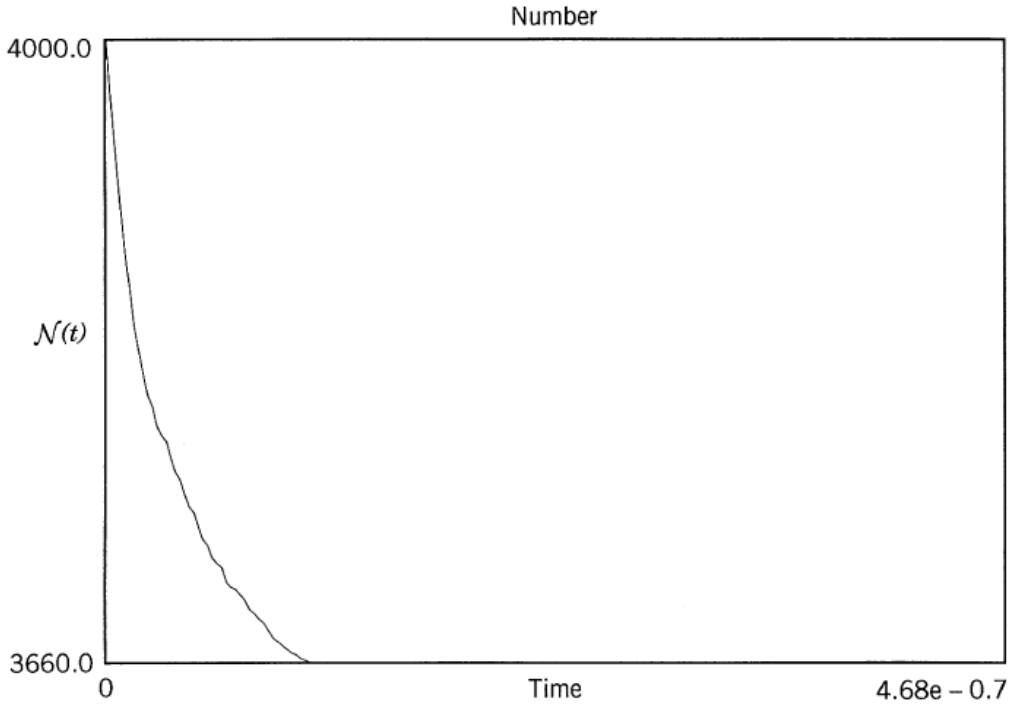

- Note 340 electron sheets lost to walls to form sheaths

Source: https://people.eecs.berkeley.edu/~lieber/

1D SIMULATION OF SHEATH FORMATION (CONT'D)

- Electron density $n_e(x)$ at $t = 0.77\ \mu$s

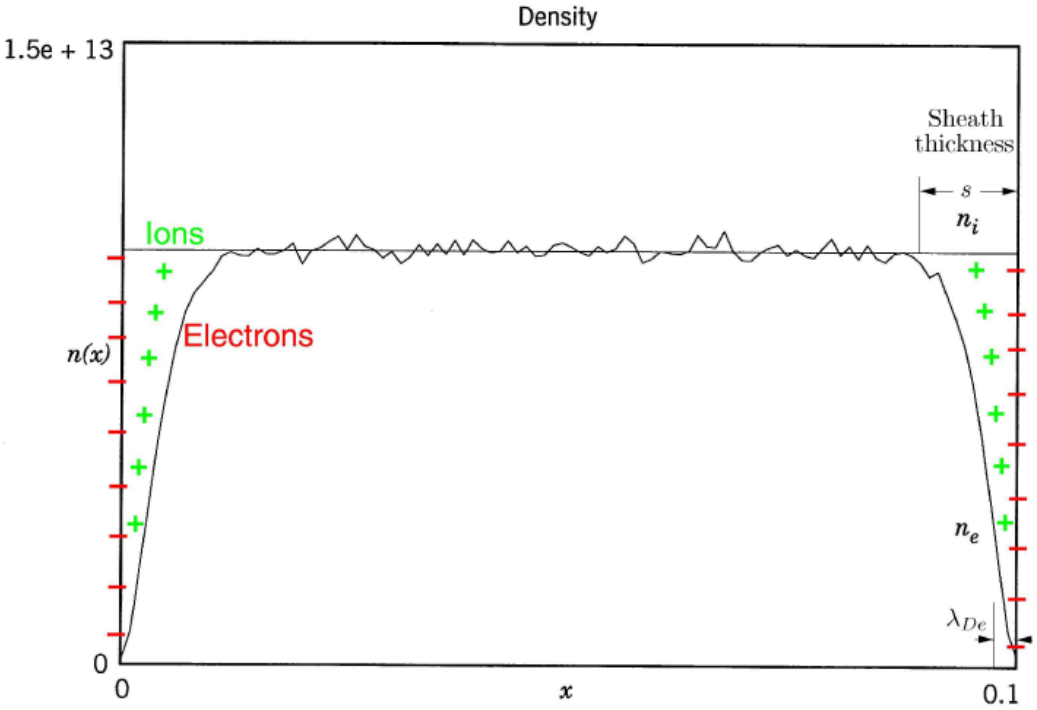

- Note sheath width is a few Debye lengths

Source: https://people.eecs.berkeley.edu/~lieber/

1D SIMULATION OF SHEATH FORMATION (CONT'D)

- Electric field $E(x)$ at $t = 0.77\ \mu$s

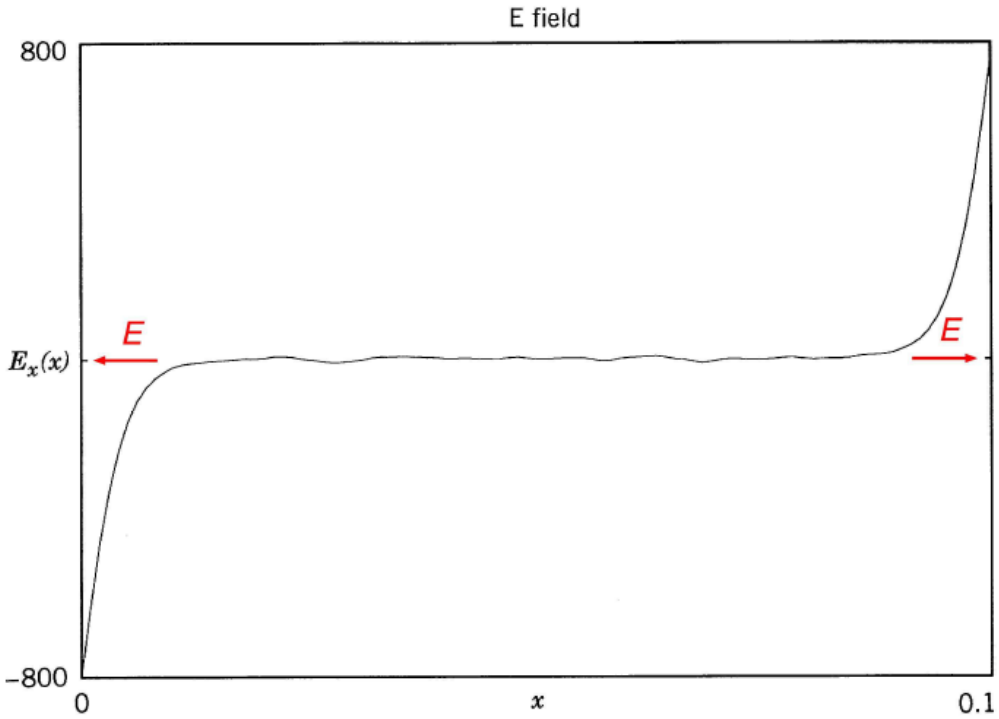

- Note electric field retards electrons, accelerates ion into walls

Source: https://people.eecs.berkeley.edu/~lieber/

1D SIMULATION OF SHEATH FORMATION (CONT'D)

- Potential $\Phi(x)$ at $t = 0.77\ \mu$s

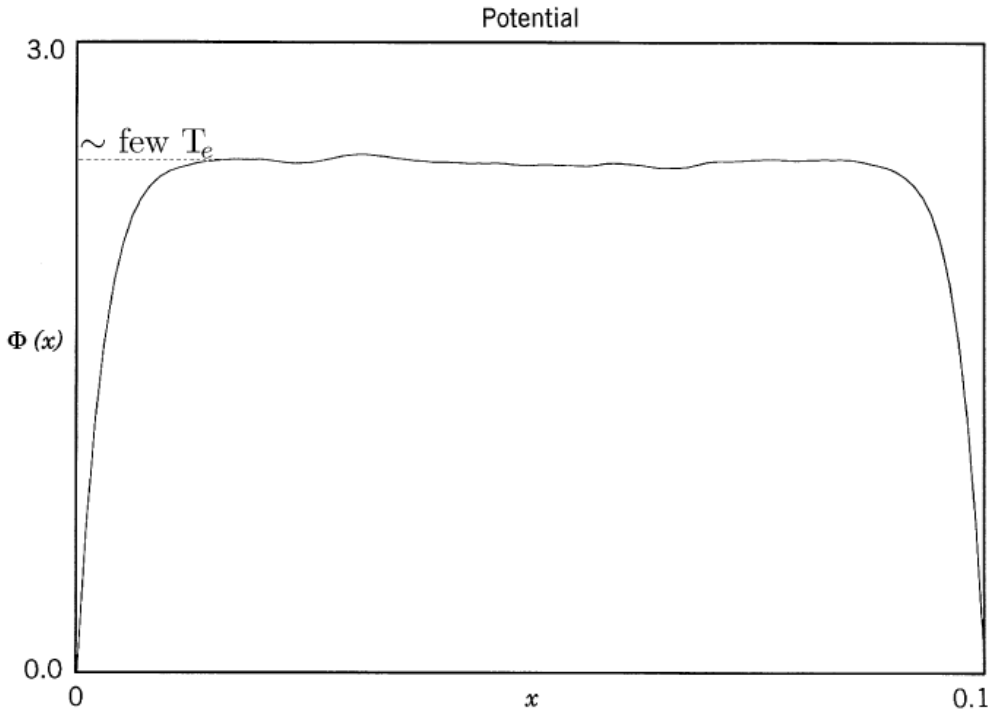

- Note plasma potential builds up to a few T_e with respect to wall

Source: https://people.eecs.berkeley.edu/~lieber/

1D SIMULATION OF SHEATH FORMATION (CONT'D)

- Right hand potential $\Phi(x = l)$ versus t

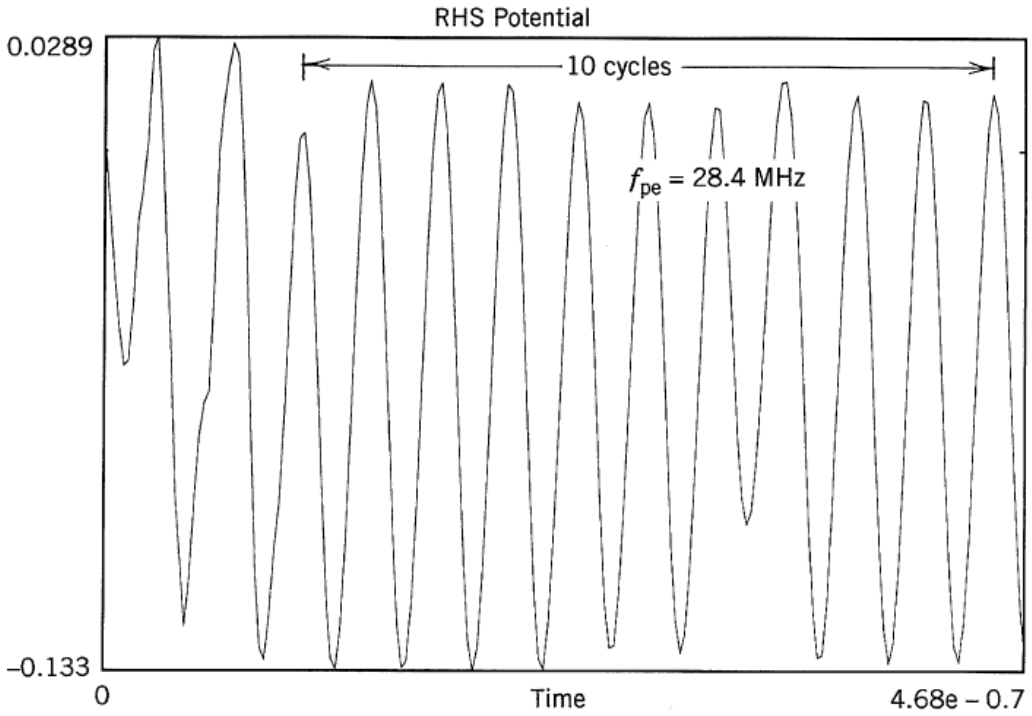

- Due to asymmetric electron initial conditions, a small oscillation of the right hand potential is excited at the plasma frequency

PLASMA DIELECTRIC CONSTANT ϵ_p

- RF discharges are driven at a frequency ω

$$E(t) = \mathrm{Re}\,(\widetilde{E}\,\mathrm{e}^{j\omega t}), \quad \text{etc. [p. 15]}$$

- Define ϵ_p from the total current in Maxwell's equations [p. 14]

$$\nabla \times \tilde{H} = \underbrace{\tilde{J}_c + j\omega\epsilon_0\widetilde{E}}_{\text{Total current } \tilde{J}} \equiv j\omega\epsilon_p\widetilde{E}$$

- Conduction current $\tilde{J}_c = -en_e\tilde{u}_e$ is due to electrons
- Newton's law (electric field and neutral drag) is [p. 18]

$$j\omega m\tilde{u}_e = -e\widetilde{E} - m\nu_m\tilde{u}_e$$

- Solve for $\tilde{u}_e$ and evaluate $\tilde{J}_c$ to obtain

$$\boxed{\epsilon_p \equiv \epsilon_0\kappa_p = \epsilon_0\left[1 - \frac{\omega_{pe}^2}{\omega(\omega - j\nu_m)}\right]}$$

with $\omega_{pe} = (e^2 n_e/\epsilon_0 m)^{1/2}$ the electron plasma frequency [p. 23]

- For $\omega \gg \nu_m$, ϵ_p is mainly real (nearly lossless dielectric)
  For $\nu_m \gg \omega$, ϵ_p is mainly imaginary (very lossy dielectric)

RF FIELDS IN LOW PRESSURE DISCHARGES

- Consider mainly lossless plasma ($\omega \gg \nu_m$)

$$\epsilon_p = \epsilon_0 \left(1 - \frac{\omega_{pe}^2}{\omega^2} \right)$$

- For rf discharges, $\omega_{pe} \gg \omega \Longrightarrow \epsilon_p$ is negative ($\epsilon_p = -1000\,\epsilon_0$)
- RF current density $\tilde{J}$ is continuous across the discharge [p. 14]

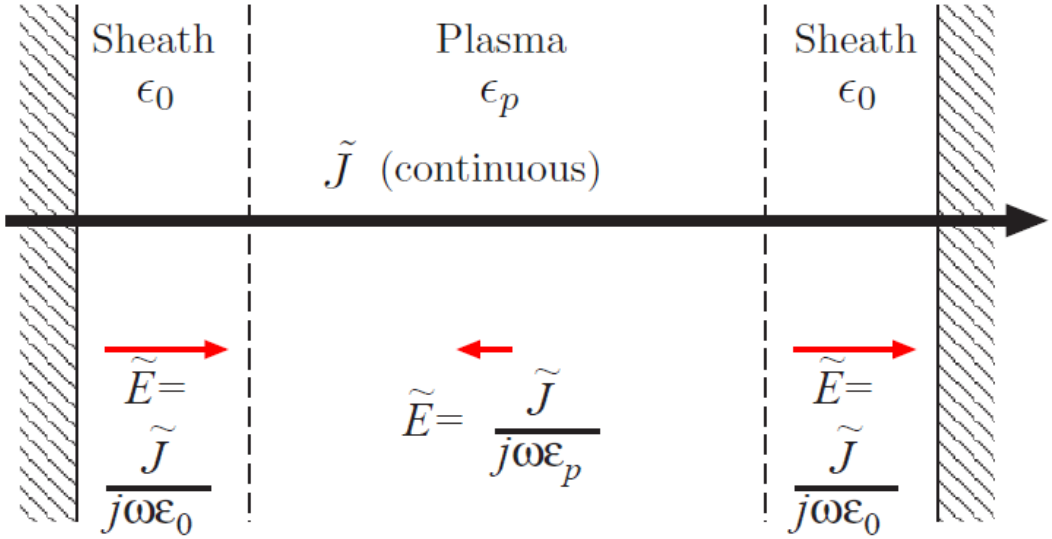

- Electric field in plasma is 1000 × smaller than in sheaths!
- Although field in plasma is small, it sustains the plasma!

Source: https://people.eecs.berkeley.edu/~lieber/

PLASMA CONDUCTIVITY σ_p

- It is useful to introduce rf plasma conductivity $\tilde{J}_c \equiv \sigma_p \tilde{E}$
- Find $\tilde{J}_c$ to be a linear function of $\tilde{E}$ [p. 31]

$$\sigma_p = \frac{e^2 n_e}{m(\nu_m + j\omega)}$$

- DC plasma conductivity ($\omega \ll \nu_m$)

$$\boxed{\sigma_{\rm dc} = \frac{e^2 n_e}{m\nu_m}}$$

- The plasma dielectric constant and conductivity are related by

$$j\omega\epsilon_p = \sigma_p + j\omega\epsilon_0$$

- RF current flowing through the plasma heats electrons (just like a resistor)

OHMIC HEATING POWER

- Time average power absorbed/volume

$$p_d = \langle \mathbf{J}(t) \cdot \mathbf{E}(t) \rangle = \frac{1}{2} \mathrm{Re}\,(\tilde{J} \cdot \tilde{E}^*) \qquad [\mathrm{W/m^3}]$$

Here $\tilde{E}^*$ = complex conjugate of $\tilde{E}$

- Since $\tilde{J}$ is the same everywhere in the discharge [p. 32], put $\tilde{E} = \tilde{J}/j\omega\epsilon_p$ to find p_d in terms of $\tilde{J}$ alone

- For discharges with $\omega \ll \omega_{pe}$ (all rf discharges)

$$p_d = \frac{1}{2}|\tilde{J}|^2 \frac{1}{\sigma_{\mathrm{dc}}} \qquad [\mathrm{W/m^3}]$$

ELECTRON COLLISIONS WITH ARGON

- Maxwellian electrons collide with Ar atoms (density n_g)

$$\frac{\#\text{ collisions of a particular kind}}{\text{s-m}^3} = \nu n_e = K n_g\, n_e$$

ν = collision frequency [s^{-1}], $K(T_e)$ = rate coefficient [m^3/s]

- Electron-Ar collision processes

$\text{e} + \text{Ar} \longrightarrow \text{Ar}^+ + 2\text{e}$ (ionization)

$\text{e} + \text{Ar} \longrightarrow \text{e} + \text{Ar}^* \longrightarrow \text{e} + \text{Ar} + \text{photon}$ (excitation)

$\text{e} + \text{Ar} \longrightarrow \text{e} + \text{Ar}$ (elastic scattering)

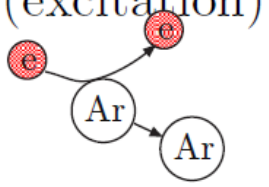

- Rate coefficient $K(T_e)$ is average of cross section $\sigma(v_R)$ [m^2] for process, over Maxwellian distribution

$$K(T_e) = \langle \sigma\, v_R \rangle_{\text{Maxwellian}}$$

v_R = relative velocity of colliding particles

Source: https://people.eecs.berkeley.edu/~lieber/

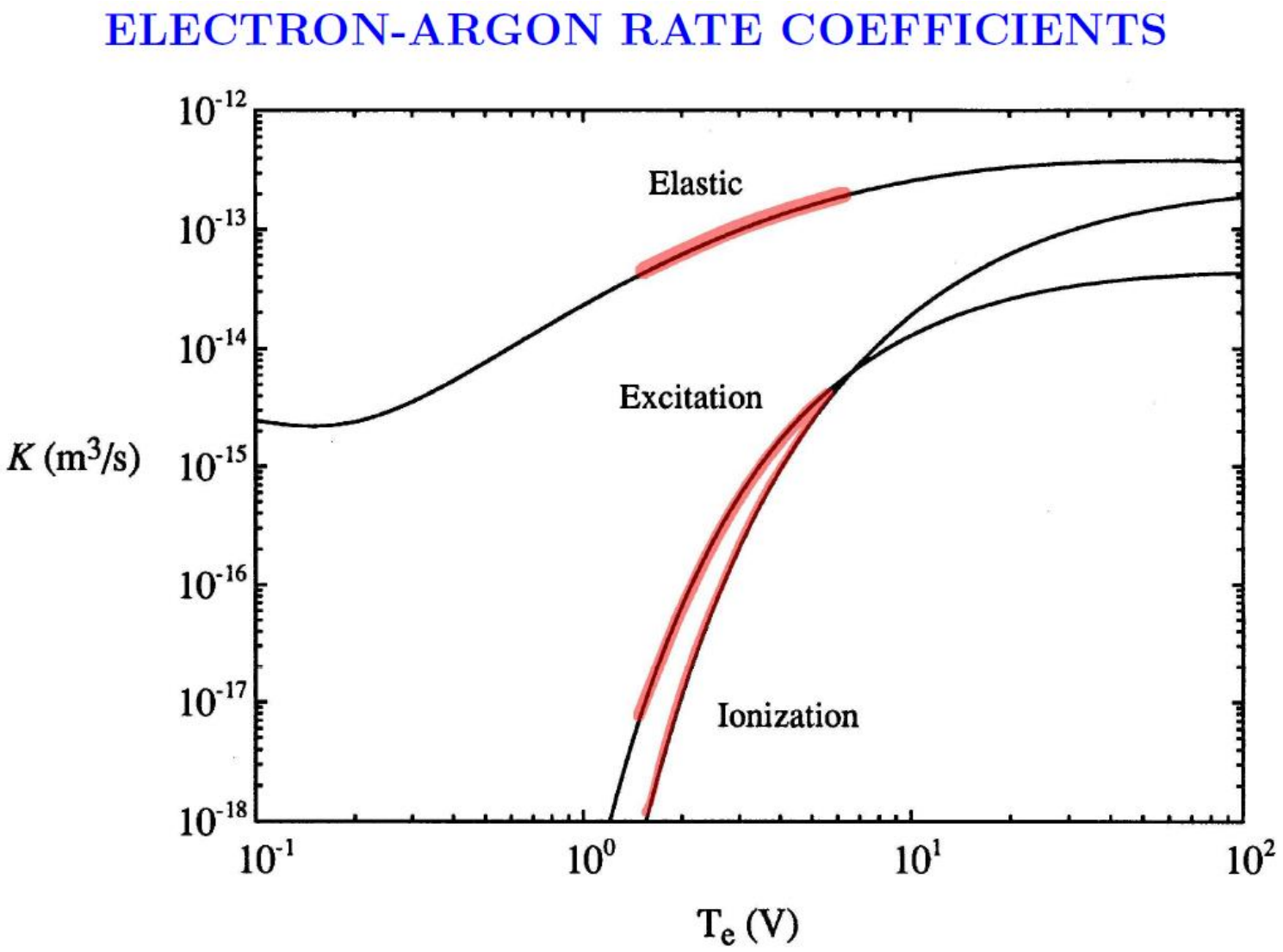

Source: https://people.eecs.berkeley.edu/~lieber/

ION COLLISIONS WITH ARGON

- Argon ions collide with Ar atoms

$$Ar^+ + Ar \longrightarrow Ar^+ + Ar \qquad \text{(elastic scattering)}$$
$$Ar^+ + Ar \longrightarrow Ar + Ar^+ \qquad \text{(charge transfer)}$$

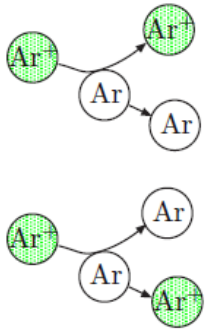

- Total cross section for room temperature ions $\sigma_i \approx 10^{-14}$ cm^2
- Ion-neutral mean free path (distance ion travels before colliding)

$$\boxed{\lambda_i = \frac{1}{n_g \sigma_i}}$$

- Practical formula

$$\boxed{\lambda_i(\text{cm}) = \frac{1}{330\,p}, \qquad p \text{ in Torr}}$$

- Ion-neutral collision frequency

$$\nu_i = \frac{\bar{v}_i}{\lambda_i}$$

with $\bar{v}_i = (8kT_i/\pi M)^{1/2}$

THREE ENERGY LOSS PROCESSES

1. Collisional energy $\mathcal{E}_c$ lost per electron-ion pair created

$$K_{\rm iz}\mathcal{E}_c = K_{\rm iz}\mathcal{E}_{\rm iz} + K_{\rm ex}\mathcal{E}_{\rm ex} + K_{\rm el}(2m/M)(3{\rm T}_e/2)$$

$$\Longrightarrow \mathcal{E}_c({\rm T}_e) \qquad \text{(voltage units)}$$

$\mathcal{E}_{\rm iz}$, $\mathcal{E}_{\rm ex}$, and $(3m/M){\rm T}_e$ are energies lost by an electron due to an ionization, excitation, and elastic scattering collision

2. Electron kinetic energy lost to walls [p. 17]

$$\mathcal{E}_e = 2\,{\rm T}_e$$

3. Ion kinetic energy lost to walls is mainly due to the dc potential $\bar{V}_s$ across the sheath

$$\mathcal{E}_i \approx \bar{V}_s$$

- Total energy lost per electron-ion pair lost to walls

$$\boxed{\mathcal{E}_T = \mathcal{E}_c + \mathcal{E}_e + \mathcal{E}_i}$$

Source: https://people.eecs.berkeley.edu/~lieber/

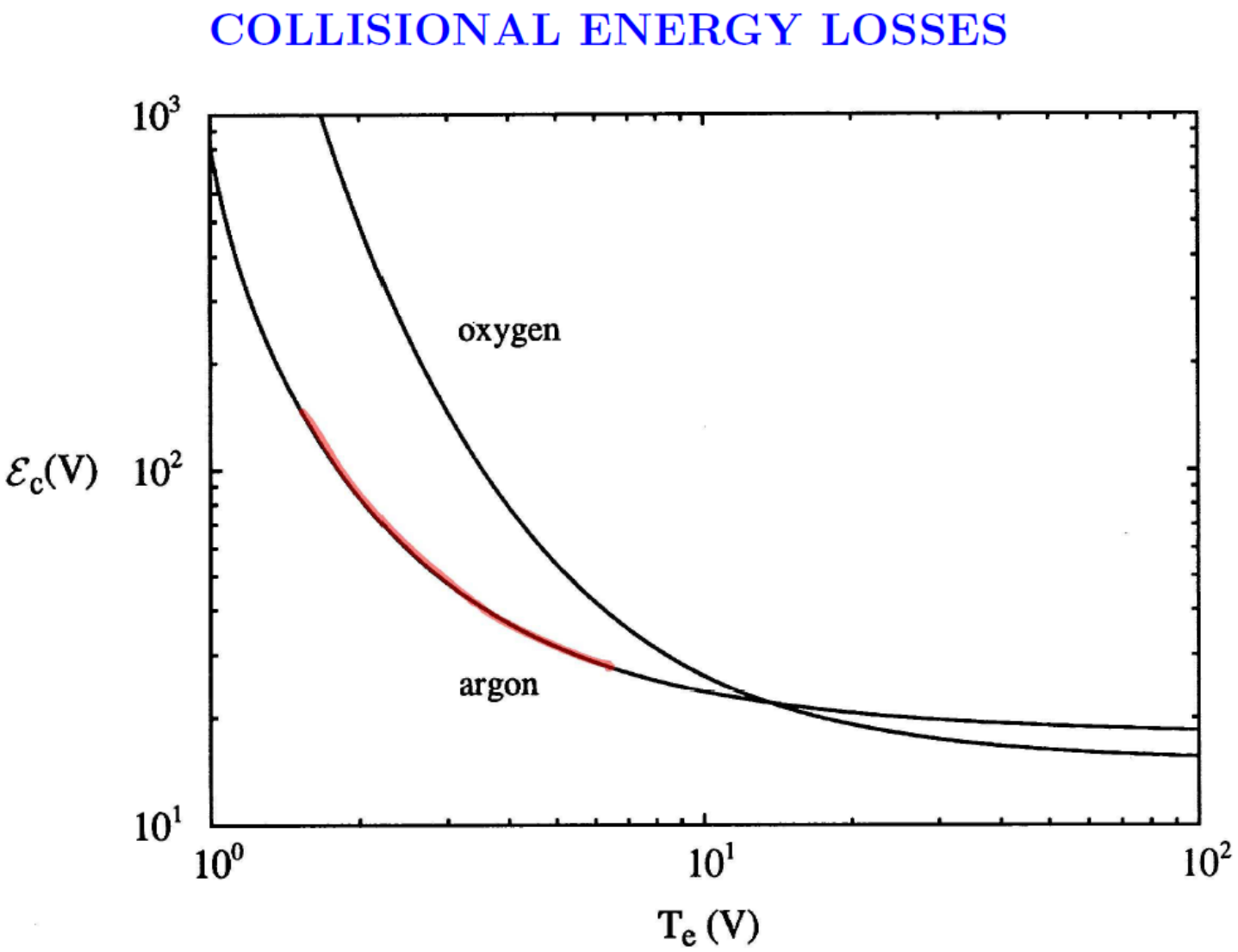

Source: https://people.eecs.berkeley.edu/~lieber/

BOHM (ION LOSS) VELOCITY u_B

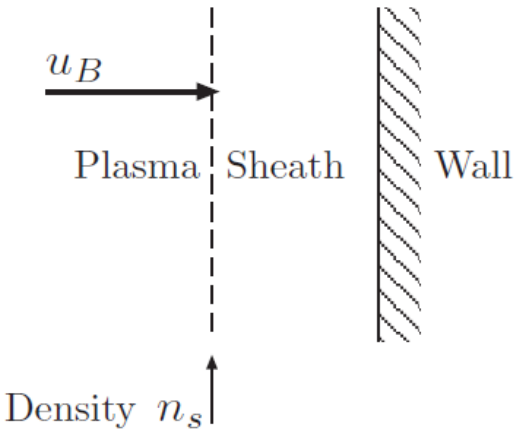

- Due to formation of a "presheath", ions arrive at the plasma-sheath edge with directed energy $kT_e/2$

$$\frac{1}{2}Mu_B^2 = \frac{kT_e}{2}$$

- Electron-ion pairs are lost at the Bohm velocity at the plasma-sheath edge (density n_s)

$$\Gamma_{\text{wall}} = n_s u_B, \qquad u_B = \left(\frac{kT_e}{M}\right)^{1/2}$$

Source: https://people.eecs.berkeley.edu/~lieber/

AMBIPOLAR DIFFUSION AT HIGH PRESSURES

- Plasma bulk is quasi-neutral ($n_e \approx n_i = n$) and the electron and ion loss fluxes are equal ($\Gamma_e \approx \Gamma_i \approx \Gamma$)
- Fick's law

$$\Gamma = -D_a \nabla n$$

with ambipolar diffusion coefficient $D_a = kT_e/M\nu_i$

- Density profile is sinusoidal

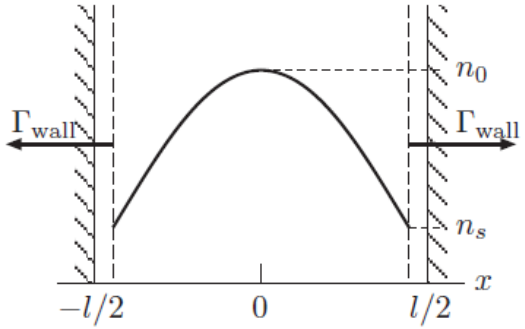

- Loss flux to the wall is

$$\Gamma_{\text{wall}} = n_s u_B \equiv h_l n_0 u_B$$

- From diffusion theory, edge-to-center density ratio is

$$h_l \equiv \frac{n_s}{n_0} = \frac{\pi}{l}\frac{u_B}{\nu_i}$$

- Applies for pressures $>$ 100 mTorr in argon

AMBIPOLAR DIFFUSION AT LOW PRESSURES

- The diffusion coefficient is not constant
- Density profile is relatively flat in the center and falls sharply near the sheath edge

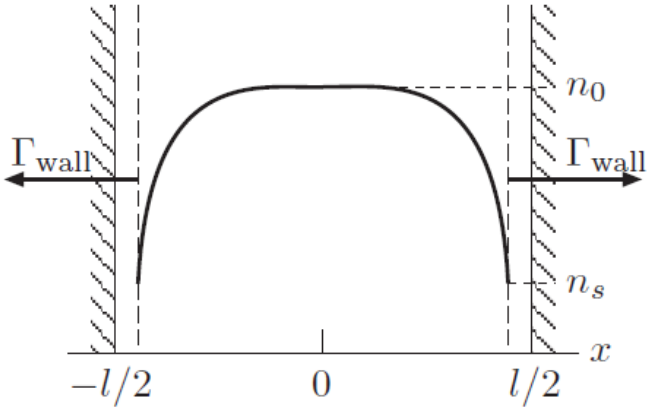

- The edge-to-center density ratio is

$$h_l \equiv \frac{n_s}{n_0} \approx \frac{0.86}{(3 + l/2\lambda_i)^{1/2}}$$

where λ_i = ion-neutral mean free path [p. 38]

- Applies for pressures < 100 mTorr in argon

AMBIPOLAR DIFFUSION IN LOW PRESSURE CYLINDRICAL DISCHARGE

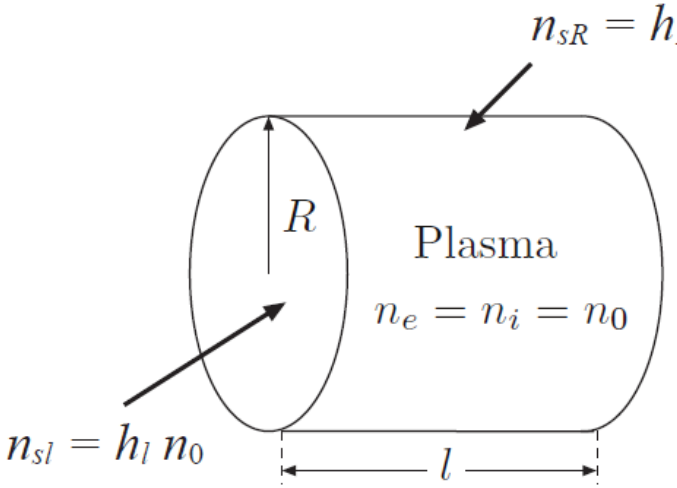

- For a cylindrical plasma of length l and radius R, loss fluxes to axial and radial walls are

$$\boxed{\Gamma_{\text{axial}} = h_l n_0 u_B, \qquad \Gamma_{\text{radial}} = h_R n_0 u_B}$$

  where the edge-to-center density ratios are

$$\boxed{h_l \approx \frac{0.86}{(3 + l/2\lambda_i)^{1/2}}, \qquad h_R \approx \frac{0.8}{(4 + R/\lambda_i)^{1/2}}}$$

- Applies for pressures < 100 mTorr in argon

PARTICLE BALANCE AND T_e

- Assume uniform cylindrical plasma absorbing power P_{abs}

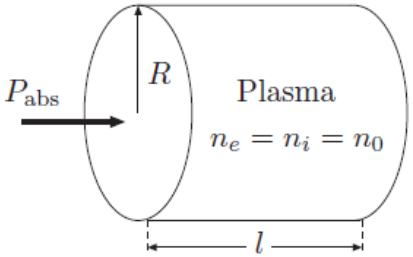

- Particle balance

Production due to ionization = loss to the walls

$$K_{\text{iz}} n_g \cancel{n_0} \pi R^2 l = (2\pi R^2 h_l \cancel{n_0} + 2\pi R l h_R \cancel{n_0}) u_B$$

- Solve to obtain

$$\frac{K_{\text{iz}}(T_e)}{u_B(T_e)} = \frac{1}{n_g d_{\text{eff}}}$$

where

$$d_{\text{eff}} = \frac{1}{2} \frac{Rl}{Rh_l + lh_R}$$

is an effective plasma size

- Given n_g and $d_{\text{eff}} \Longrightarrow$ electron temperature T_e
- T_e varies over a narrow range of 2–5 volts

Source: https://people.eecs.berkeley.edu/~lieber/

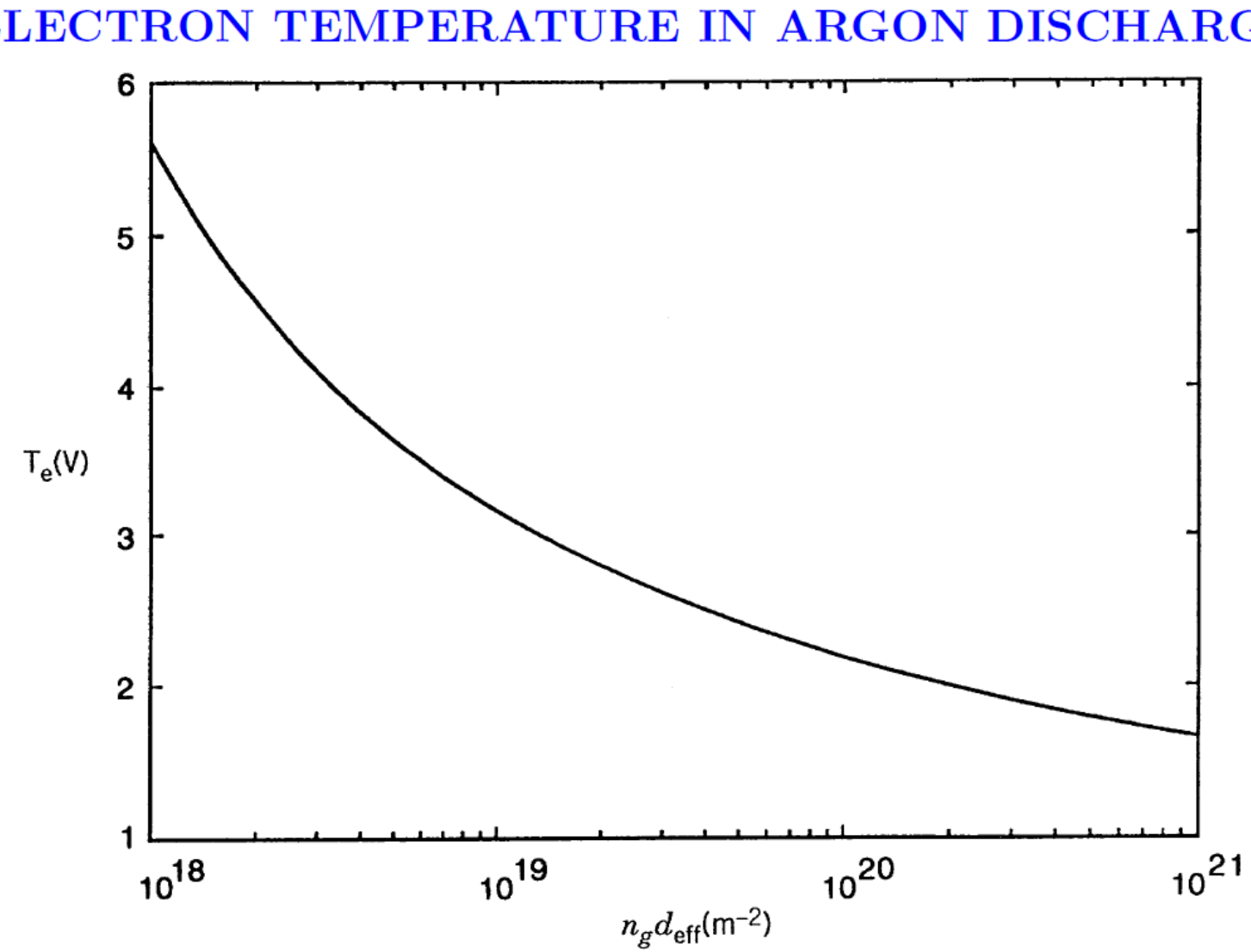

ION ENERGY FOR LOW VOLTAGE SHEATHS

- $\mathcal{E}_i$ = energy entering sheath + energy gained traversing sheath
- Ion energy entering sheath = $T_e/2$ (voltage units) [p. 41]
- Sheath voltage determined from particle conservation

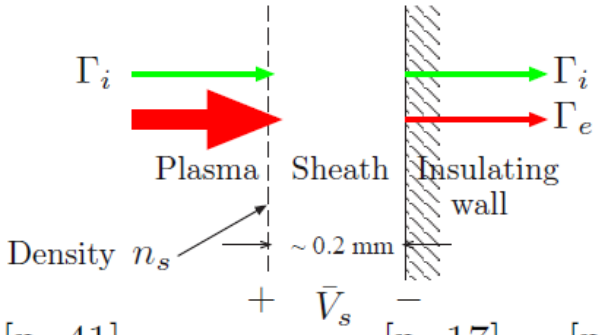

[p. 41] [p. 17] [p. 19]

$$\Gamma_i = n_s u_B, \qquad \Gamma_e = \underbrace{\tfrac{1}{4} n_s \bar{v}_e}_{\text{Random flux at sheath edge}} \, e^{-\overline{V}_s/T_e}$$

with $\bar{v}_e = (8eT_e/\pi m)^{1/2}$

- The ion and electron fluxes at the wall must balance

$$\boxed{\overline{V}_s = \frac{T_e}{2} \ln\left(\frac{M}{2\pi m}\right)}$$

or $\overline{V}_s \approx 4.7\, T_e$ for argon

- Accounting for the initial ion energy, $\mathcal{E}_i \approx 5.2\, T_e$

Source: https://people.eecs.berkeley.edu/~lieber/

ION ENERGY FOR HIGH VOLTAGE SHEATHS

- Large ion bombarding energies can be gained near rf-driven electrodes embedded in the plasma

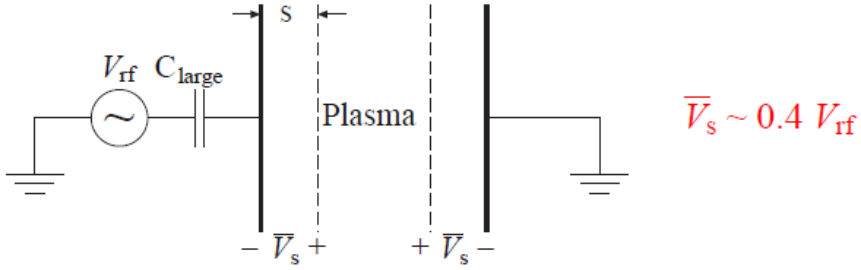

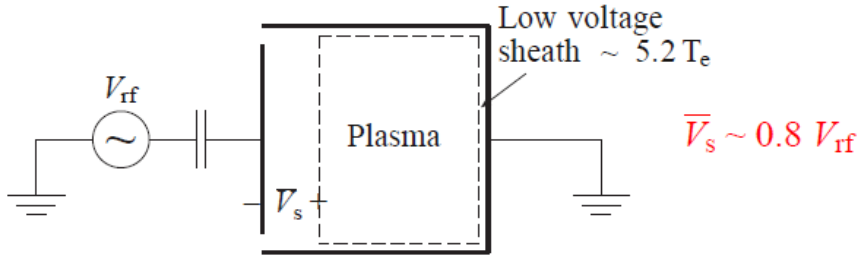

- The sheath thickness s (~ 0.5 cm) is given by the Child Law

$$\bar{J}_i = e n_s u_B = \frac{4}{9}\epsilon_0 \left(\frac{2e}{M}\right)^{1/2} \frac{\overline{V}_s^{3/2}}{s^2}$$

- Estimating ion energy is not simple as it depends on the type of discharge and the application of bias voltages

POWER BALANCE AND n_0

- Assume low voltage sheaths at all surfaces

$$\mathcal{E}_T(T_e) = \underbrace{\mathcal{E}_c(T_e)}_{\text{Collisional}} + \underbrace{2\,T_e}_{\text{Electron}} + \underbrace{5.2\,T_e}_{\text{Ion}} \qquad [\text{V}]$$

[p. 40] [p. 17] [p. 48]

- Power balance

Power in = power out

$$\boxed{P_{\text{abs}} = (h_l n_0 2\pi R^2 + h_R n_0 2\pi R l)\, u_B\, e\mathcal{E}_T} \qquad [\text{W}]$$

- Solve to obtain

$$\boxed{n_0 = \frac{P_{\text{abs}}}{A_{\text{eff}} u_B e \mathcal{E}_T}}$$

where

$$A_{\text{eff}} = 2\pi R^2 h_l + 2\pi R l h_R$$

is an effective area for particle loss

- Density n_0 is proportional to the absorbed power P_{abs}
- Density n_0 depends on pressure p through h_l, h_R, and T_e

Source: https://people.eecs.berkeley.edu/~lieber/

PARTICLE AND POWER BALANCE

- Particle balance $\Longrightarrow$ electron temperature T_e
  (independent of plasma density)

- Power balance $\Longrightarrow$ plasma density n_0
  (once electron temperature T_e is known)

Source: https://people.eecs.berkeley.edu/~lieber/

EXAMPLE 1

- Let $R = 0.15$ m, $l = 0.3$ m, $n_g = 3.3 \times 10^{19}$ m^{-3} ($p = 1$ mTorr at 300 K), and $P_{\text{abs}} = 800$ W
- Assume low voltage sheaths at all surfaces
- Find $\lambda_i = 0.03$ m [p. 38]. Then $h_l \approx h_R \approx 0.3$ [p. 44] and $d_{\text{eff}} \approx 0.17$ m [p. 46]
- T_e versus $n_g d_{\text{eff}}$ figure gives $\mathrm{T}_e \approx 3.5$ V [p. 47]
- $\mathcal{E}_c$ versus T_e figure gives $\mathcal{E}_c \approx 42$ V [p. 40]. Adding $\mathcal{E}_e = 2\mathrm{T}_e \approx 7$ V and $\mathcal{E}_i \approx 5.2\mathrm{T}_e \approx 18$ V yields $\mathcal{E}_T = 67$ V [p. 39]
- Find $u_B \approx 2.9 \times 10^3$ m/s [p. 41] and find $A_{\text{eff}} \approx 0.13$ m^2 [p. 50]
- Power balance yields $n_0 \approx 2.0 \times 10^{17}$ m^{-3} [p. 50]
- Ion current density $J_{il} = e h_l n_0 u_B \approx 2.9$ mA/cm^2 [p. 46]
- Ion bombarding energy $\mathcal{E}_i \approx 18$ V [p. 48]

Source: https://people.eecs.berkeley.edu/~lieber/

EXAMPLE 2

- Apply a strong dc magnetic field along the cylinder axis
  $\Longrightarrow$ particle loss to radial wall is inhibited
- Assume no radial losses, then $d_{\text{eff}} = l/2h_l \approx 0.5$ m
- From the T_e versus $n_g d_{\text{eff}}$ figure, $T_e \approx 3.3$ V (was 3.5 V)
- From the $\mathcal{E}_c$ versus T_e figure, $\mathcal{E}_c \approx 46$ V. Adding $\mathcal{E}_e = 2T_e \approx 6.6$ V and $\mathcal{E}_i \approx 5.2T_e \approx 17$ V yields $\mathcal{E}_T = 70$ V
- Find $u_B \approx 2.8 \times 10^3$ m/s and find $A_{\text{eff}} = 2\pi R^2 h_l \approx 0.043$ m^2
- Power balance yields $n_0 \approx 5.8 \times 10^{17}$ m^{-3} (was 2×10^{17} m^{-3})
- Ion current density $J_{il} = eh_l n_0 u_B \approx 7.8$ mA/cm^2
- Ion bombarding energy $\mathcal{E}_i \approx 17$ V

  $\Longrightarrow$ Slight decrease in electron temperature T_e

  $\Longrightarrow$ Significant increase in plasma density n_0

EXPLAIN WHY!

- What happens to T_e and n_0 if there is a sheath voltage $V_s = 500$ V at each end plate?

Source: https://people.eecs.berkeley.edu/~lieber/

CAPACITIVE RF DISCHARGES

SYMMETRIC HOMOGENEOUS MODEL

Source: https://people.eecs.berkeley.edu/~lieber/

BASIC PROPERTIES

- Simplicity of concept
- RF rather than microwave powered
- Inherent high sheath voltages
- No independent control of plasma density and ion energy
- Control parameters

  RF current $\tilde{I}_{\rm rf}$ (1–10 mA/cm^2)
  Driving frequency ω (2–13.56 MHz)
  Neutral gas density n_g (10^{14}–10^{16} cm^{-3})
  Electrode separation l (1–10 cm)
- Discharge parameters to find

  Plasma density n (10^9–10^{10} cm^{-3})
  Electron temperature T_e (2–4 V)
  Discharge voltage $V_{\rm rf}$ (100–1000 V)
  Discharge power $P_{\rm rf}$ (50–500 W)
  Ion bombarding energy $\mathcal{E}_i$ (50–500 V)

Source: https://people.eecs.berkeley.edu/~lieber/

CONFIGURATIONS

- Multi-wafer parallel plate and "hex" configurations (1980's)

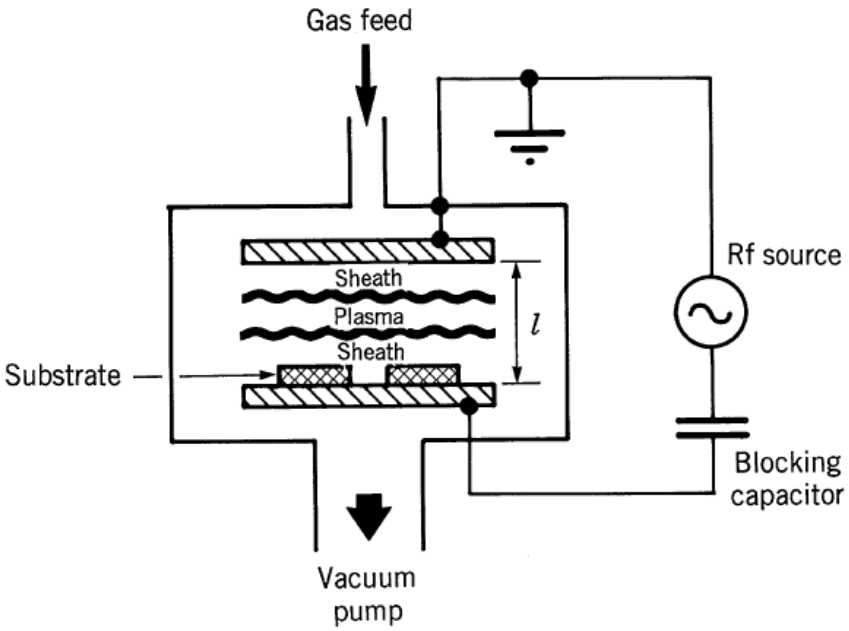

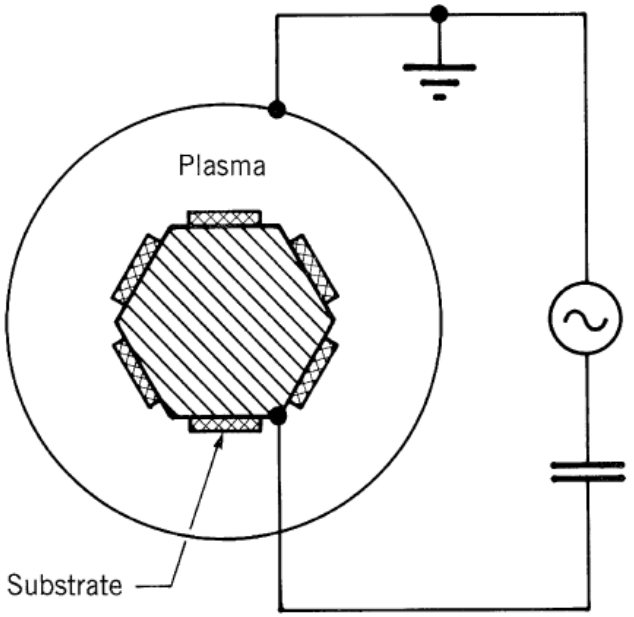

- Modern configurations are single wafer parallel plate, sometimes driven at multiple rf frequencies

Source: https://people.eecs.berkeley.edu/~lieber/

CURRENT-DRIVEN HOMOGENEOUS MODEL

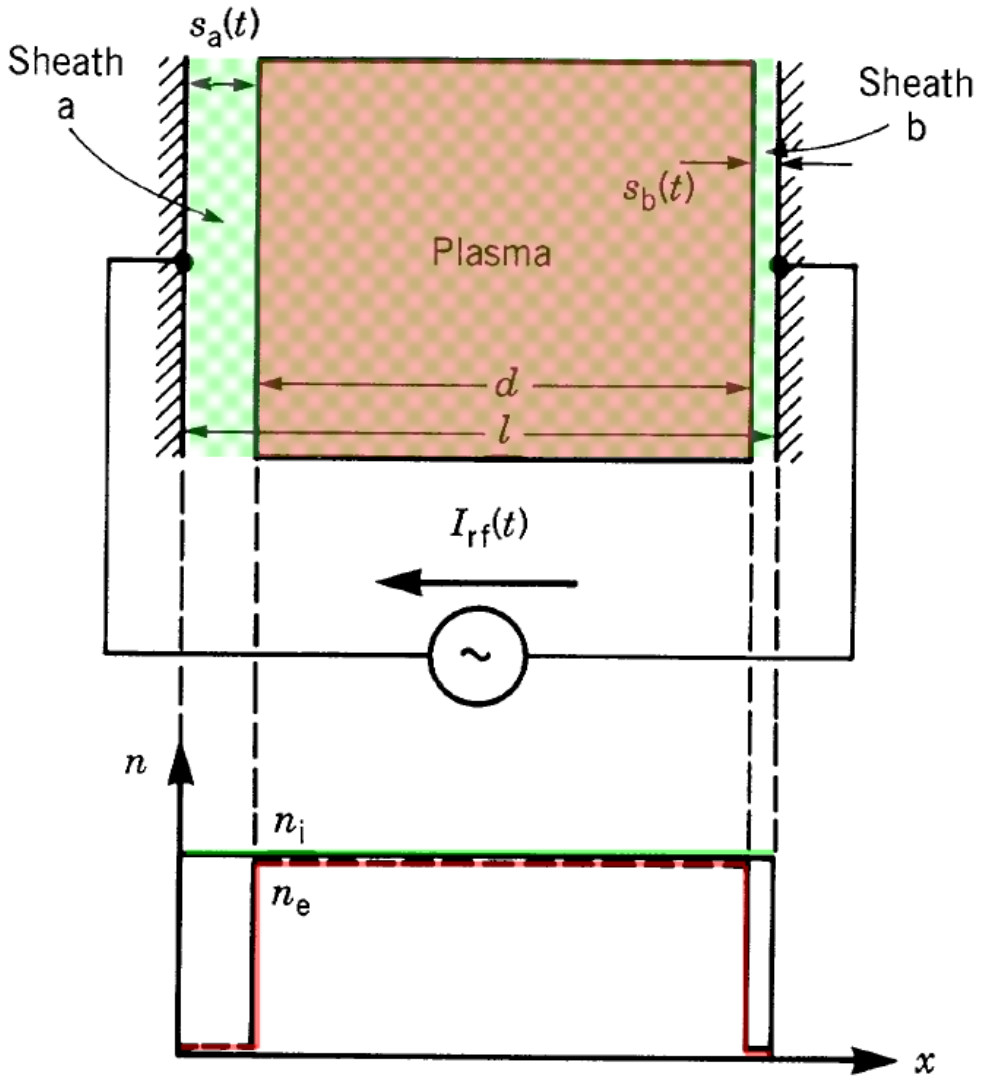

Source: https://people.eecs.berkeley.edu/~lieber/

HOMOGENEOUS MODEL ASSUMPTIONS

- No transverse variations (along the electrodes)
- Electrons respond to instantaneous electric fields
- Ions respond to only time-average electric fields
- Electron density is zero in the sheath regions
- Ion density is constant in the plasma and sheath regions

  $$n_i(z) = n_0$$

  (We will correct this later)

Source: https://people.eecs.berkeley.edu/~lieber/

ELECTRON SHEATH EDGE MOTION

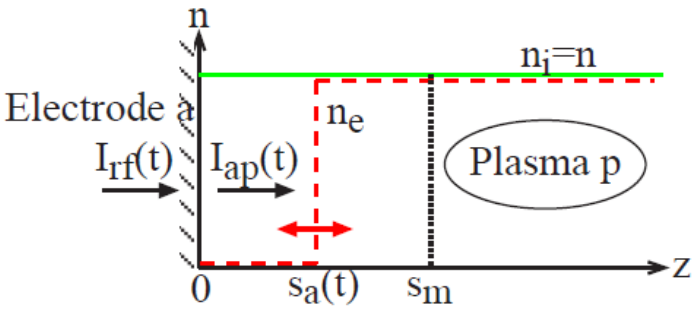

- The electric field is found by integrating the charge density in the sheath [p. 12]

$$\frac{dE}{dz} = \frac{en}{\epsilon_0}, \qquad z < s_a(t)$$

to obtain

$$E(z,t) = \frac{en}{\epsilon_0}\big(z - s_a(t)\big)$$

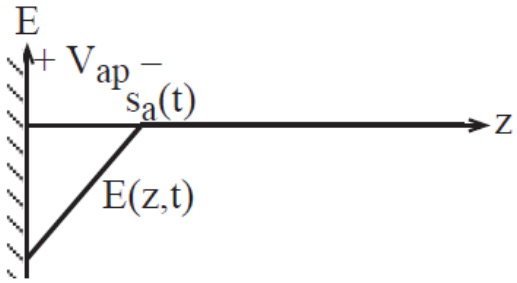

ELECTRON SHEATH EDGE MOTION (CONT'D)

- The displacement current in the sheath is [p. 14]

$$I_{ap} = \epsilon_0 A \frac{\partial E}{\partial t} = -enA \frac{ds_a}{dt}$$

- Let $I_{\rm rf}(t) = \tilde{I}_0 \cos \omega t$ and integrate to obtain

$$s_a(t) = \bar{s}_0 - \tilde{s}_0 \sin \omega t$$

$$\boxed{\tilde{s}_0 = \frac{\tilde{I}_0}{en\omega A}}$$

- The oscillation amplitude of the sheath motion is $\tilde{s}_0$, but what is the "constant of integration" $\bar{s}_0$?

CONDUCTION CURRENT

- Assume a steady loss of ions to electrode a

$$I_i = enu_B A$$

- The time-average total conduction current to the electrode is zero
- Hence electrons must be lost to the electrode
- The sheath thickness $s_a(t)$ must then collapse to zero at some time during the rf cycle $\Longrightarrow \bar{s}_0 = \tilde{s}_0$

$$\boxed{s_a(t) = \tilde{s}_0(1 - \sin\omega t)}$$

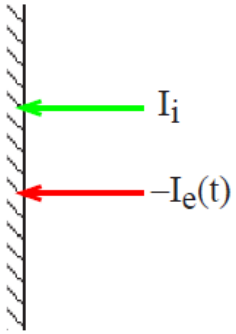

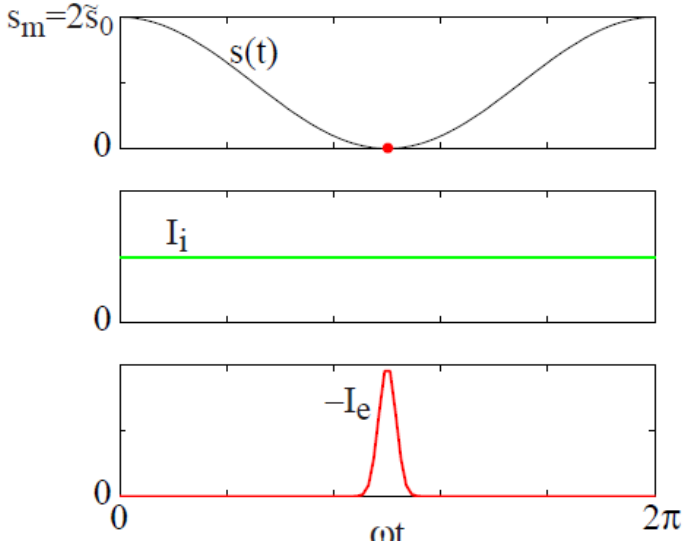

Source: https://people.eecs.berkeley.edu/~lieber/

VOLTAGE ACROSS THE SHEATH

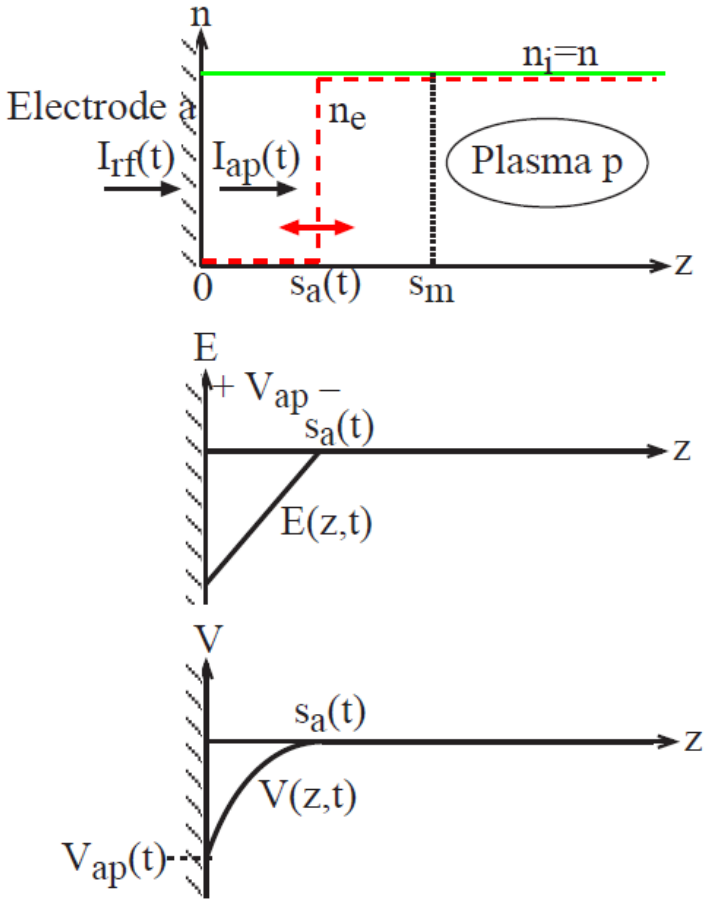

The voltage is found by integrating the electric field in the sheath

$$\frac{dV}{dz} = -E$$

VOLTAGE ACROSS THE SHEATH (CONT'D)

- Integrating the electric field in the sheath [p. 12]

$$\frac{dV}{dz} = -E$$

we obtain

$$V_{ap}(t) = \int_0^{s_a(t)} E(z,t)\, dz = -\frac{en}{\epsilon_0}\frac{s_a^2(t)}{2}$$

- Using $s_a(t)$ [p. 61]

$$\boxed{V_{ap}(t) = -\frac{en}{2\epsilon_0}\tilde{s}_0^2\left(1-\sin\omega t\right)^2}$$

- $V_{ap}(t)$ is a nonlinear function of $I_{\rm rf}$; there are second harmonics

VOLTAGE ACROSS BOTH SHEATHS

- By symmetry $s_b(t) = \tilde{s}_0(1 + \sin\omega t)$; since $s_a(t) = \tilde{s}_0(1 - \sin\omega t)$

$$\boxed{s_a(t) + s_b(t) = 2\,\tilde{s}_0 = \text{const}}$$

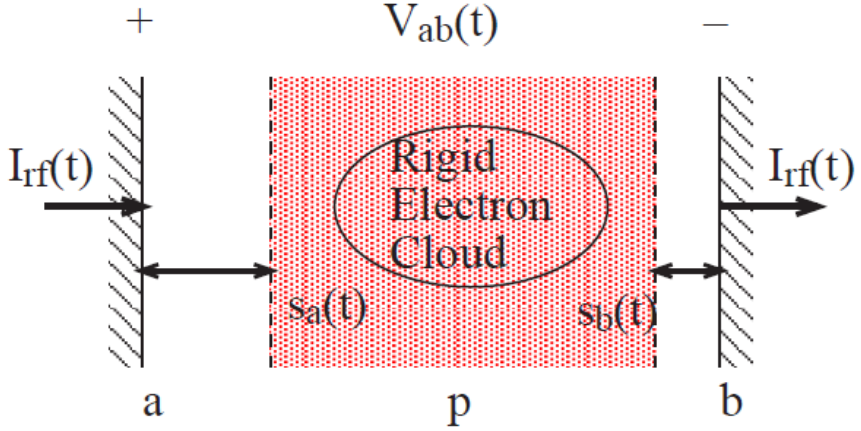

- There is a rigid bulk electron cloud oscillation

VOLTAGE ACROSS BOTH SHEATHS (CONT'D)

- Voltage across sheath b is

$$V_{bp}(t) = -\frac{en}{2\epsilon_0}\tilde{s}_0^2\left(1+\sin\omega t\right)^2$$

- Voltage across the plasma is small because $I_{\rm rf} = j\omega\epsilon_p EA$ and ϵ_p is large $\Longrightarrow$ E across bulk plasma is small
- Discharge voltage is $V_{\rm rf} = V_{ap} + V_{pb}$

$$\boxed{V_{\rm rf}(t) = \frac{2en\tilde{s}_0^2}{\epsilon_0}\sin\omega t}$$

- Each sheath is nonlinear, but the combination of both sheaths is linear

Source: https://people.eecs.berkeley.edu/~lieber/

DC VOLTAGE ACROSS ONE SHEATH

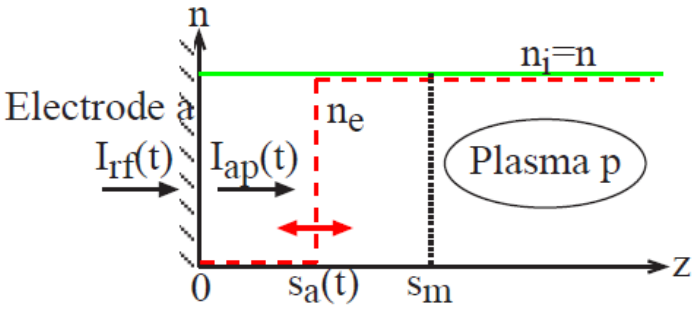

$$V_{pa}(t) = \frac{en}{2\epsilon_0}\tilde{s}_0^2\left(1 - 2\sin\omega t + \sin^2\omega t\right)$$

- Take time average

$$\overline{V}_s = \frac{3}{4}\frac{en}{\epsilon_0}\tilde{s}_0^2 = \mathcal{E}_i$$

- Compare to rf voltage across discharge [p. 65]

$$\Longrightarrow \overline{V}_s = \frac{3}{8}\widetilde{V}_{\rm rf}$$

- We can think of $\widetilde{V}_{\rm rf}$ as divided equally across the two sheaths

$$\boxed{\overline{V}_s = \frac{3}{4}\widetilde{V}_s \qquad \text{with} \qquad \widetilde{V}_s = \frac{1}{2}V_{\rm rf}}$$

Source: https://people.eecs.berkeley.edu/~lieber/

SHEATH VOLTAGES VERSUS TIME

Sheath voltages $V_{ap}(t)$, $V_{pb}(t)$, and their sum $V_{ab}(t) = V_{\mathrm{rf}}(t)$; the time average $\overline{V}_s$ of $V_{pb}(t)$ is also shown

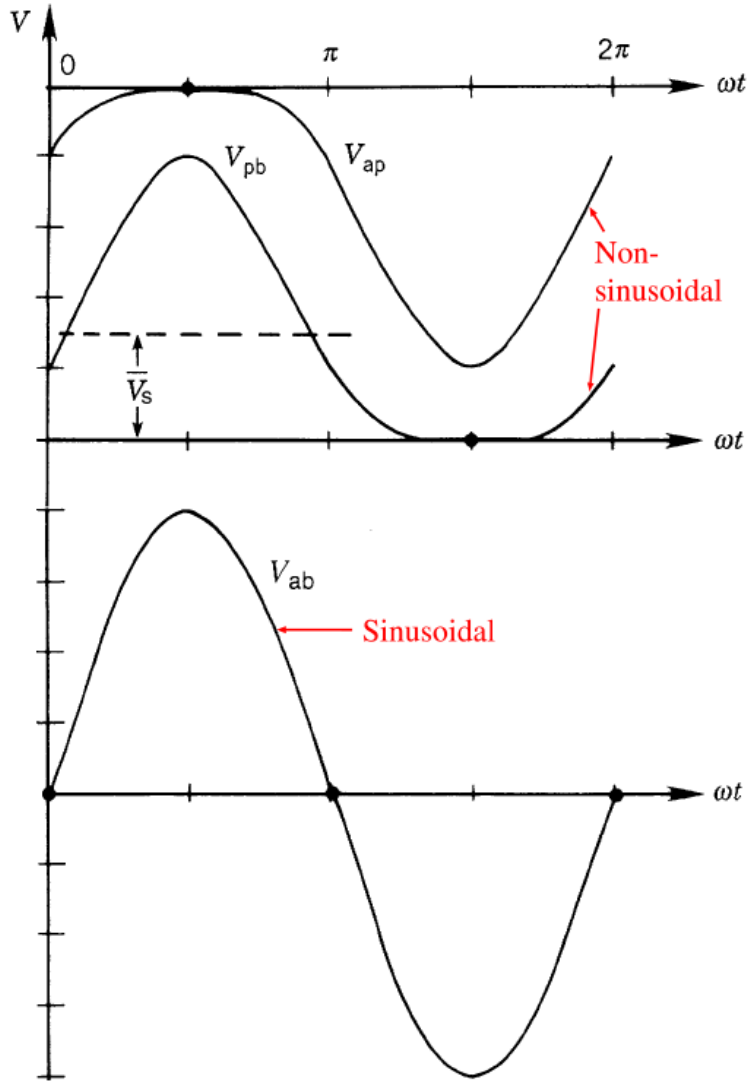

Source: https://people.eecs.berkeley.edu/~lieber/

SHEATH POTENTIAL VERSUS POSITION AT VARIOUS TIMES

Spatial variation of the total potential Φ (solid curves) for the homogeneous model at four different times during the rf cycle. The dashed curve shows the spatial variation of the time-average potential $\bar{\Phi} \equiv \overline{V}_s$

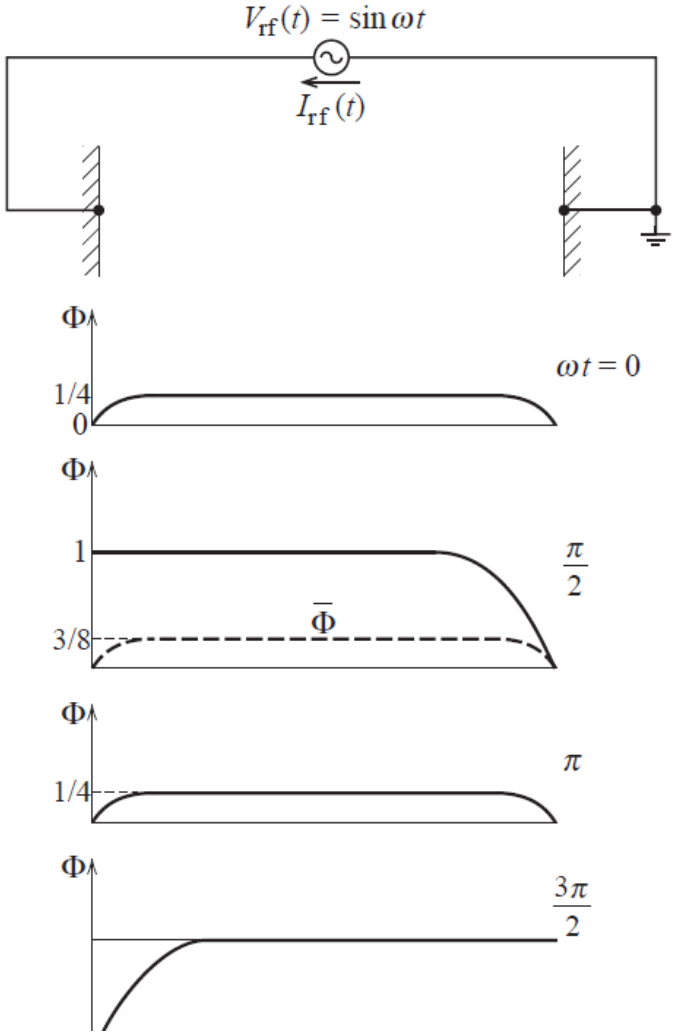

SHEATH CAPACITANCE

- Define total discharge capacitance by

$$I_{\rm rf}(t) = \tilde{I}_0 \cos\omega t, \qquad V_{\rm rf}(t) = \frac{2en\tilde{s}_0^2}{\epsilon_0} \sin\omega t \quad [p.\ 65]$$

which yields

$$\boxed{I_{\rm rf} = C_s \frac{dV_{\rm rf}}{dt} \qquad \text{with} \qquad C_s = \frac{\epsilon_0 A}{2\tilde{s}_0}}$$

- We can think of each sheath as having a capacitance

$$\boxed{C_a = C_b = \frac{\epsilon_0 A}{\tilde{s}_0}}$$

- We now have a lossless discharge model

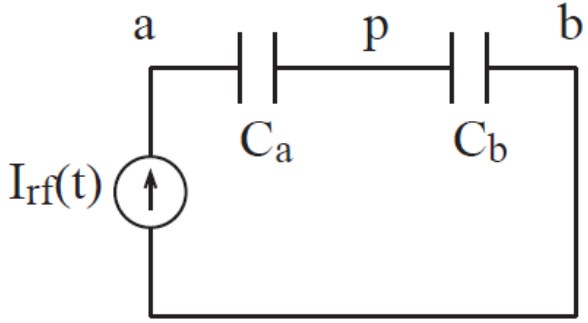

OHMIC AND STOCHASTIC HEATING

- Ohmic heating in the bulk plasma [p. 34]

$$P_\Omega = \frac{1}{2}|\tilde{J}_{\rm rf}|^2 \frac{m\nu_m d}{e^2 n} A \qquad \text{[watts]}$$

- Stochastic heating by oscillating sheaths

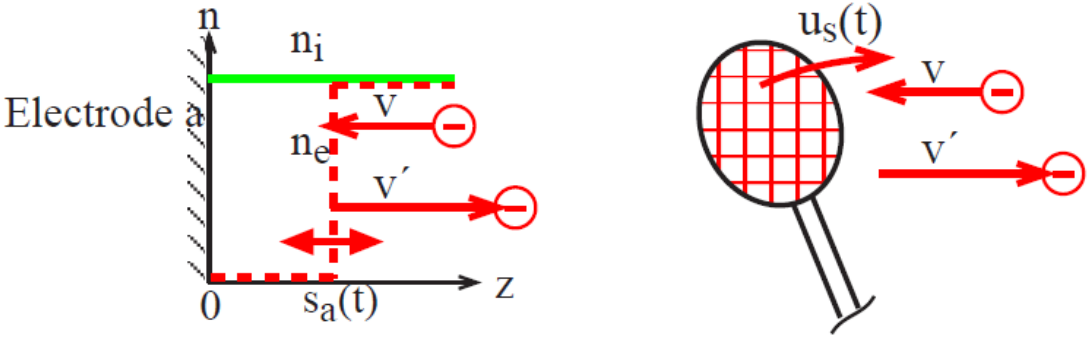

$$v' = -v + 2\,u_s(t)$$

with

$$u_s(t) = \frac{ds_a}{dt} = \tilde{u}_0 \cos\omega t \qquad \text{with} \qquad \tilde{u}_0 = \omega \tilde{s}_0$$

- Average energy transferred is

$$\Delta\mathcal{E}_e = \left[\frac{1}{2}m\big(-v + 2\,u_s(t)\big)^2 - \frac{1}{2}mv^2\right] = m\tilde{u}_0^2$$

- $\Delta\mathcal{E}_e$ is positive, so the oscillating sheath heats electrons

STOCHASTIC HEATING POWER

- For a Maxwellian distribution, the electron flux incident on a sheath is [p. 17]

$$\Gamma_e = \frac{1}{4} n \bar{v}_e$$

with

$$\bar{v}_e = (8eT_e/\pi m)^{1/2}$$

the mean electron speed

- The time-average stochastic heating power is found to be

$$\boxed{P_{sa} = \Gamma_e A \cdot 2\,\Delta\mathcal{E}_e = \frac{1}{2} m n \bar{v}_e \omega^2 \tilde{s}_0^2 A \qquad \text{[watts]}}$$

- This is a powerful electron heating mechanism in a capacitive discharge

HEATING POWERS VERSUS DRIVING VOLTAGE

- For stochastic heating [p. 71]

$$P_{sa} = \frac{1}{2} m n \bar{v}_e \omega^2 \tilde{s}_0^2 A$$

Using $\widetilde{V}_{\rm rf} = 2en\tilde{s}_0^2/\epsilon_0$ [p. 65] we obtain for the two sheaths

$$\boxed{P_s = P_{sa} + P_{sb} = \frac{m}{2e}\epsilon_0 \bar{v}_e \omega^2 \widetilde{V}_{\rm rf} A}$$

- For bulk ohmic heating [p. 70]

$$P_\Omega = \frac{1}{2}|\tilde{J}_{\rm rf}|^2 \frac{m\nu_m d}{e^2 n} A$$

Using $\tilde{J}_{\rm rf} = en\omega\tilde{s}_0$ and $\widetilde{V}_{\rm rf}$ given above

$$\boxed{P_\Omega = \frac{m}{4e}\epsilon_0 \nu_m d\, \omega^2 \widetilde{V}_{\rm rf} A}$$

Ohmic and stochastic heating powers depend on $\widetilde{V}_{\rm rf}$

Introduction to Plasma Simulation

Equations for neutral transport phenomena

Momentum conservation

$$\nabla \bullet (\rho_{mix} \vec{V} u_i) = -\frac{\partial P}{\partial x_i} + \nabla \bullet (\mu_{mix} \nabla u_i) + S_i$$

Mixed Viscosity by Kinetic theory

$$\mu_{mix} = f(\mu_i, x_i, \Phi_{ij}) \leftarrow \mu_i = f(coefficent, M_i, T, \sigma_i, \Omega_\mu)$$

Function of ( )

Energy conservation

$$\nabla \bullet (\rho_{mix} \vec{V} h_0) = \nabla \bullet (k_{mix} \nabla T + P + \bar{\tau} \vec{V}) + S_h$$

$$h_0 = i + \frac{P}{\rho} + \frac{1}{2}(u^2 + v^2 + w^2)$$

h_0 : the total enthalpy

Mixed Conductivity by Kinetic theory

$$k_{mix} = f(k_i, x_i, \Phi_{ij}) \leftarrow k_i = f(coefficent, MW_i, C_{p,i}, R, \mu_i)$$

Mixed Molecular weight

$$MW_{mix} = \sum x_i M_i$$

Ideal gas

$$\rho_{mix} = \frac{(P + P_{ref}) MW_{mix}}{RT}$$

MW_{mix} : Mixed Molecular weight

Diffusivity by Kinetic theory

$$D_i = f(x_t, x_j, D_{ij}(M_{i_{or\,j}}, P, \Omega_D \sigma_{ij}))$$

$$D_i^T = f(x_t, x_j, T, D_{ij}(M_{i_{or\,j}}, P, \Omega_D \sigma_{ij}))$$

Species transport

$$\nabla \bullet (\rho_{mix} u_j Y_i) = \nabla \bullet (\Gamma \frac{\partial Y_i}{\partial x_j}) + (\dot{m}_k)_{evap}$$

$$Y_i = \sum \xi_{ik} f_k$$

f_k : The mixture fraction for the k mixture

Y_i : The mass fraction of species

ξ_{ik} : mass fraction of the I species in the k mixture

If Multi-component Diffusion

$$\Gamma \frac{\partial Y_i}{\partial x_j} = j_i \qquad j_i = j_i^C + j_i^T$$

$j_i^C = -\rho D_i \nabla Y_i$: concentration-driven diffusion

$j_i^T = -\rho D_i^T \nabla(\ln T)$: Thermo-diffusion or soret diffusion

μ_i : Viscosity of species i

T : Temperature

M_i : Molecular weight of species i

x_i : Mole fraction of species i

σ_i : Lennard-Jones collision diameter

Ω : collision integral

Φ_{ij} : dimensionless quantity

-> function of Molecualr weight

Importance of careful consideration of diffusion

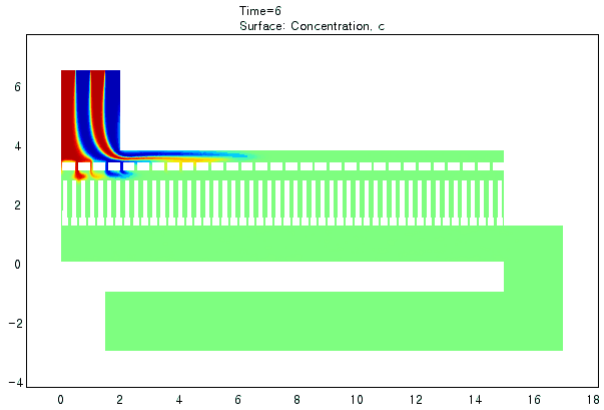

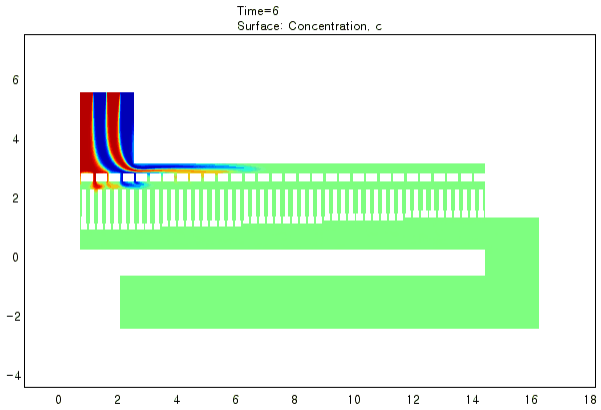

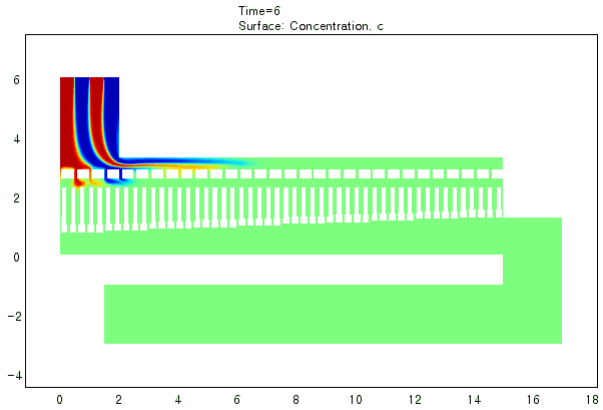

- Scalar fields are described by convection, diffusion and reaction.
- Convection → important in a transient problem, odd-order error, wave propagation
- Diffusion → important in a steady problem, even-order error, artificial diffusion
- In a vacuum system (i.e., P_{op} < 200 Torr), reactor is under the diffusion dominating condition because Re is low.
- In an RF discharge problem, if the system is assumed as a continuum regime, normally thermal velocity is much larger than electron velocity. Thus inertia term can be neglected, and we can use “drift-diffusion approximation”. This drift-diffusion approximation makes electron energy equation diffusion dominating.
- Thus accurate solving for diffusion term is critical to simulate semiconductor fabrication system.

Transport of neutral species (stable molecules, radicals, …)

$$\frac{\partial}{\partial t}\left(\rho Y_i\right) = -\nabla\cdot\left(\rho \mathbf{v} Y_i\right) - \nabla\cdot\left(j_i^C + j_i^T\right) + \left(G_i - L_i\right) M_i$$

ρ - the overall density
v - the overall velocity
Y_i - the mass fraction of species i
j_i^C - the flux of species i due to the concentration gradients
j_i^T - the thermal diffusion flux of species i
G_i - the generation rate of species i
L_i - the depletion rate of species i
M_i - the molar mass of species i

Equations for charged species (Fluid model)

$$\frac{\partial n_p}{\partial t} + \nabla \cdot \left(n_p \mathbf{v}_p \right) = n_e N k_i$$

positive ion continuity

$$n_p \mathbf{v}_p = n_p \mu_p \mathbf{E} - D_p \nabla n_p$$

drift-diffusion approximation

$$\frac{\partial n_n}{\partial t} + \nabla \cdot \left(n_n \mathbf{v}_n \right) = n_e N k_i$$

negative ion continuity

$$n_n \mathbf{v}_n = n_n \mu_n \mathbf{E} - D_n \nabla n_n$$

drift-diffusion approximation

$$\frac{\partial n_e}{\partial t} + \nabla \cdot \left(n_e \mathbf{v}_e \right) = n_e N k_i$$

electron continuity

$$n_e \mathbf{v}_e = -n_e \mu_e \mathbf{E} - D_e \nabla n_e$$

drift-diffusion approximation

Continuity Equation

$$\frac{\partial n_e \varepsilon_e}{\partial t} + \nabla \cdot \left(\frac{5}{3} n_e \varepsilon_e \mathbf{v}_e + \mathbf{q}_e \right) = -e n_e \mathbf{v}_e \cdot \mathbf{E} - n_e N k_L$$

$$\mathbf{q}_e = -\frac{2}{3} \kappa \nabla \varepsilon_e$$

$$\kappa = \frac{5}{2} n_e D_e$$

Electron Energy Equation

$$\mathbf{E} = -\nabla V$$

$$\Delta V = -\frac{e}{\varepsilon_0} \left(n_p - n_n - n_e \right)$$

Poisson equation

D_e eventually governs the dissociation rate profile in the gas phase.

If the gas phase reaction is more active than surface reaction, deposition profile will be a function of N_e distribution.

Surface phenomena: sticking model & molecular dynamics

Deposition by radical species can be described by utilization of a phenomenological approach called as a sticking model.

$$-D_i \frac{\partial n_i}{\partial z} = -R_{i,s}\left(n_{i,s}\right) = \Gamma_i^{in} + \Gamma_i^{out}$$

$$\Gamma_i^{in} = \frac{s_i + \gamma_i}{1 - \left(s_i + \gamma_i\right)/2} n_{i,s} \sqrt{\frac{k_B T_g}{2\pi m_i}}$$

$$\Gamma_i^{out} = -\sum_{j \neq i} \frac{\gamma_j}{s_j + \gamma_j} \Gamma_j^{in}$$

where subscript i, D_i, n_i, z, $n_{i,s}$, and $R_{i,s}$ are the species index, the diffusion coefficient, the density of species i, the axial coordinate, the density of species i at the surface, and the surface reaction rate of species i, respectively.

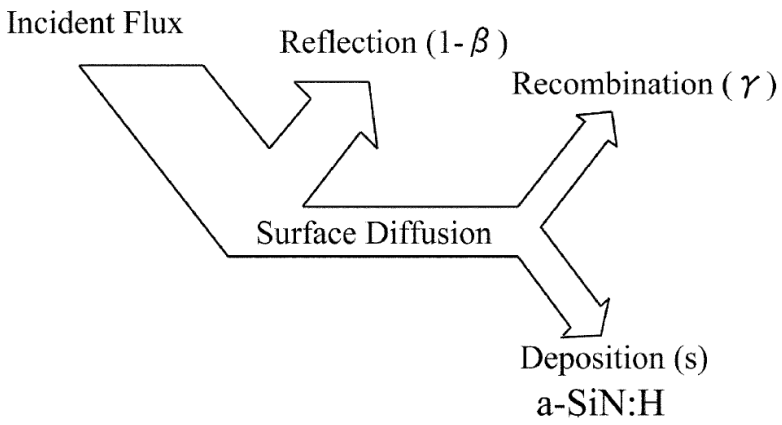

Molecular Dynamics Simulations (s, β, γ)

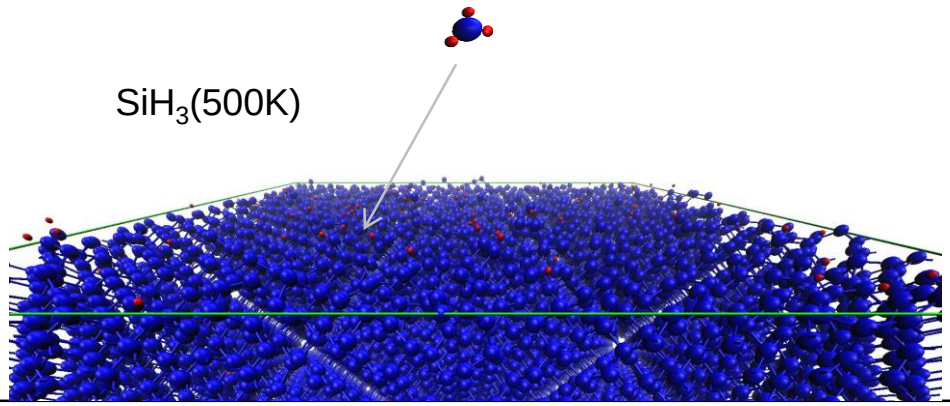

Case Studies

Non-uniformity issues observed in the wafer edge

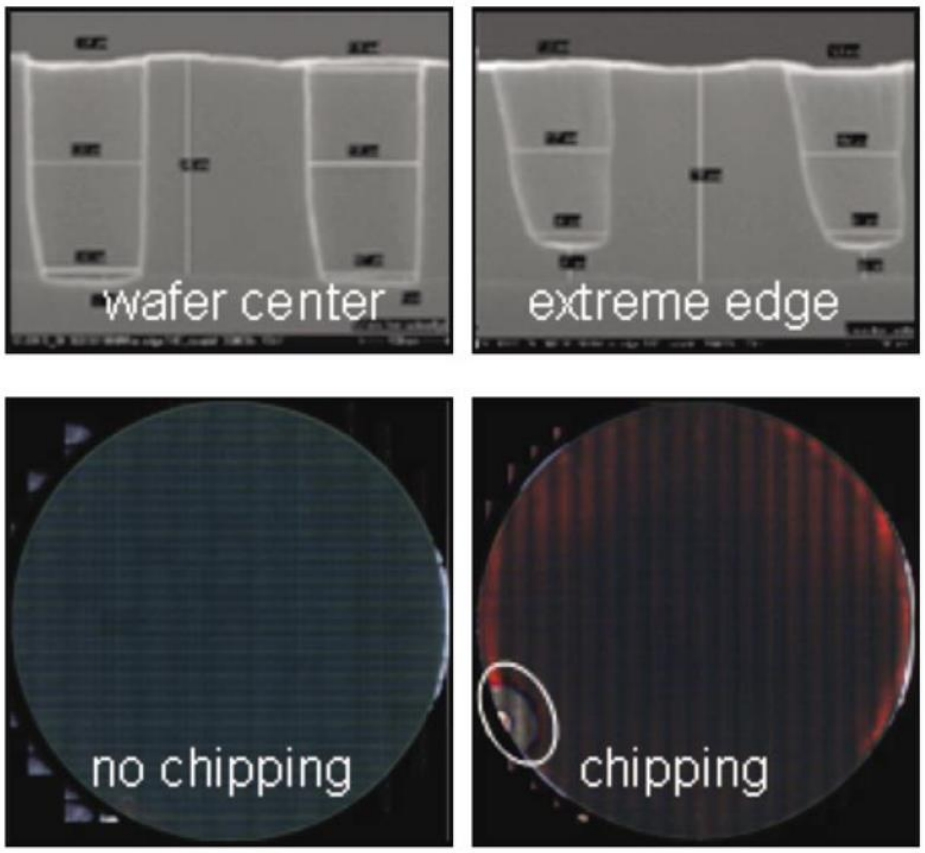

Figure 1. SEM image of regular and deformed hard mask (top). Optical image of a wafer without and with chipping (bottom).

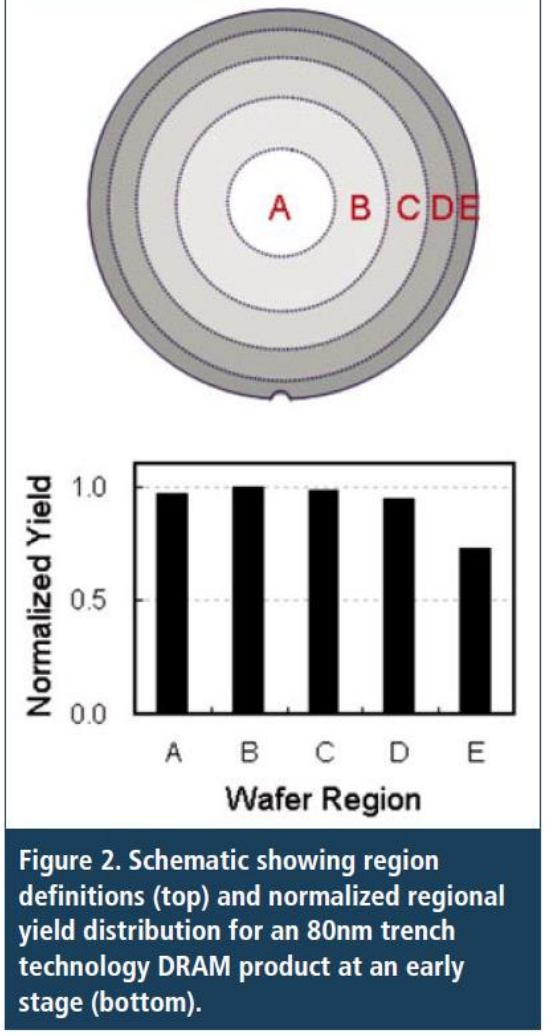

Figure 2. Schematic showing region definitions (top) and normalized regional yield distribution for an 80nm trench technology DRAM product at an early stage (bottom).

Source: Wafer-edge yield engineering in leading-edge DRAM manufacturing
by Oguz Yavas, Ernst Richter, Christian Kluthe & Markus Sickmoeller, Qimonda AG

Non-uniformity issues observed in the wafer edge

Ho Jun Kim and Hae June Lee **2017** Effects of the wall boundary conditions of a showerhead plasma reactor on the uniformity control of RF plasma deposition *Journal of Applied Physics* **122** 053301

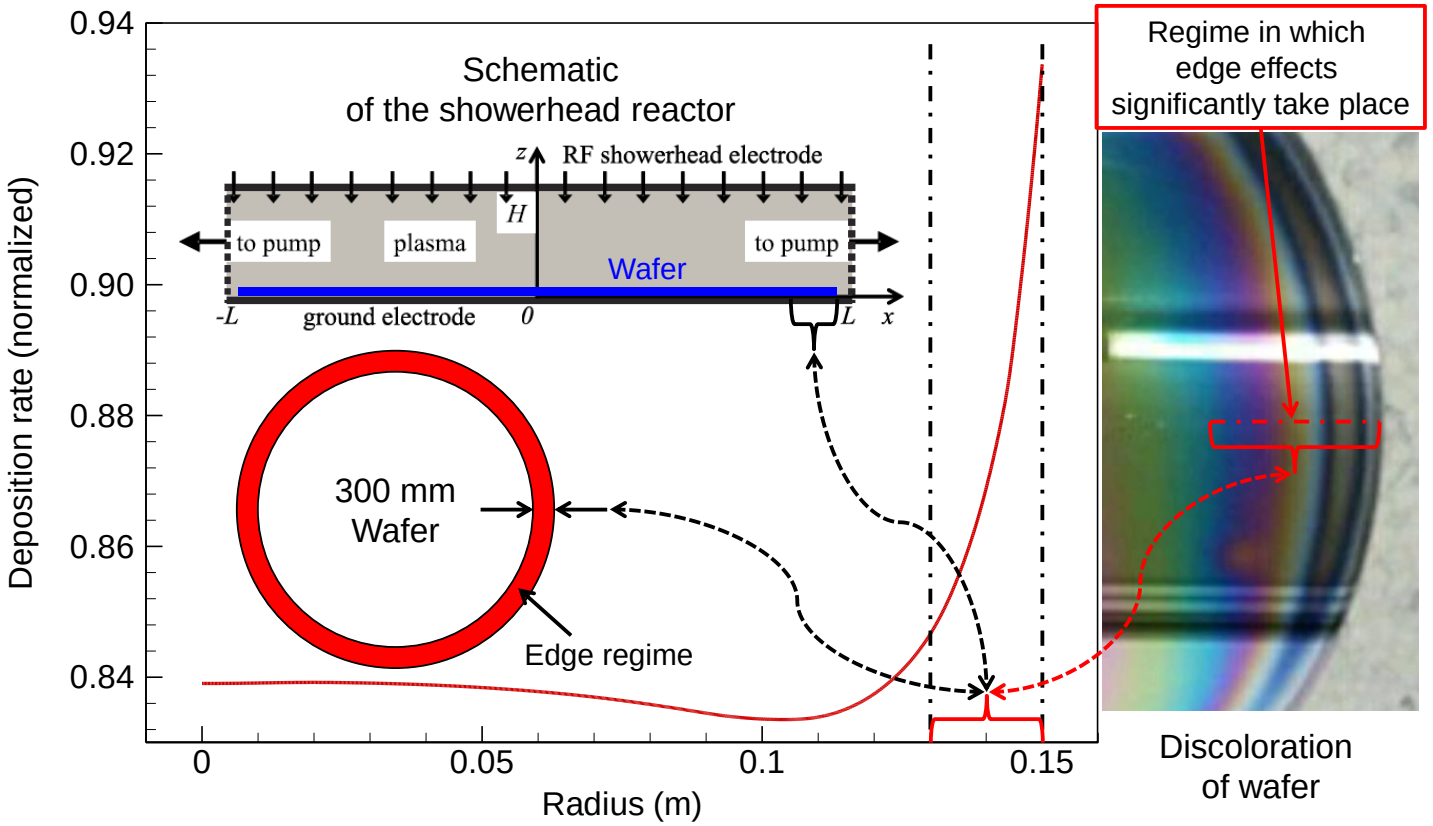

For a typical case with nonuniformity in the edge thickness, its deposition rate profile is plotted along the electrode radius ($0 \le r \le 150$ mm, where r is the radial coordinate) with a solid red line. Near the edge ($r \ge 120$ mm), the deposition rate varies greatly, and concomitantly the corresponding area of wafer shows discoloration (see inset). As shown in the schematic of the showerhead reactor, the geometric configuration of a reactor can give rise to significant spatial changes in various physical aspects.

Plasma reactor simulation: Capacitively Coupled Plasma

Domain for simulation

❖ Domain

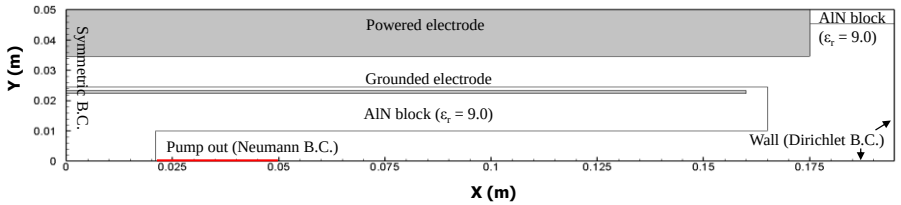

Normally, the reactor is
Cylindrical → due to a wafer shape
Axi-symmetric

The off-axis maximum of the electron density is observed!

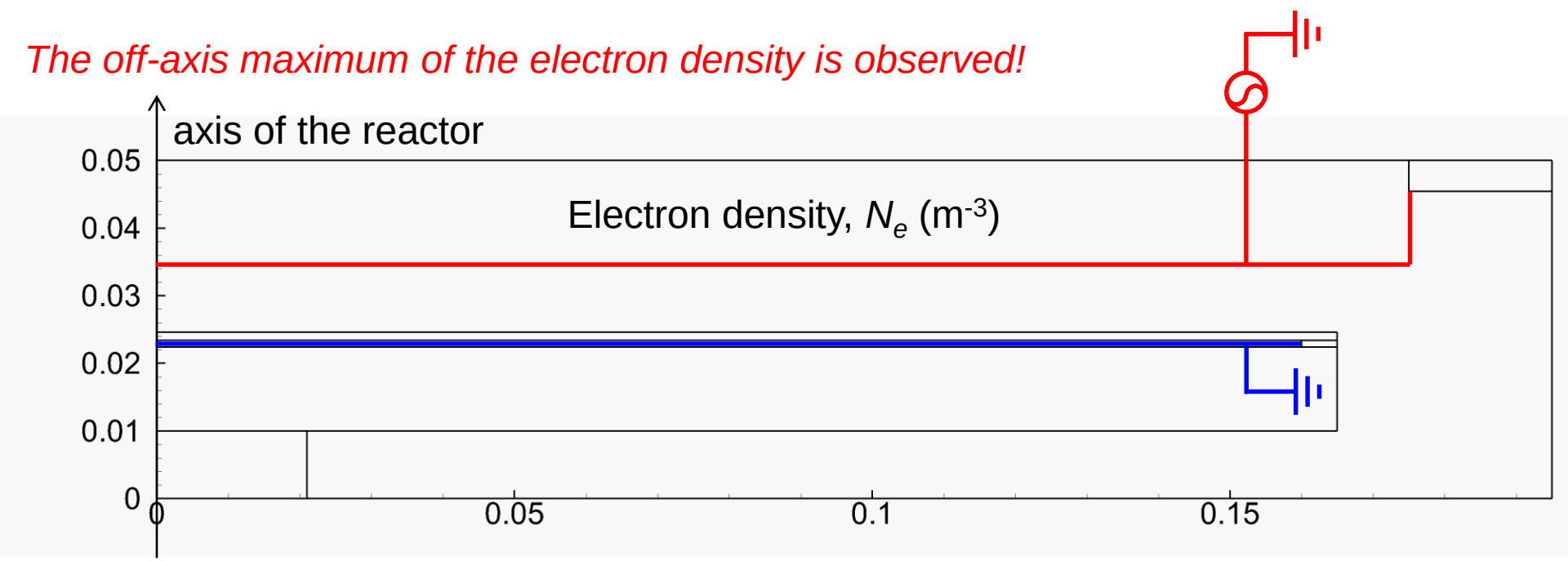

PIC simulation from Kim *et al*. of PNU

Application:

SiN_xH_y layer deposition
a-Si:H layer deposition

SiN_xH_y film utilized in the memory fabrication

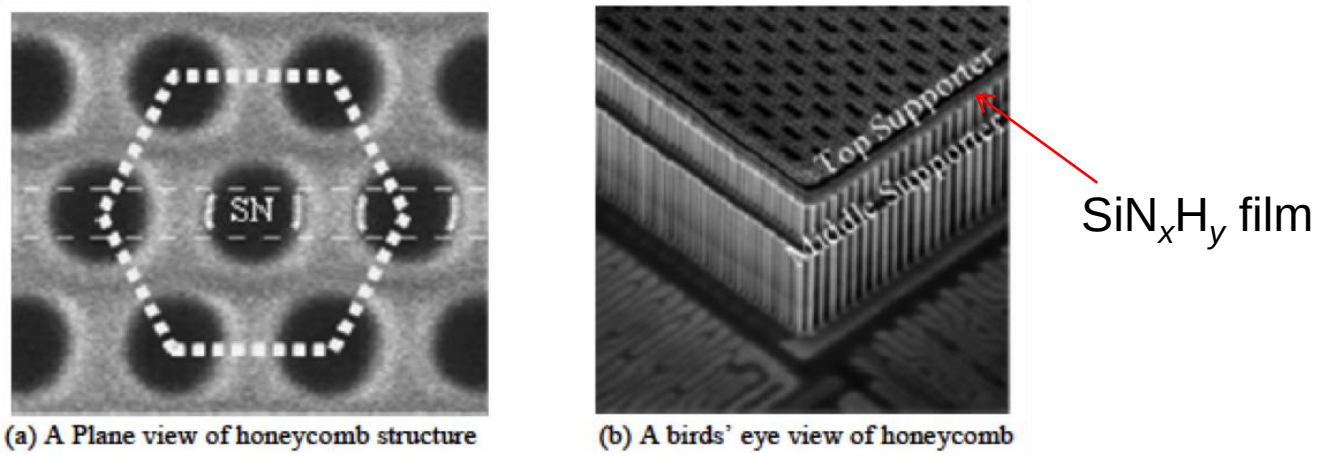

(a) A Plane view of honeycomb structure (b) A birds' eye view of honeycomb

Pan-view images of Samsung 20 nm DRAM

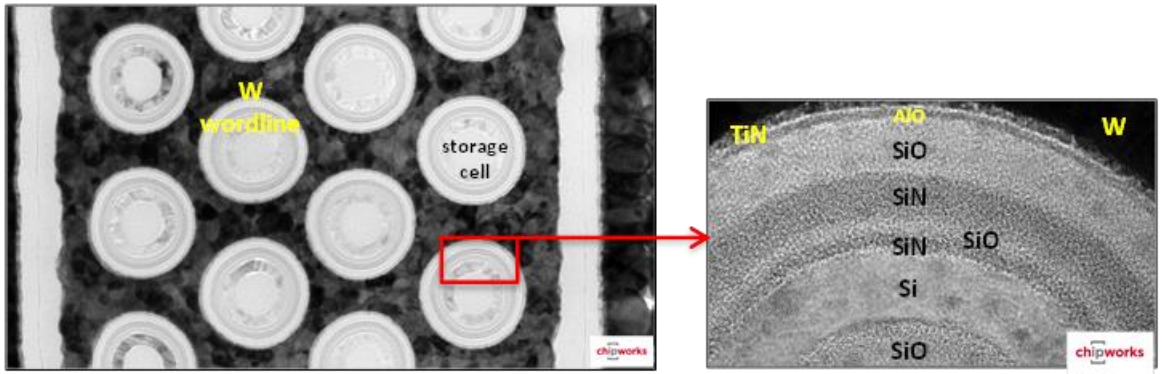

Plan-view images of Samsung V-NAND flash array

Reactor configuration used for SiN_xH_y deposition

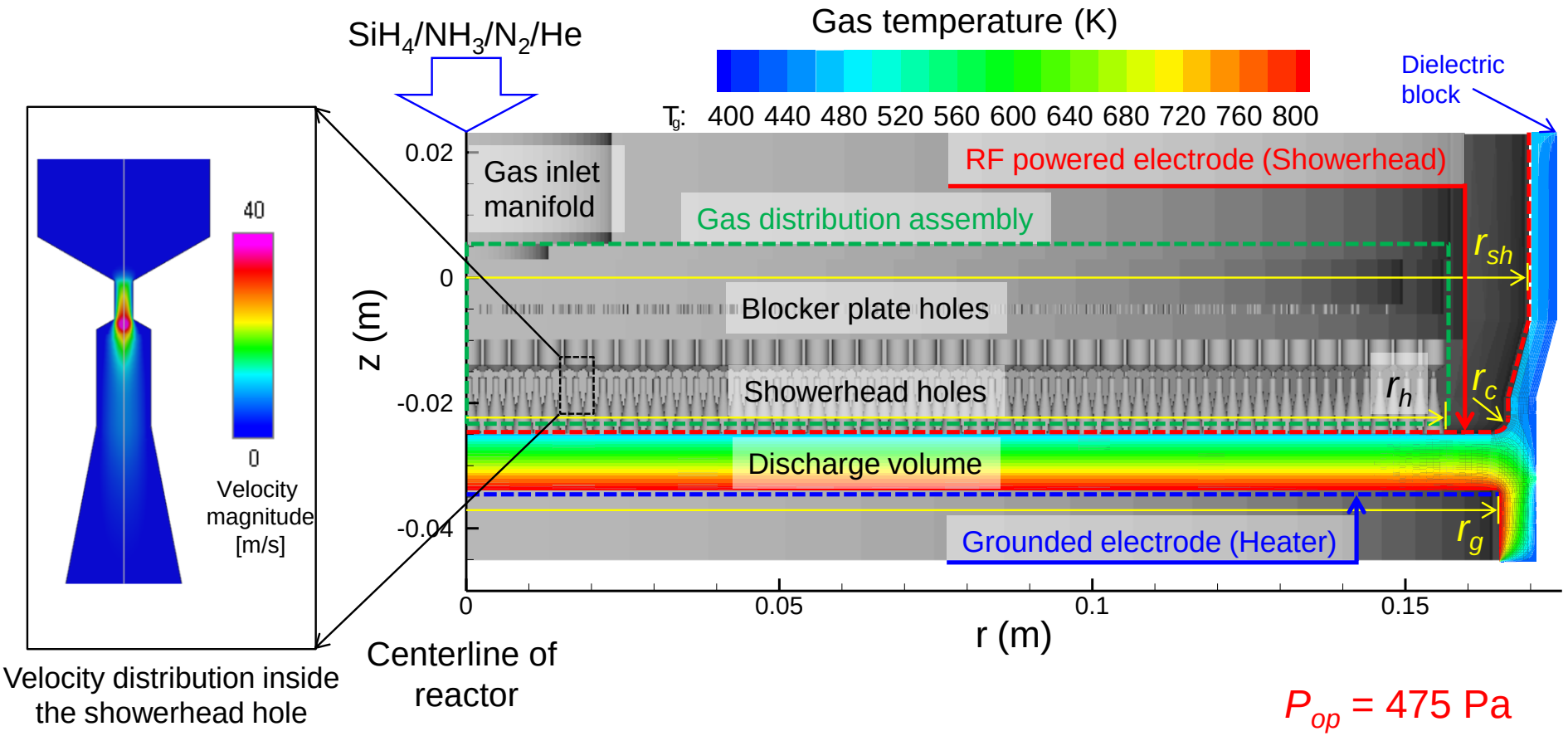

CCP reactor configuration is plotted together with the spatial variation of the gas temperature. The inset shows the velocity distribution obtained by a numerical simulation of neutral gas flow in the showerhead hole. The reactor dimensions are also depicted.

Deposition rate contour experimentally measured

In the center of the deposition rate contour, non-negligible variation can be observed.

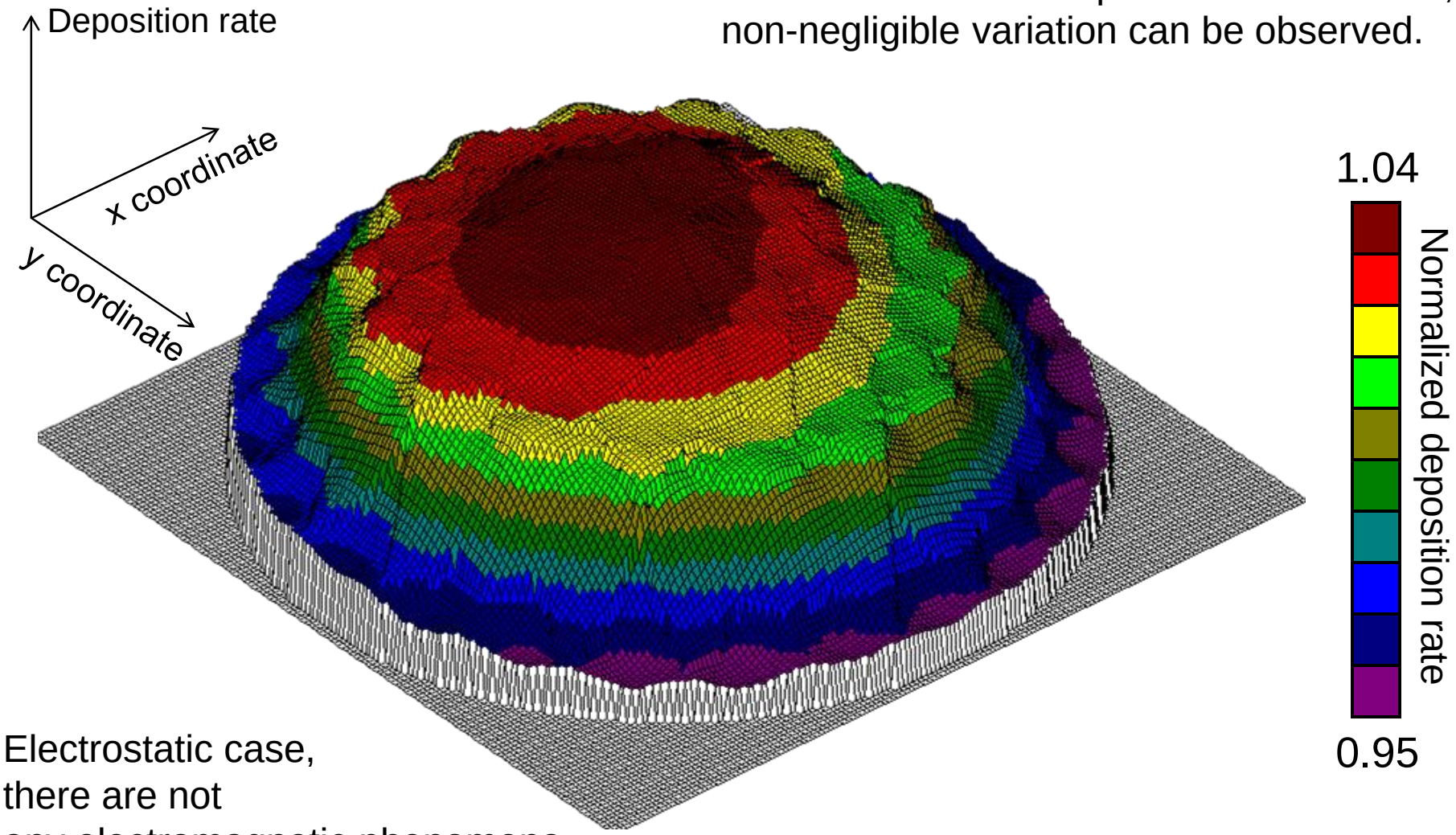

Electrostatic case,
there are not
any electromagnetic phenomena.

Gas flow simulation performed with a realistic 3D geometry

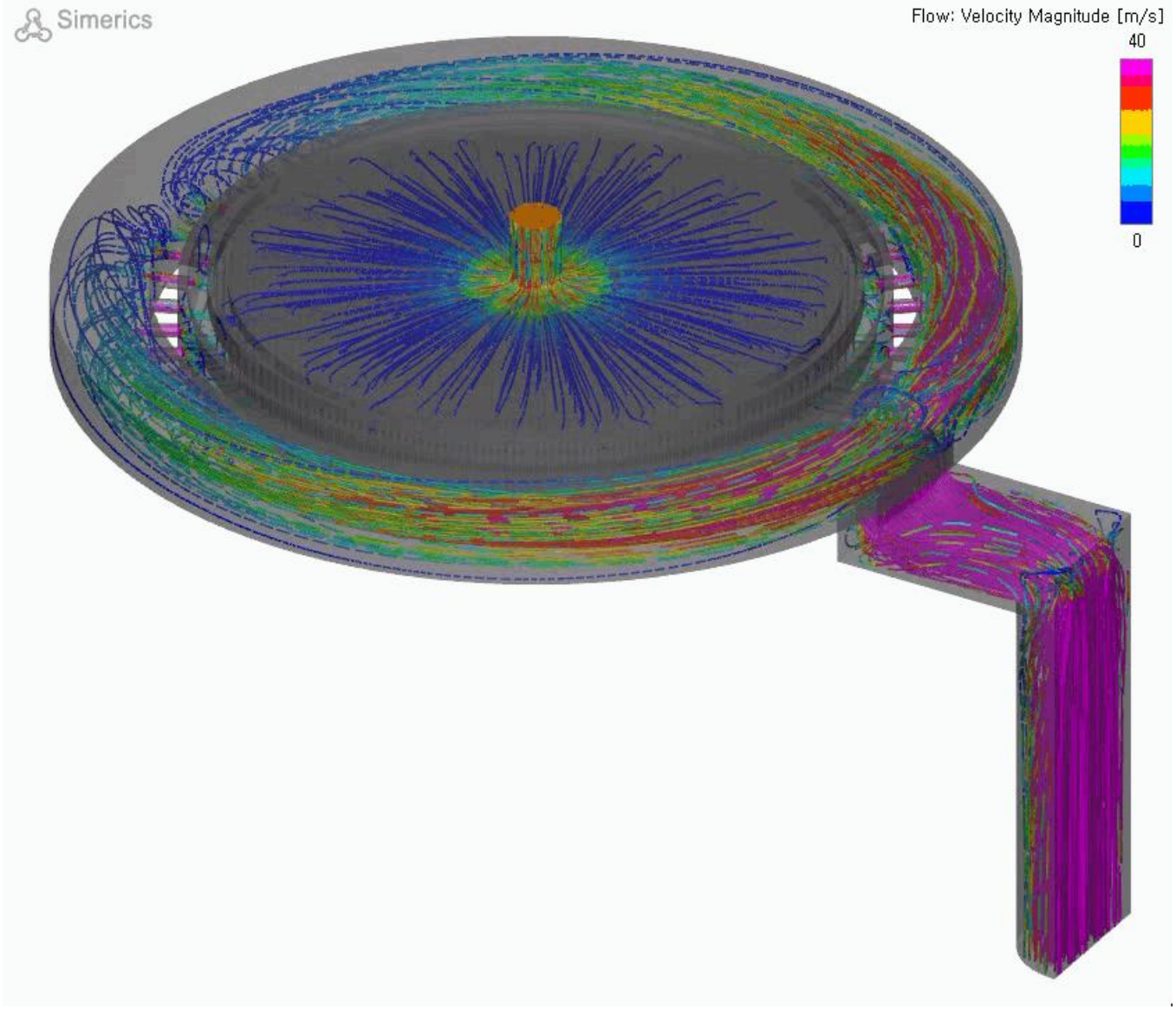

Gas flow simulation performed with a realistic 3D geometry

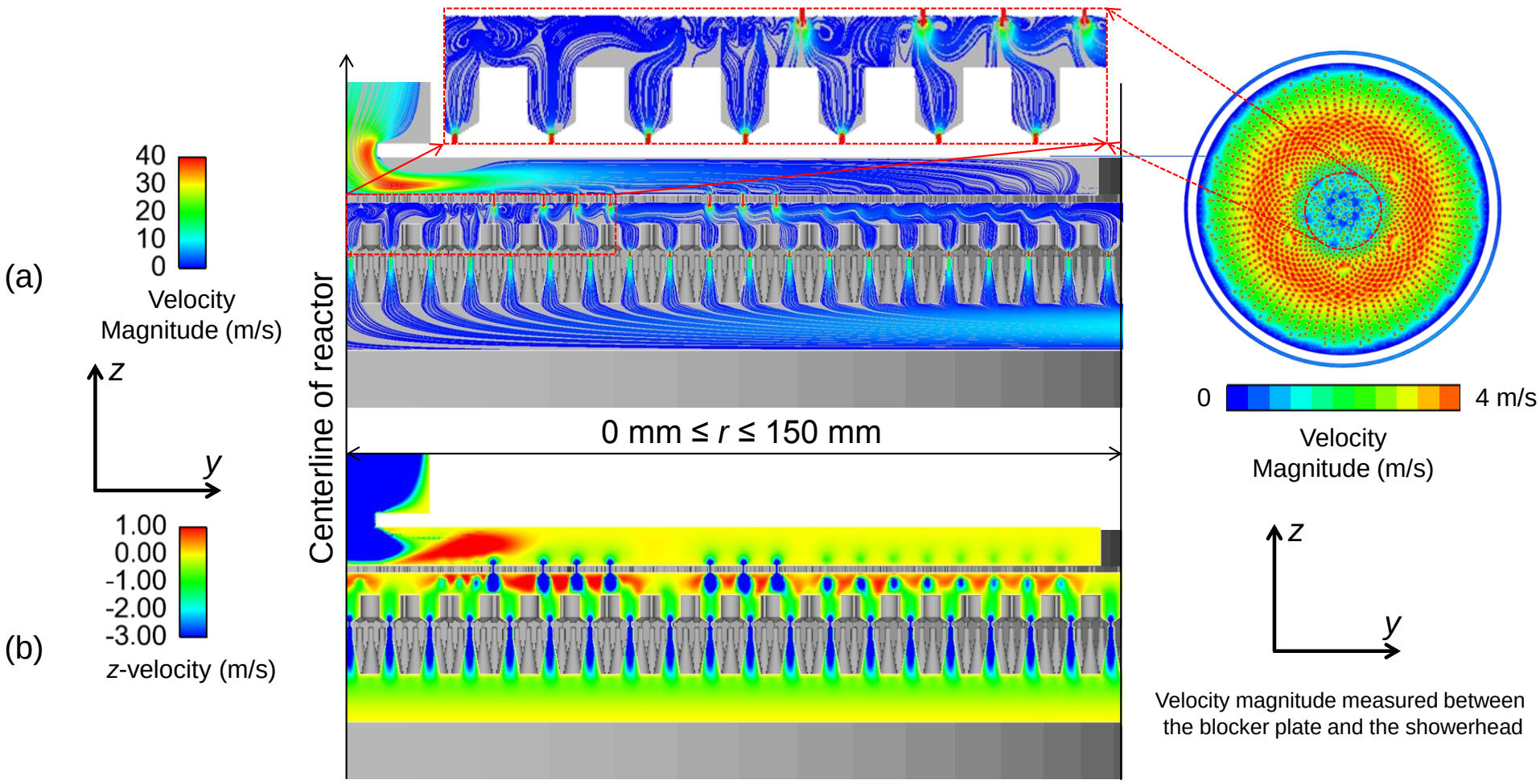

Results of the 3D gas flow simulation: (a) streamlines and velocity magnitude and (b) *z*-velocity contour plot. In the inset of (a), it is observed that the streamlines of the interim space between the blocker plate and showerhead are most curled at the center of the reactor ($r \leq 50$ mm).

Validation: deposition rate profiles

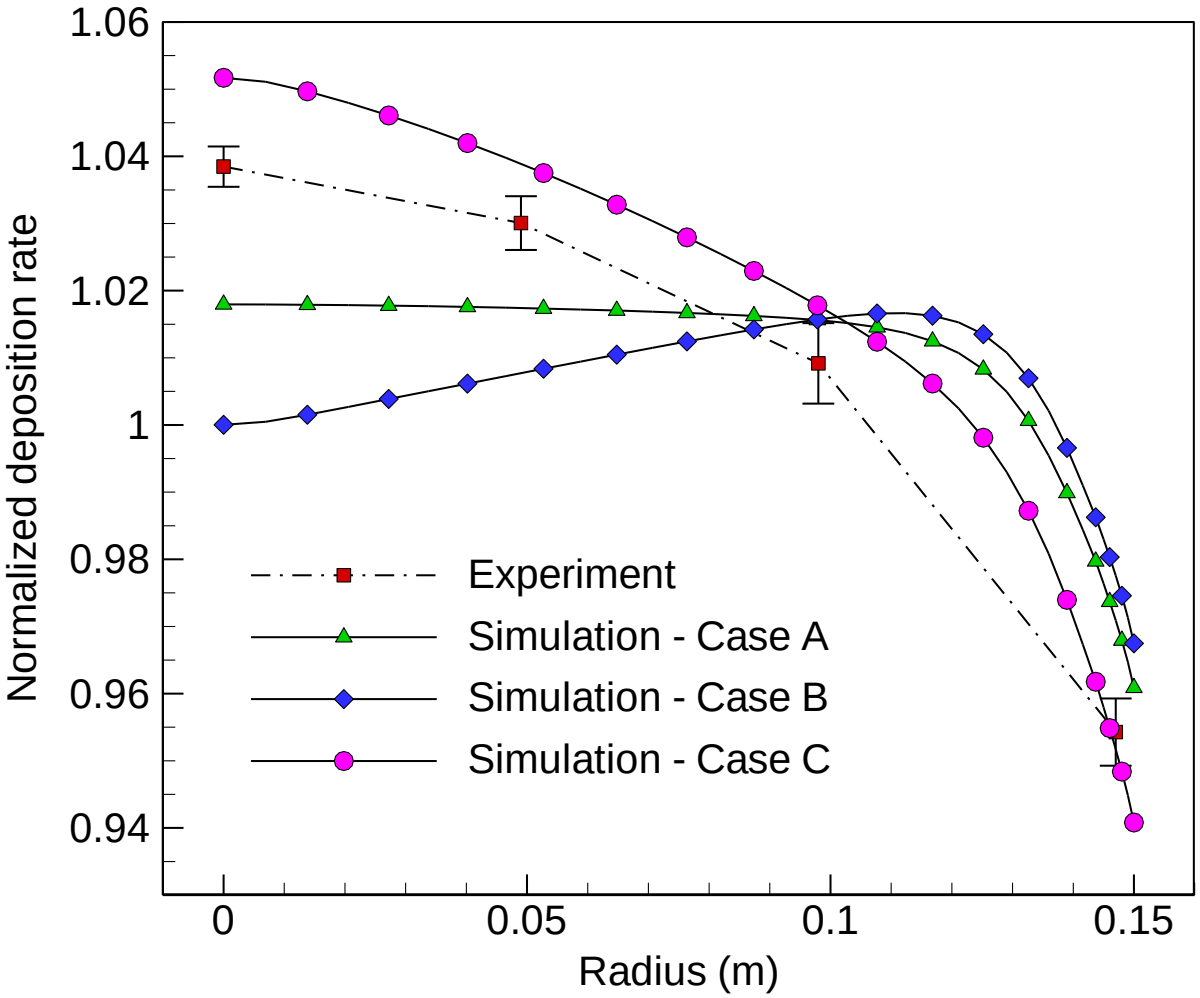

The simulated deposition rates along the wafer radius are depicted for the three different profiles of inlet gas density at the showerhead and compared with the experimental results.

Showerhead analysis

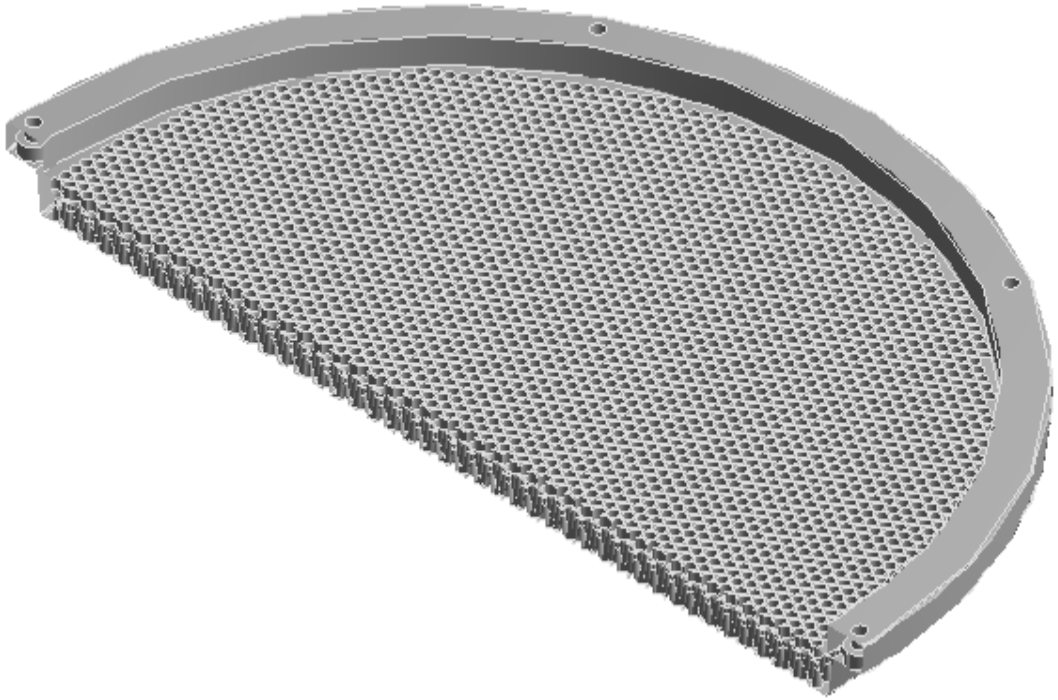

Effects of the shower radius

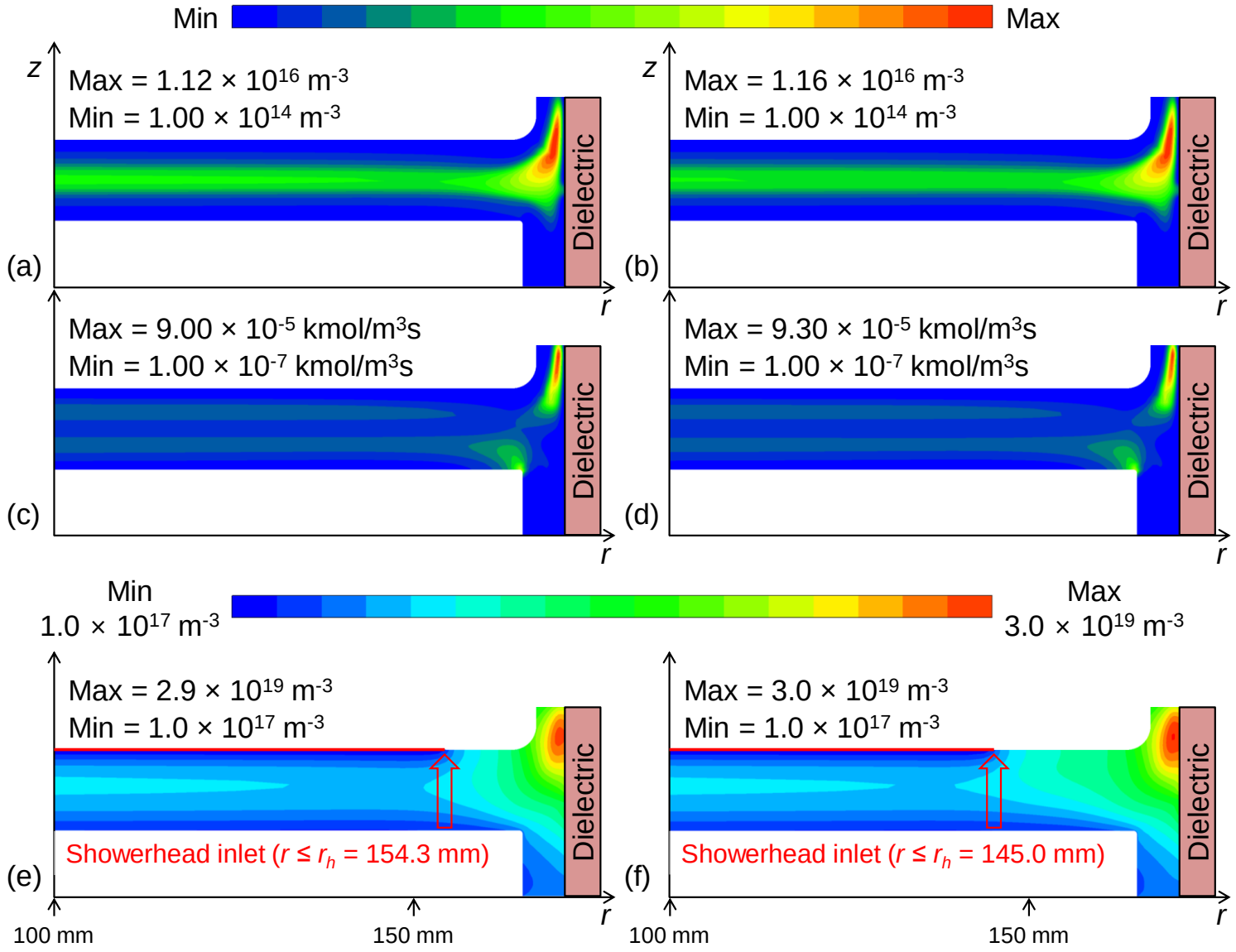

Effects of the shower radius

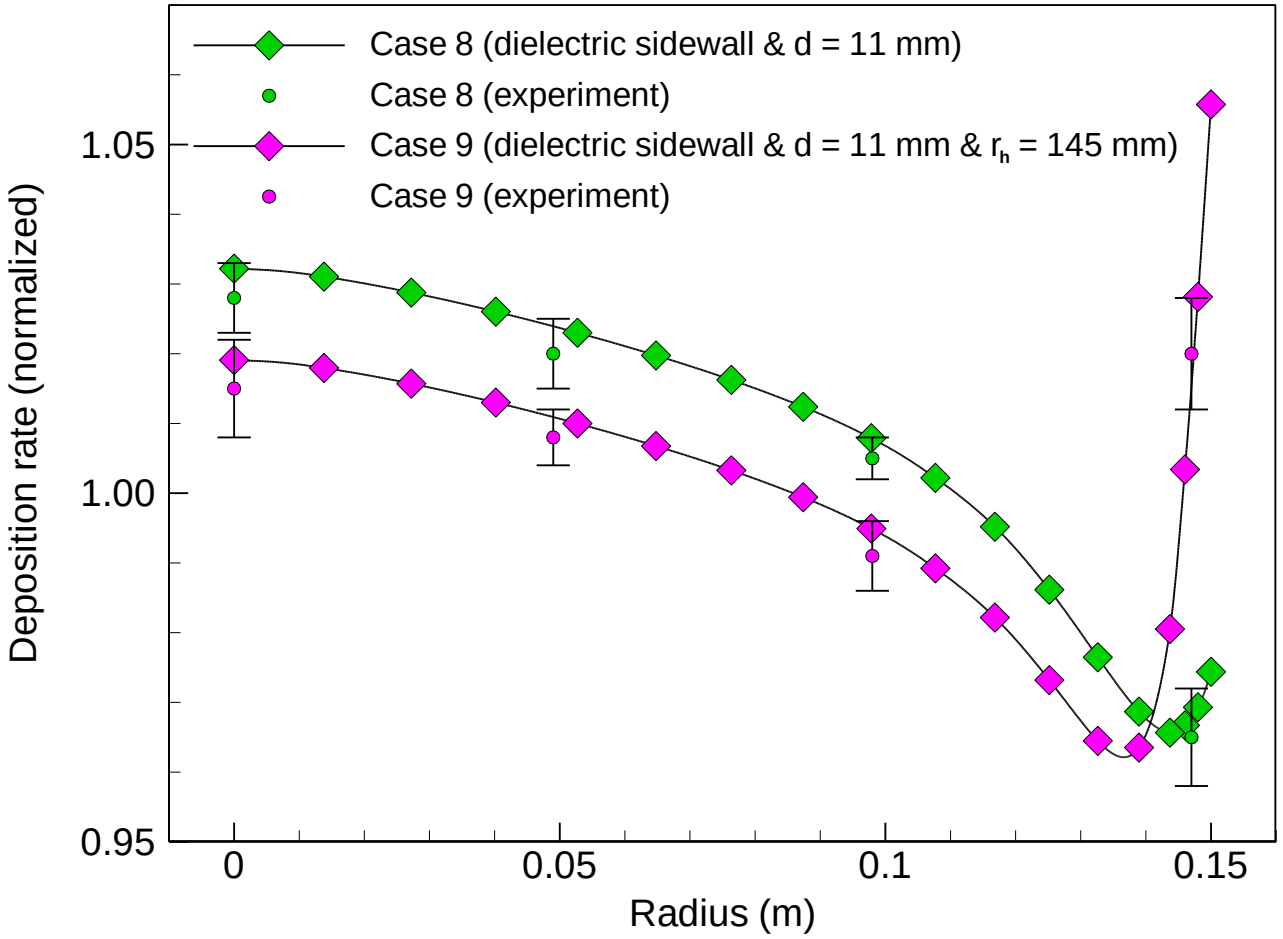

The deposition rate profiles of experimental measurement agree well with the simulation results for the variation of shower radius, with r_h = 154.3mm (case 8) and r_h = 145mm (case 9). The increased N density near the electrode radius induces an increase of the deposition rate profile near the edge for the case with r_h = 145 mm.

Hydrogenated amorphous silicon: a-Si:H

- The term “amorphous” commonly applied to non-crystalline materials prepared by deposition from gases. In amorphous silicon the long range order is not present. Rather, the atoms form a continuous random networks.
- The electronic-grade amorphous silicon is called hydrogenated amorphous silicon (a-Si:H). It is also an alloy of silicon and hydrogen.
- In early studies of amorphous silicon, it was determined that plasma-deposited amorphous silicon contained a significant percentage of hydrogen atoms bonded into the amorphous silicon structure.
- These atoms were discovered to be essential to the improvement of the electronic properties of the material.

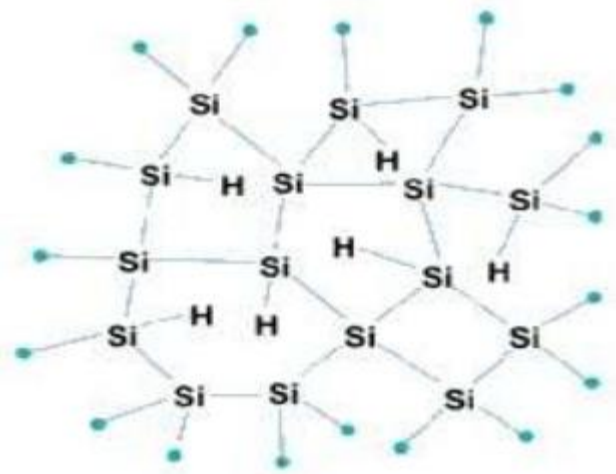

a-Si:H Structure

Reactor configuration used for a-Si:H deposition

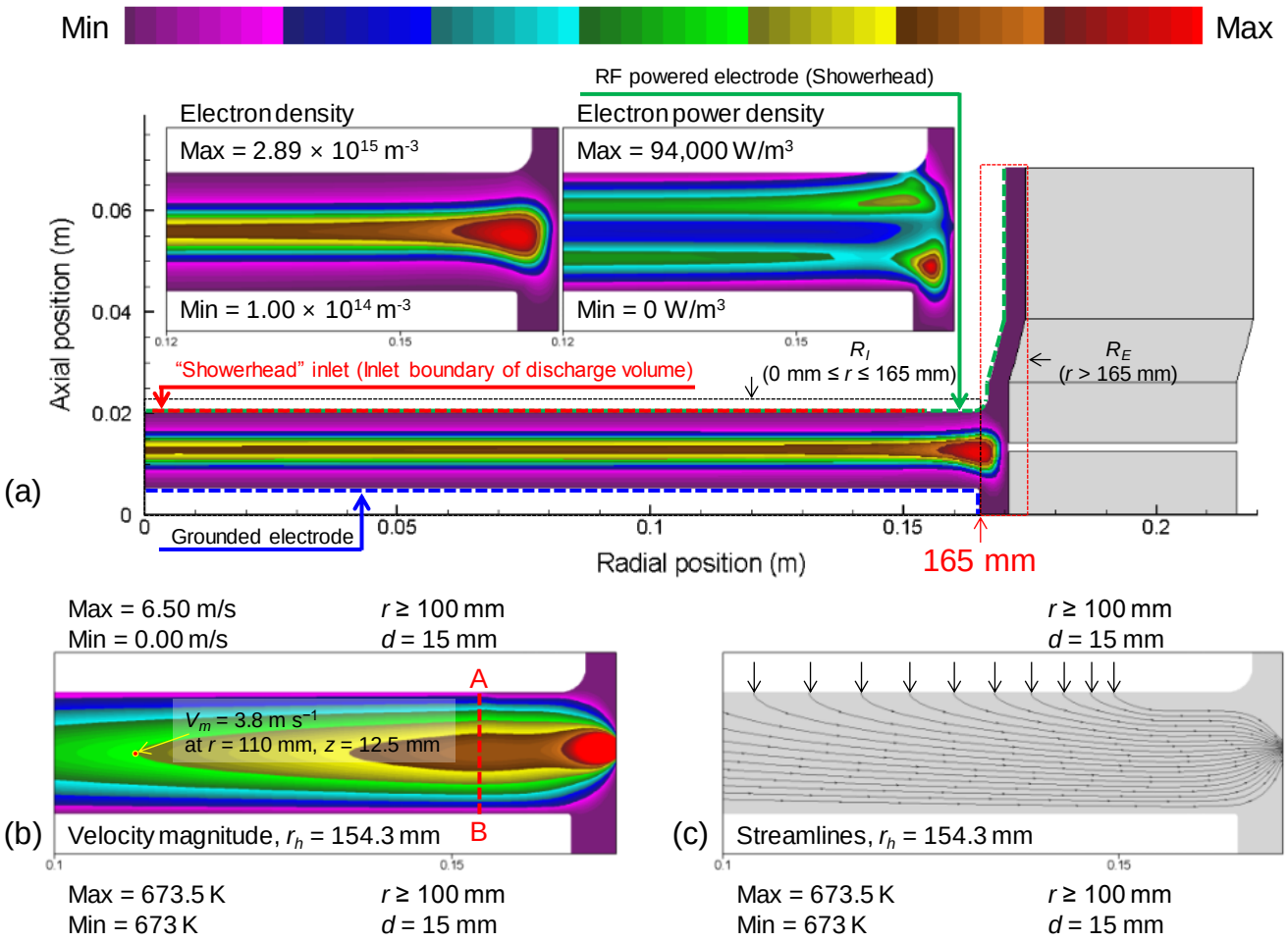

Schematic diagram of a cylindrically symmetric showerhead reactor. Because of its geometric axisymmetry, only half of the reactor is shown. The left boundary denotes the axis of symmetry, and the right boundary denotes the radial wall (i.e., the sidewall). The spatial variations in (a) electron density, N_e (m^{-3}) and (b) velocity magnitude, V_m ($m\ s^{-1}$), are depicted for the base case (Case 1). In the inset of (a), the spatial variation of time-averaged electron power density, P_e ($W\ m^{-3}$), is also depicted. (c) The streamlines are drawn in black.

Effects of the gas distribution

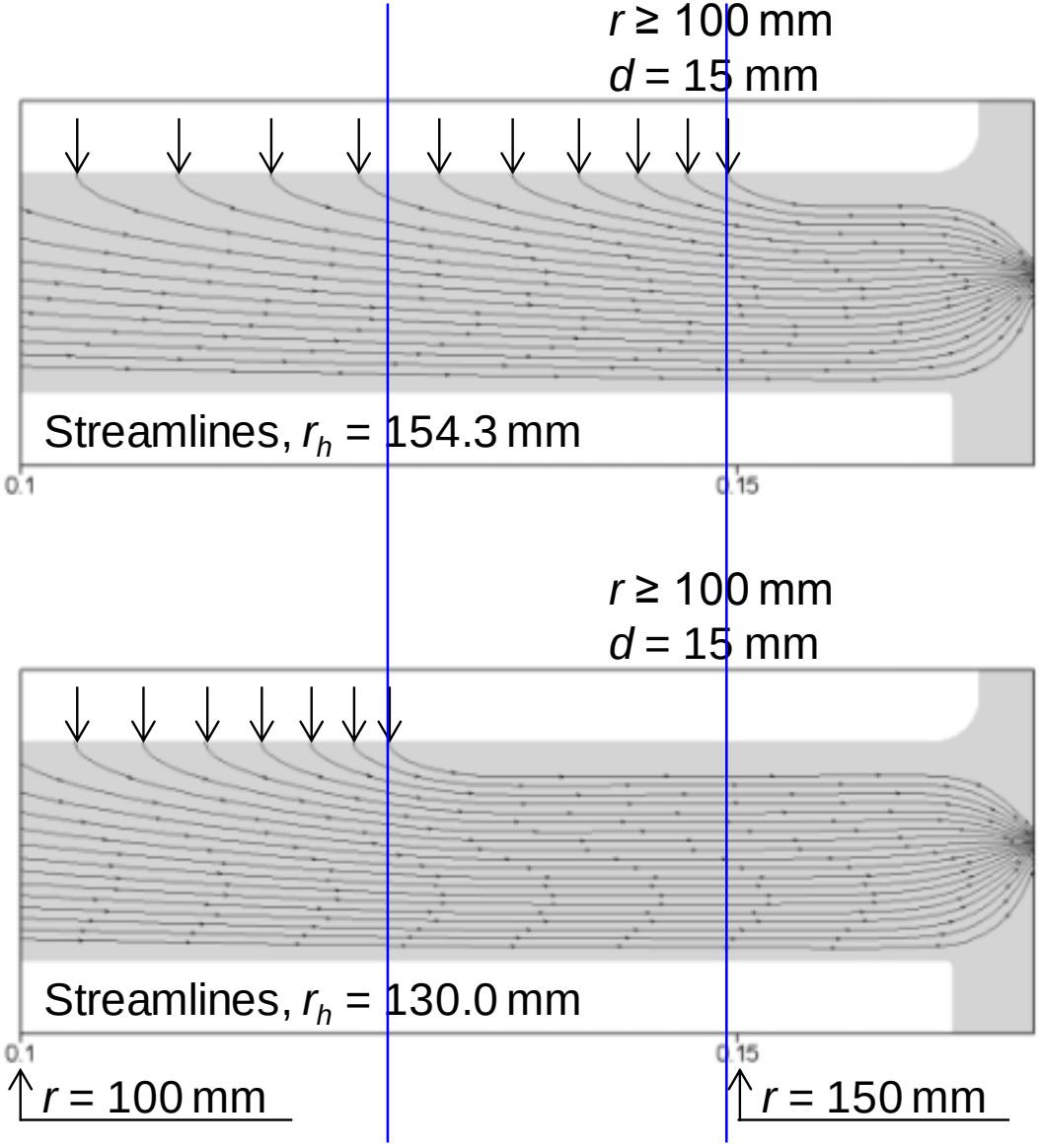

Effects of the gas distribution

Simple change makes the big difference !

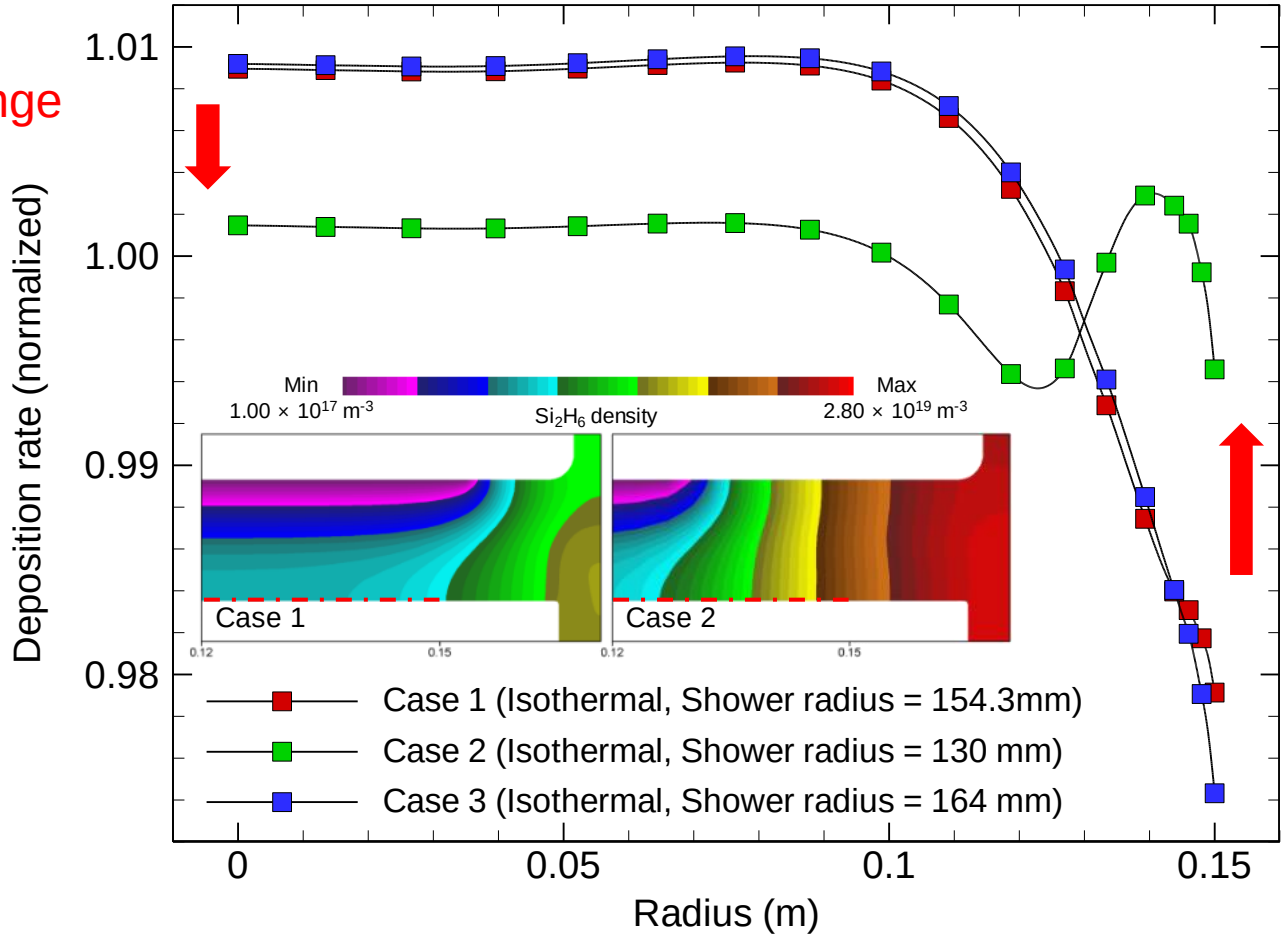

Simulated deposition rates measured along the radial direction for Cases 1 (red square), 2 (green square), and 3 (blue square). The rates are normalized to their corresponding averaged values. In the inset, the spatial variations of Si_2H_6 densities are depicted for Cases 1 and 2.

Effects of the thermal diffusion

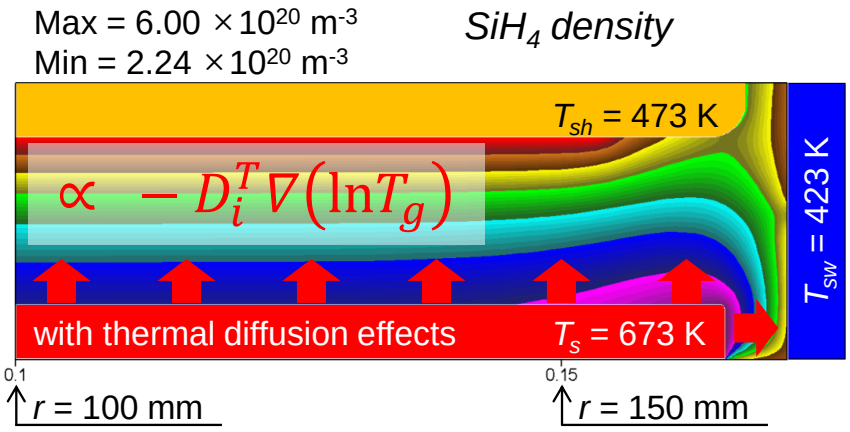

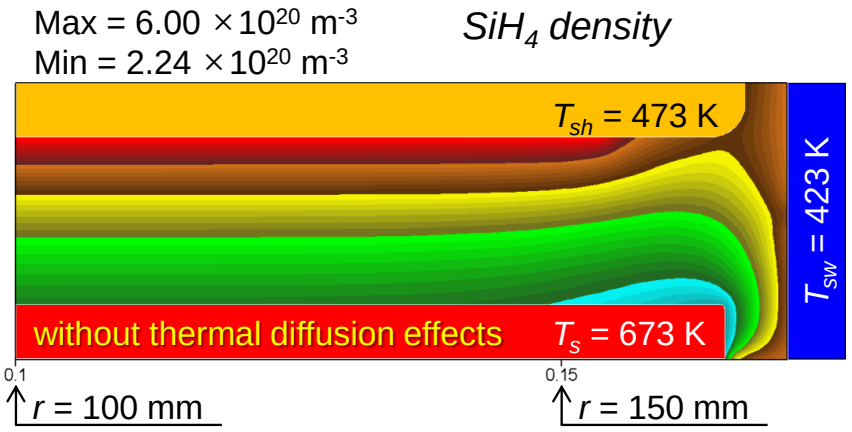

$$j_i^T = -D_i^T \nabla(\ln T_g)$$

$$D_i^T = \alpha D_i M_i M_j c_g^2 / \rho_g$$

$$\alpha = \frac{1}{6\lambda_{ij}}\left(\frac{S^{(i)} f_i - S^{(j)} f_j}{X_\lambda + Y_\lambda}\right)\left(6C_{ij}^* - 5\right)$$

$$S^{(i)} = \left(\frac{M_i + M_j}{2M_j}\right)\frac{\lambda_{ij}}{\lambda_i} - \frac{15}{4A_{ij}^*}\left(\frac{M_j - M_i}{2M_i}\right) - 1$$

$$S^{(j)} = \left(\frac{M_j + M_i}{2M_i}\right)\frac{\lambda_{ij}}{\lambda_j} - \frac{15}{4A_{ij}^*}\left(\frac{M_i - M_j}{2M_j}\right) - 1$$

$$X_\lambda = \frac{f_i^2}{\lambda_i} + \frac{2 f_i f_j}{\lambda_{ij}} + \frac{f_j^2}{\lambda_j}$$

$$Y_\lambda = \frac{f_i^2}{\lambda_i}U^{(i)} + \frac{2 f_i f_j}{\lambda_{ij}}U^{(Y)} + \frac{f_j^2}{\lambda_j}U^{(j)}$$

$$U^{(i)} = \frac{4}{15}A_{ij}^* - \frac{1}{12}\left(\frac{12}{5}B_{ij}^* + 1\right)\frac{M_i}{M_j} + \frac{1}{2}\frac{\left(M_i - M_j\right)^2}{M_i M_j}$$

$$U^{(j)} = \frac{4}{15}A_{ij}^* - \frac{1}{12}\left(\frac{12}{5}B_{ij}^* + 1\right)\frac{M_j}{M_i} + \frac{1}{2}\frac{\left(M_j - M_i\right)^2}{M_i M_j}$$

$$U^{(Y)} = \frac{4}{15}A_{ij}^*\left(\frac{\left(M_i + M_j\right)^2}{4M_i M_j}\right)\frac{\lambda_{ij}^2}{\lambda_i \lambda_j} - \frac{1}{12}\left(\frac{12}{15}B_{ij}^* + 1\right) - \frac{5}{32A_{ij}^*}\left(\frac{12}{5}B_{ij}^* - 5\right)\frac{\left(M_i - M_j\right)^2}{M_i M_j}$$

$$\lambda_i = 8.32\times10^{-4}\frac{\left(T_g / M_i\right)^{1/2}}{\sigma_i^2 \Omega_i^{(2,2)*}}$$

$$\lambda_{ij} = 8.32\times10^{-4}\frac{\left[T_g\left(M_i + M_j\right)/2M_i M_j\right]^{1/2}}{\sigma_{ij}^2 \Omega_{ij}^{(2,2)*}}$$

$$A_{ij}^* = \Omega_{ij}^{(2,2)*} / \Omega_{ij}^{(1,1)*}$$

$$B_{ij}^* = \left[5\Omega_{ij}^{(1,2)*} - 4\Omega_{ij}^{(1,3)*}\right] / \Omega_{ij}^{(1,1)*}$$

$$C_{ij}^* = \Omega_{ij}^{(1,2)*} / \Omega_{ij}^{(1,1)*}$$

$$\sigma_{ij} = \left(\sigma_i + \sigma_j\right)/2$$

Effects of the thermal diffusion

T_{sh} = 473 K
T_{sw} = 423 K
T_s = 673 K

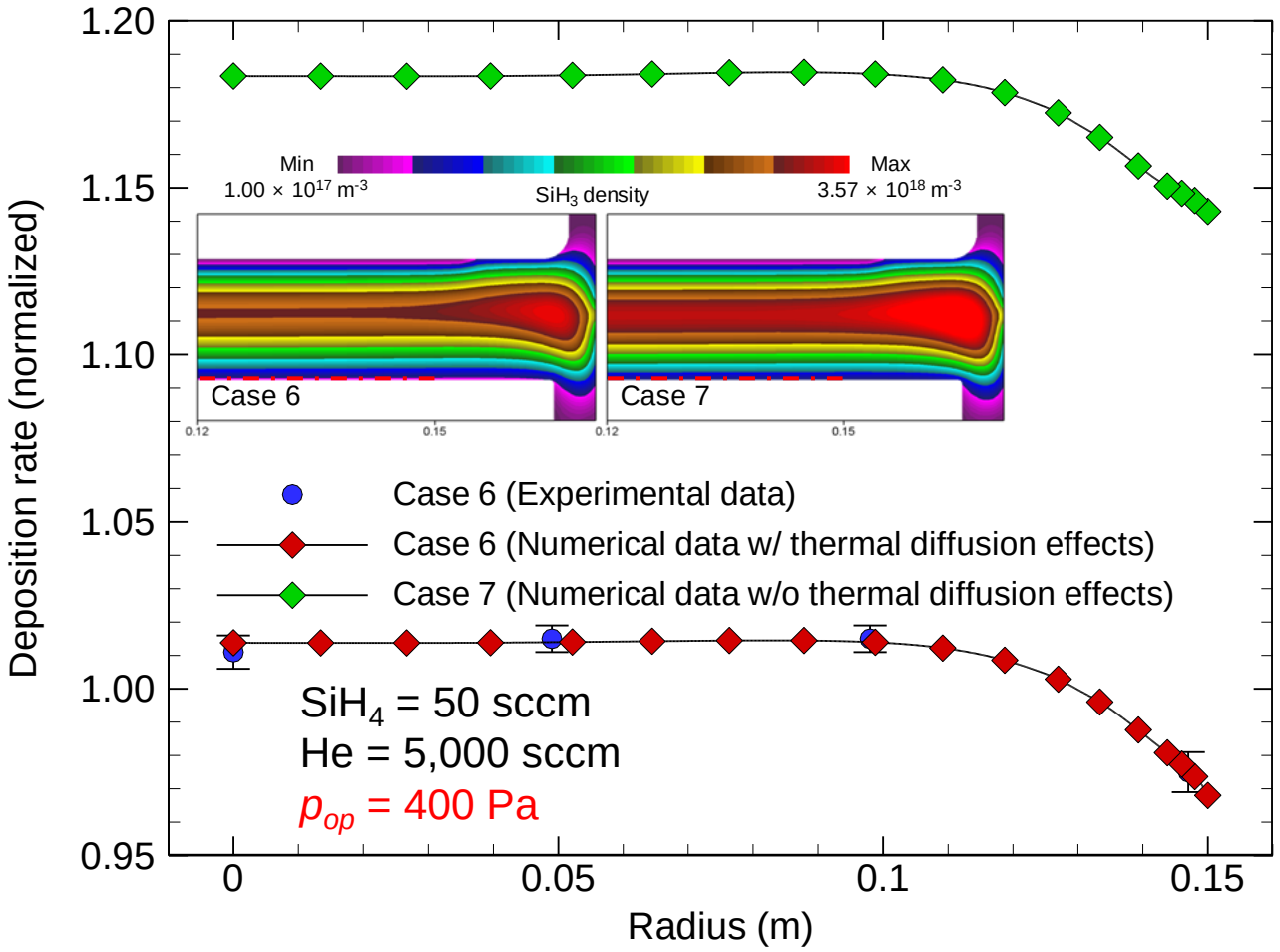

Simulated deposition rates measured along the radial direction are given for Cases 6 (red diamond) and 7 (green diamond). In addition, the experimental data for Case 6 (blue circle) are superimposed. For Case 6, the numerical and experimental data are both normalized to their corresponding averaged values. However, the profile of Case 7 is normalized to the averaged value of the profile of Case 6 to serve as a quantitative comparison of the deposition rates. A deposition rate discrepancy of about 17% can be seen between Cases 6 and 7. The inset depicts the spatial variations of SiH_3 densities for Cases 6 and 7; the SiH_3 density of Case 6 is lower than that of Case 7 near the "hot susceptor."

These two methods can have “the chemistry dependency.”

Then, which method can be more "physically general?"

Sidewall and electrode spacing

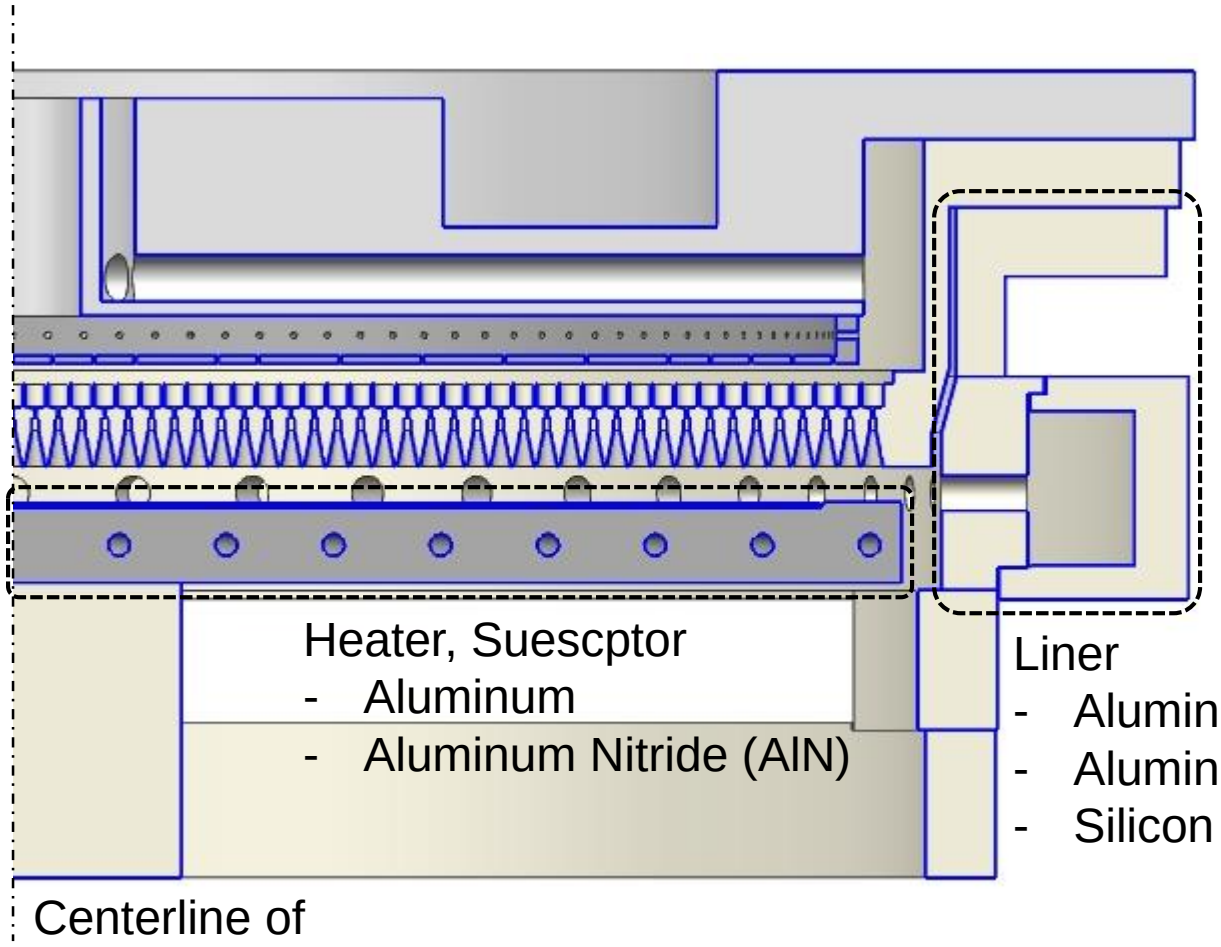

Heater, Suescptor
- Aluminum
- Aluminum Nitride (AlN)

Liner
- Aluminum
- Aluminum Oxide (Al_2O_3)
- Silicon Carbide (SiC)

Centerline of reactor

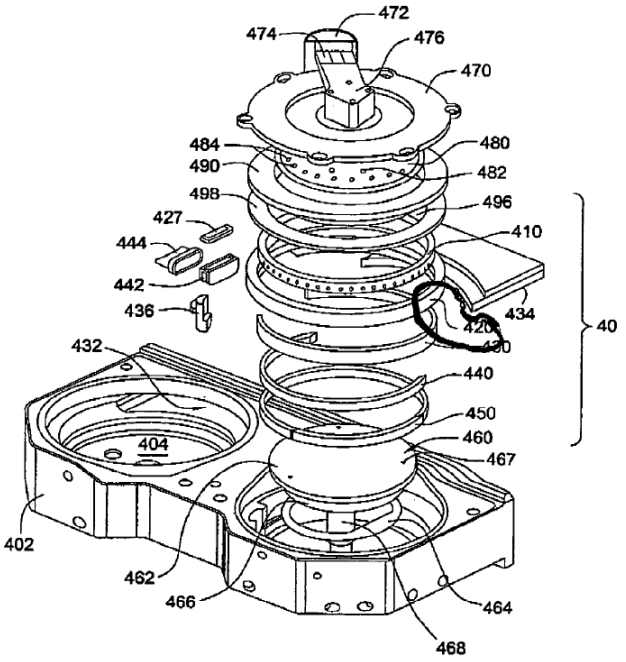

Sidewall effects: $SiH_4/NH_3/N_2/He$ mixture

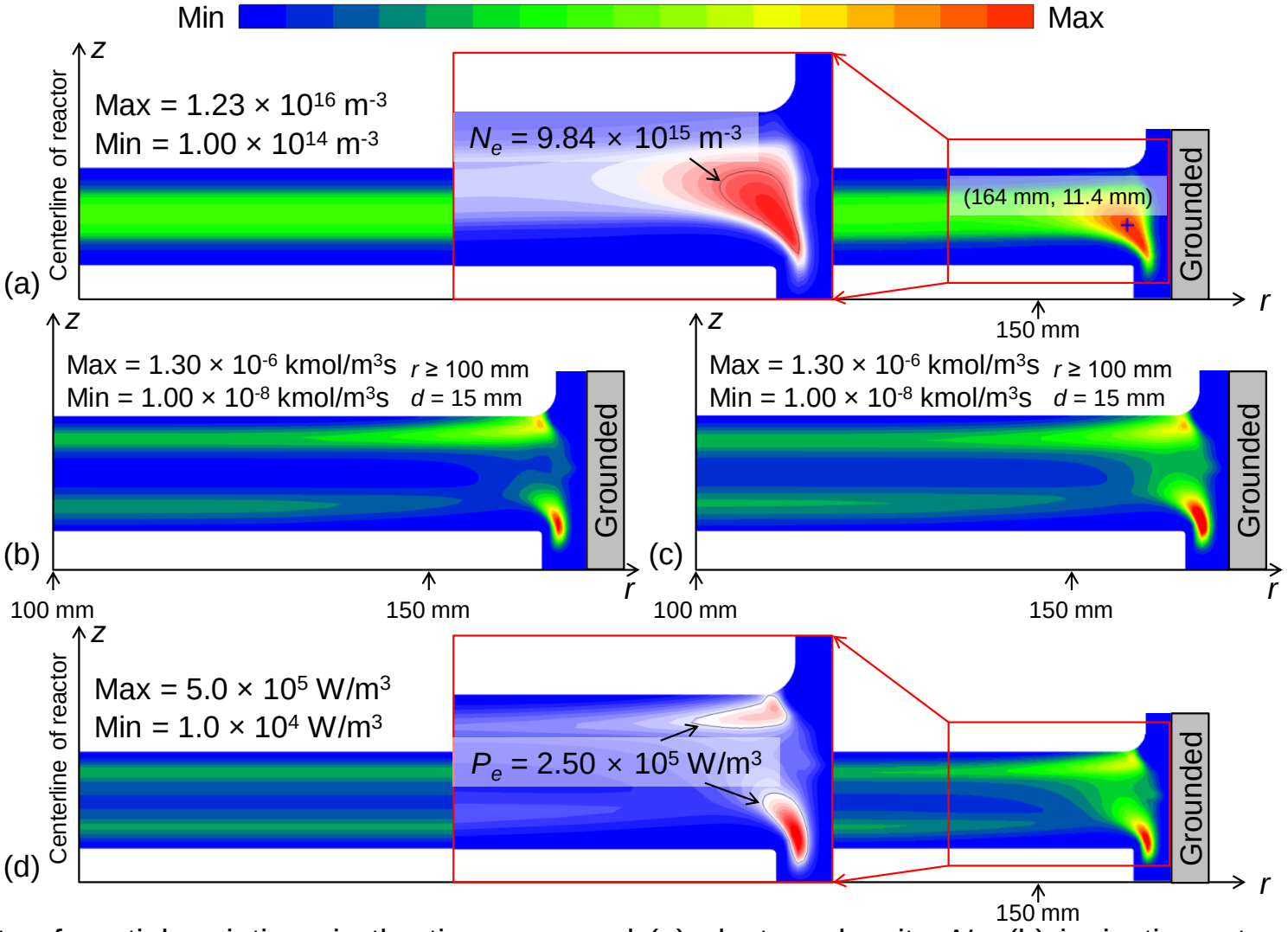

Contour plots of spatial variations in the time-averaged (a) electron density, N_e, (b) ionization rate of SiH_2^+, (c) ionization rate of NH_3^+, and (d) electron power density, P_e for case with the grounded sidewall. The profiles are radially uniform at r < 100mm as shown in (a) and (d), and thus (b) and (c) are shown only for $r \geq 100$ mm.

Sidewall effects: $SiH_4/NH_3/N_2$/He mixture

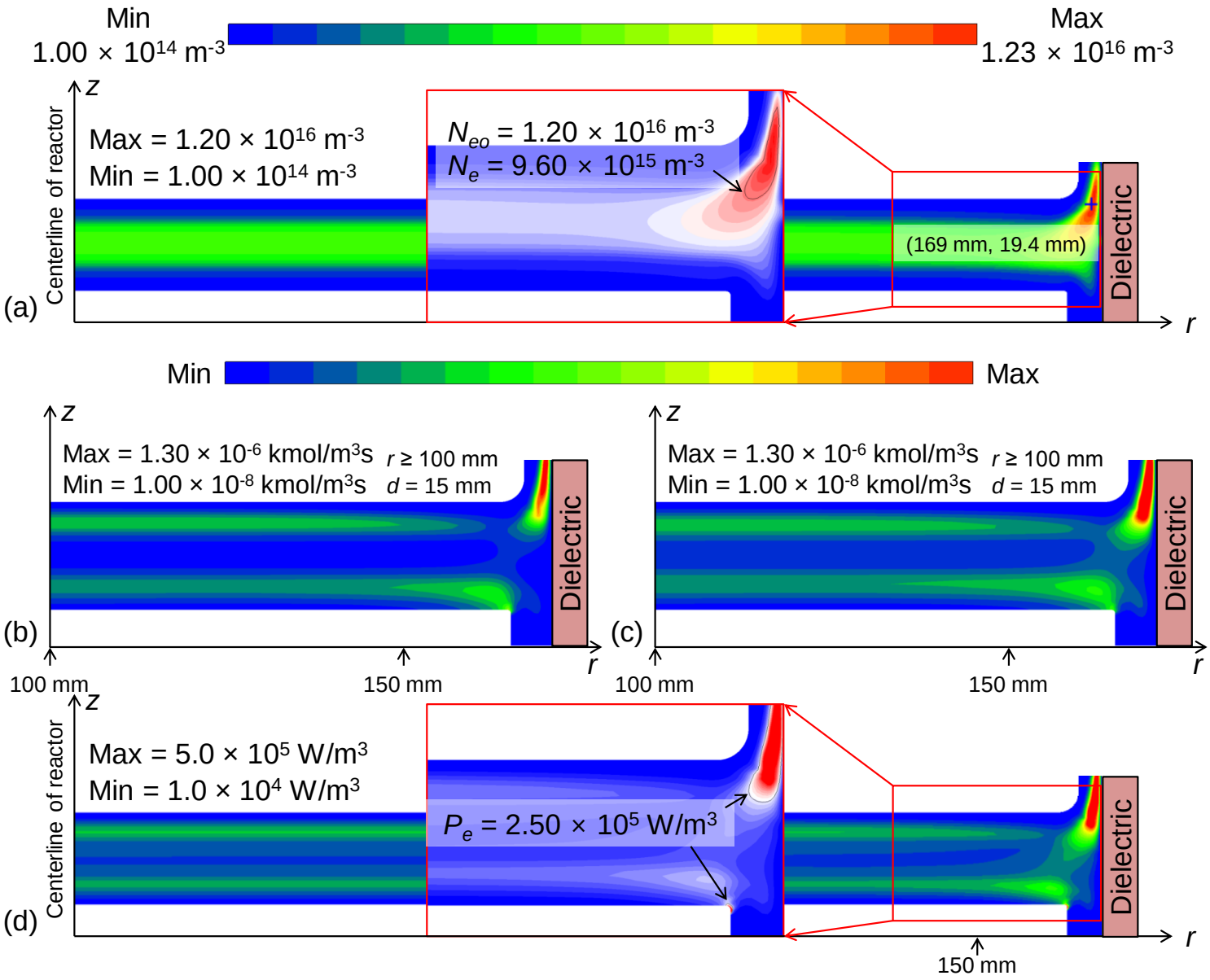

Sidewall effects: $SiH_4/NH_3/N_2$/He mixture

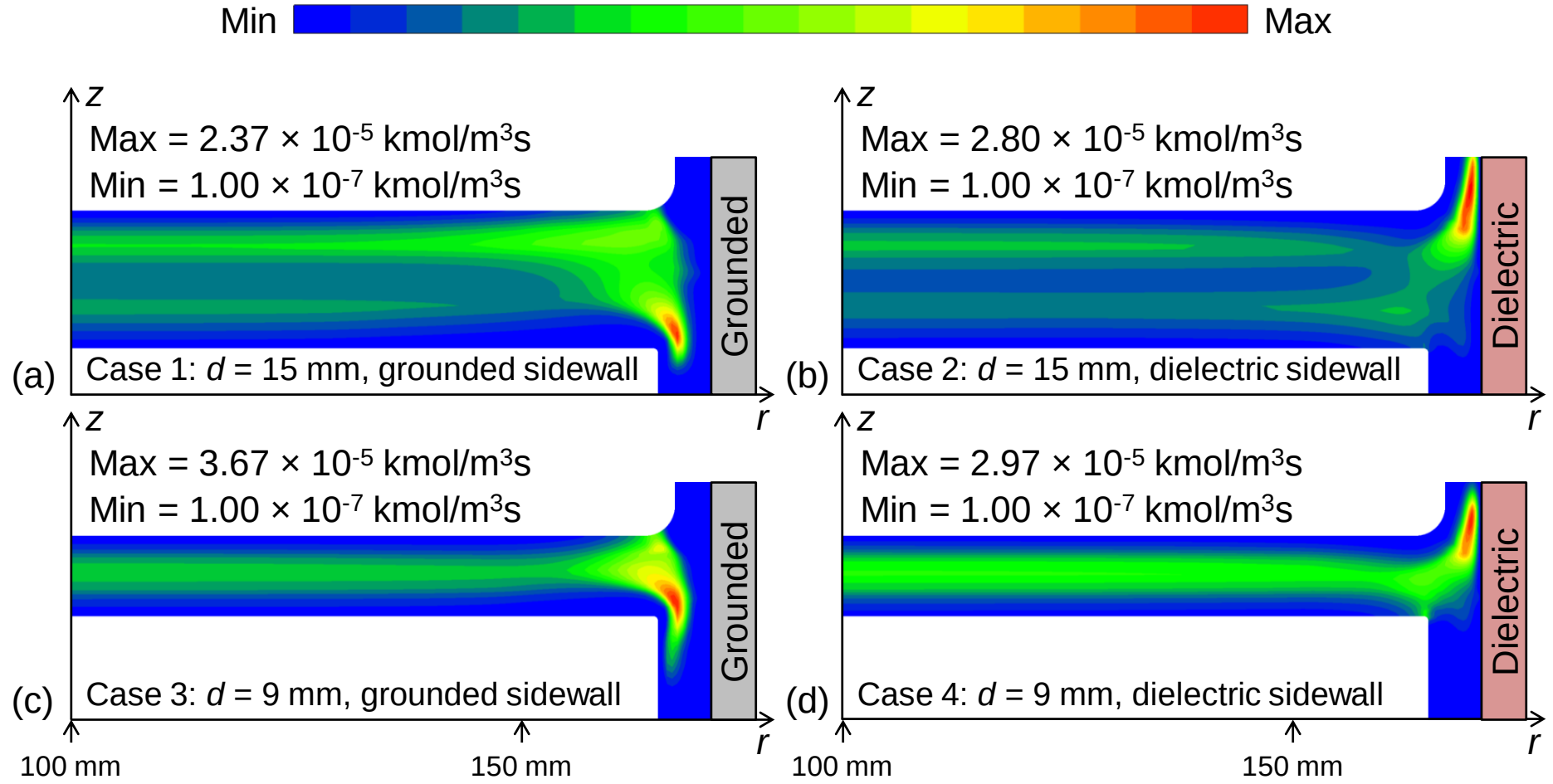

Contour plots of the time-averaged dissociation rates of SiH_4 molecules ($e^- + SiH_4 \rightarrow SiH_3 + H + e^-$) for (a) case 1, (b) case 2, (c) case 3, and (d) case 4. As the profiles are radially uniform for $r < 100$ mm, contours are shown only for $r \geq 100$ mm.

$SiH_4/NH_3/N_2$/He mixture

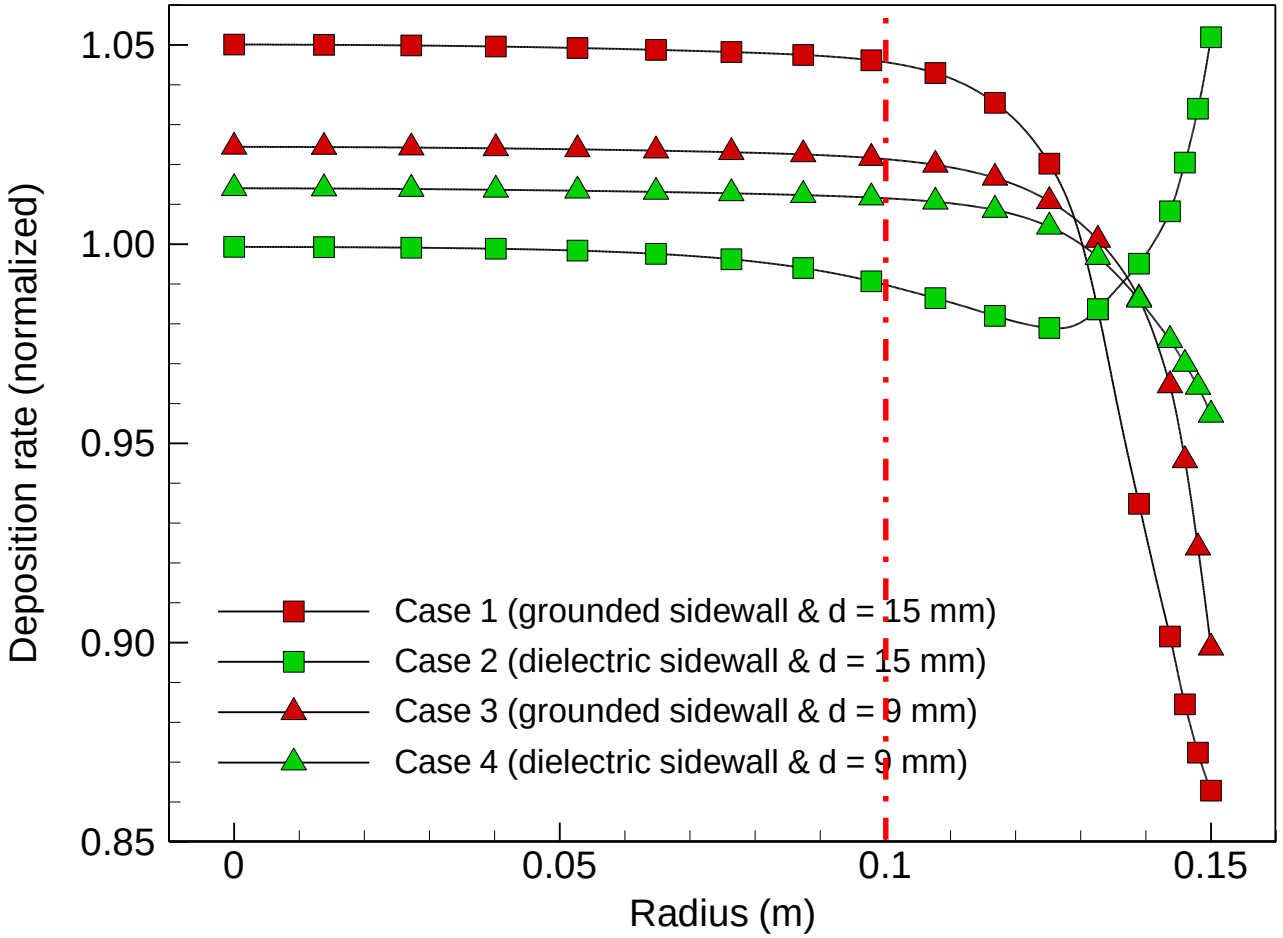

Normalized deposition rate profiles for cases 1, 2, 3, and 4. Owing to the axi-symmetry of the reactor, the simulated deposition rate profiles are plotted along the electrode radius.

Concluding remarks

- In this study, we numerically demonstrated that modulation of the sidewall conditions could contribute to controlling distributions of the plasma variables in an intermediate pressure CCP-PECVD.
- A cylindrical discharge volume was set to be radially surrounded by a lateral sidewall. To vary the sidewall conditions, we toggled its electrical condition from grounded to dielectric.
- Some important findings were observed.
  - ✓ First, we found that the case with the grounded sidewall has the spatial distributions of the ionization rate, ion and electron densities more heavily weighted toward the larger radius than the cases with the thick insulator.
  - ✓ By utilization of the thick insulator, noticeable reduction of the peak ionization rate could be achieved near the sidewall without significant changes of the ion and electron densities in the inter-electrode region.
  - ✓ These observations were owing to the fact that the effective size of the electrode of the case with the thick insulator becomes more comparable due to the higher impedance of the sidewall, as compared with that of the case with the grounded sidewall.
  - ✓ As a result, the thick insulator induced significant improvement in the uniformity of the deposition rate profile.

Other Works

Remote plasma cleaning (RPC)

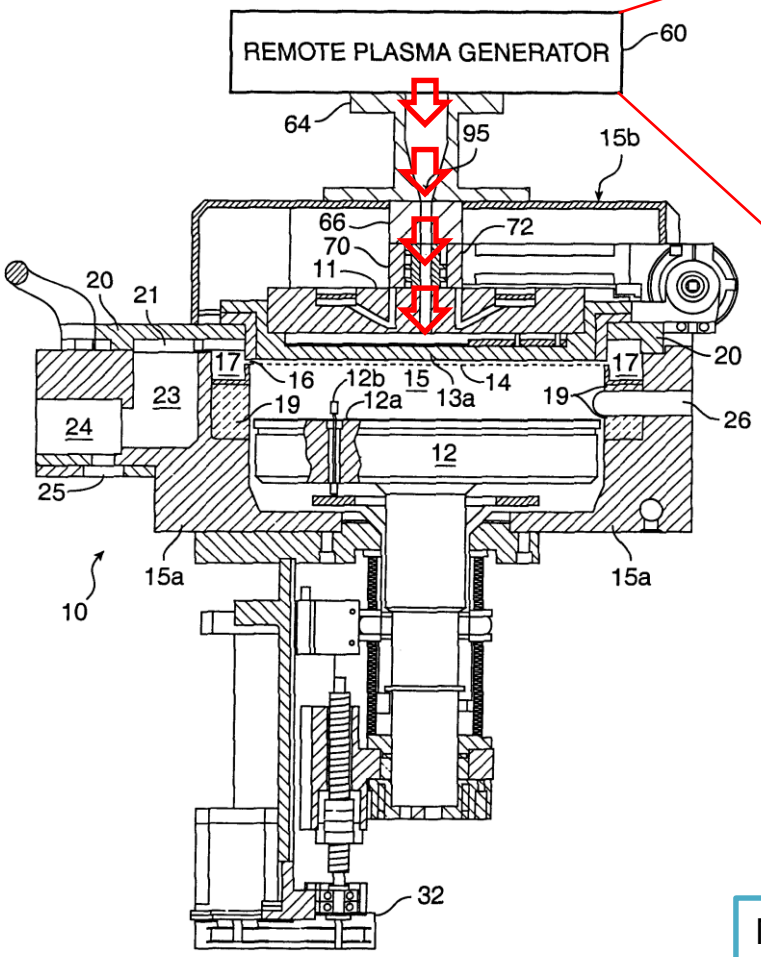

Reaction pathways	Description
$e + NF_3 \rightarrow e + NF_2 + F$	Direct electron impact dissociation
$e + NF_3 \rightarrow NF_2 + F-$	Electron impact dissociative attachment
Excitation and successive dissociation	
$e + NF_3 \rightarrow e + NF_3^a + e$	Vibrational and electronic excitation
$e + NF_3^a \rightarrow NF_2 + F$	Dissociative attachment after excitation
$e + NF_3^a \rightarrow +NF_2 + F + e$	Dissociation from excitation
Thermal pathway	
$NF_3 + M \rightarrow NF_2 + F + M$	Thermal dissociation

[a] Indicates an electronically or vibrationally excited state.

- Remote NF_3 plasmas have now been adopted for cleaning most CVD/ALD reactors due to faster clean times, reduced reactor damage and substantially lower emissions of gases having high GWPs.
- An NF_3 plasma is generated upstream of the reactor, generating F atoms that are then transported to the reactor where they react with the residue such as SiO_x or SiN_x covering the reactor surfaces.
- Since the discharge is confined to the plasma source, the surfaces of the chamber are not exposed to a flux of energetic ions.
- Hence, the residues are cleaned by a chemical etch.

Number densities of reactive radicals are calculated in the RPG model and their flux values are introduced as a boundary condition of reactor inlet.

Reference:
Integration of remote plasma generator with semiconductor processing chamber
US 6387207 B1

▷ Plasma Chemistry

NF_3 Dissociation: $e + NF_3 + Ar \rightarrow e + NF_2 + F + Ar + Ar^* + \ldots$

$e + NF_3 \rightarrow e + NF_2 + F$

▷ Radical Chemistry

1. Gas Phase Reaction

Volume Recombination: $F + F + M \rightarrow F_2 + M$

2. Surface Reaction

Surface Adsorption: $F \rightarrow F_S$
Surface Recombination: $F + F_S \rightarrow F_2$
Surface Desorption: $F_S \rightarrow F$
Oxide Etching: $SiO_2 + 4F \rightarrow SiF_4 + O_2$

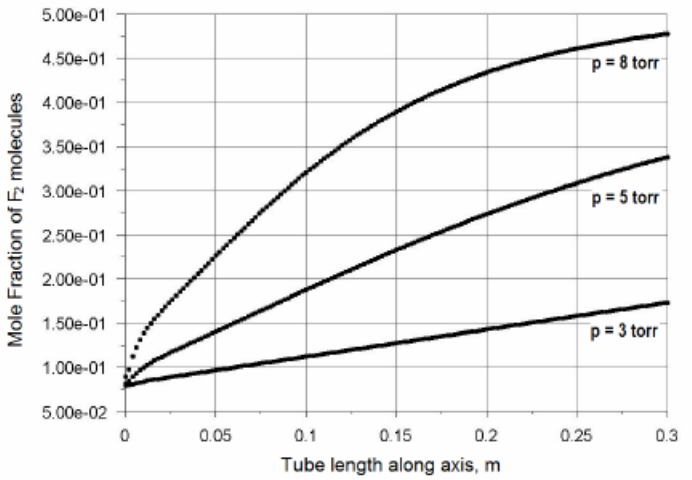

Mole fractions of F_2 molecules in transport tube length. The curves show computed values for three different pressures: 3, 5 and 8 Torr.

Remote plasma cleaning (RPC)

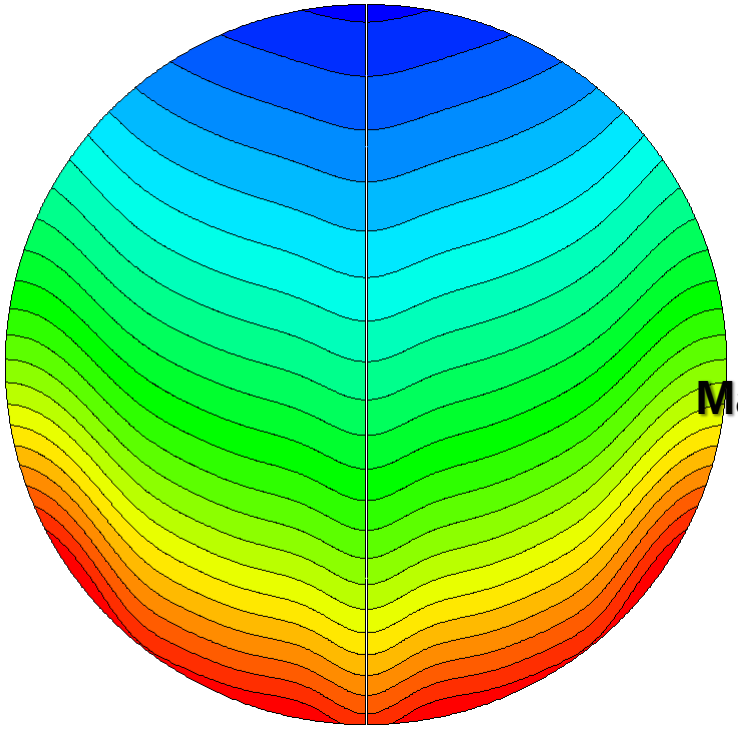

Simulation

Well Matched

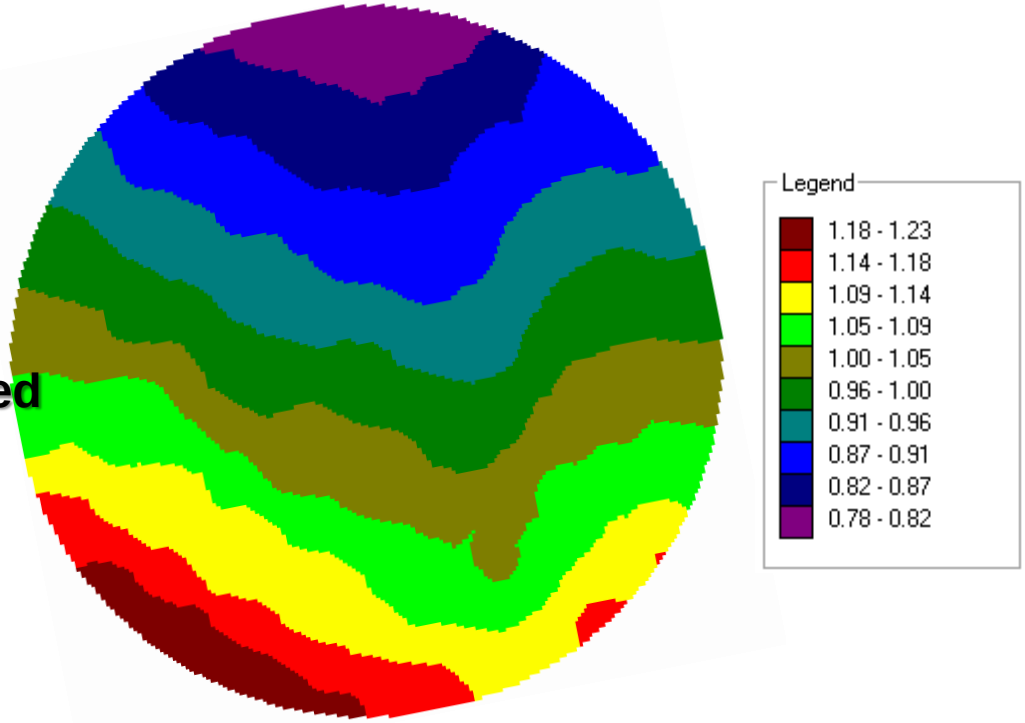

Experiment

Thank you